CURE CYCLE DETERMINATION OF NEAT AND NANO-REINFORCED CARBON/EPOXY COMPOSITES USED IN AEROSPACE APPLICATIONS THROUGH INVESTIGATION OF CURE KINETICS BY DIFFERENTIAL SCANNING CALORIMETRY AND RHEOMETER

by

AYŞE NUR SÜMBÜL BOZTAŞ

Submitted to the Graduate School of Engineering and Natural Sciences

in partial fulfillment of
the requirements for the degree of
Master of Science

SABANCI UNIVERSITY
July 2021

CURE CYCLE DETERMINATION OF NEAT AND NANO-REINFORCED CARBON/EPOXY COMPOSITES USED IN AEROSPACE APPLICATIONS THROUGH INVESTIGATION OF CURE KINETICS BY DIFFERENTIAL SCANNING CALORIMETRY AND RHEOMETER

Approv	red by		
Date of	Approval:		

AYŞE NUR SÜMBÜL BOZTAŞ 2021 © All Rights Reserved

ABSTRACT

CURE CYCLE DETERMINATION OF NEAT AND NANO-REINFORCED CARBON/EPOXY COMPOSITES USED IN AEROSPACE APPLICATIONS THROUGH INVESTIGATION OF CURE KINETICS BY DIFFERENTIAL SCANNING CALORIMETRY AND RHEOMETER

AYŞE NUR SÜMBÜL BOZTAŞ

MSc. Thesis, July 2021

Thesis supervisor: Assoc. Prof. Dr. Bekir Dızman

Keywords: Cure cycle, Cure kinetics, Differential Scanning Calorimetry, Rheometer, Carbon/epoxy composites

In carbon/epoxy composite laminates, epoxy resin has an important role as a component that holds the carbon fibers together and provides load distribution. Particularly, the interfacial bond between carbon fiber and epoxy resin should be good against shear stresses and stresses occurring in the perpendicular direction to the fibers. In order to achieve this, it is necessary to maximize the adhesion and strength properties of the epoxy resin and to remove the voids in the structure. This depends on a good examination of the epoxy resin curing kinetics. For this purpose, in this thesis, dynamic and isothermal tests were performed under different pressure conditions using HP-DSC for two different resins and prepregs, the rheological behavior of the resin and prepregs were examined, and then rheology and HP-DSC data were combined to determine cure cycles. The proposed cure cycles were applied for the manufacturing of carbon/epoxy composite laminate in the autoclave, and the working condition of the cure cycle was evaluated with the thermal and mechanical tests. In the first part of the thesis, materials, devices, and test methods used were introduced. In the second part, the curing kinetics of epoxy resin and the effect of pressure on the curing behavior were examined in the light of the literature. Afterwards, the curing kinetic behavior was investigated with HP-DSC under different pressures, heating rates and temperatures. These tests were done for resin and twill prepregs. The results revealed that the air bubbles and the voids formed as a result of the removal of water vapor during the process in the crimp zones in the prepreg were evacuated with the application of pressure, which increased the reaction surface area and the reaction enthalpy. The application of pressure considerably increased the curing time of the resin. The effect of pressure was more pronounced at low heating rate since there was more time for molecular mobility at low temperatures and the heat distribution was more uniform. The rheological data showed that the viscosity values of the B-stage prepreg were higher than the resin. Lastly, two different cure cycles determined with 3 and 7 bar pressures were applied, and the reference characterization and mechanical test results were successfully performed. In the third part, UD prepregs were studied under similar test conditions. No effect of pressure on enthalpy was observed for UD prepregs since they have unidirectional fibers and do not have crimp zones. The differences in curing behavior between neat and nano-reinforced UD prepregs were also investigated. Small increases in reaction enthalpy were observed with the utilization of MWCNT in the reactions, and it was concluded that the curing rate increased since the use of MWCNT increased the reaction surface area. It was also observed that the viscosity increased with the incorporation of MWCNT into the structure. Finally, the cure cycle was determined for these prepregs. Two different pressures (3 and 7 bars) were used. As a result of the tests applied to the manufacturing with these cure cycles, it was seen that 3 bar did not provide the reference manufacturing values in this system, while 7 bar pressure did.

ÖZET

HAVACILIK UYGULAMALARINDA KULLANILAN KATKISIZ VE NANO-KATKILI KARBON/EPOKSİ KOMPOZİTLERİN KÜRLEME KİNETİĞİNİN DİFERANSİYEL TARAMALI KALORİMETRE VE REOMETRE İLE İNCELENMESİ VE KÜR DÖNGÜLERİNİN BELİRLENMESİ

AYŞE NUR SÜMBÜL BOZTAŞ

Yüksek Lisans Tezi, Temmuz 2021

Tez Danışmanı: Doç. Dr. Bekir Dızman

Anahtar Kelimeler: Kür döngüsü, Kür kinetiği, Diferansiyel Taramalı Kalorimetre, Reometre, Karbon/epoksi kompozit

Karbon/epoksi kompozit plakalarda epoksi reçine karbon fiberleri bir arada tutan ve yük dağılımını sağlayan bileşen olarak önemli bir göreve sahiptir. Özellikle kesme yükü gerilmelerine ve fiberlere dik doğrultuda oluşan gerilmelere karşı karbon fiber ile epoksi reçinenin ara yüzey bağının iyi olması gerekir. Bunu sağlamak için epoksi reçinenin yapışma ve mukavemet özelliklerinin en yüksek seviyeye çıkarılması ve yapıdaki boşlukların uzaklaştırılması gereklidir. Bu da epoksi reçine kür kinetiğinin ivi incelenmesine bağlıdır. Bu amaçla, bu tez çalışmasında iki farklı reçine ve bu reçinelerden elde edilen prepregler için HP-DSC kullanılarak farklı basınç koşulları altında dinamik ve izotermal testler yapıldı, reometre ile reçine ve prepreglerin reolojik davranışları incelendi ve sonrasında reoloji ve HP-DSC verileri birleştirilerek kür döngüleri oluşturuldu. Önerilen kür döngüleri otoklavda karbon/epoksi kompozit lamina üretimi için uygulandı ve yapılan termal ve mekanik testler ile kür döngüsünün çalışma durumu kontrol edildi. Tezin birinci bölümünde, kullanılan malzemeler, cihazlar ve test yöntemleri tanıtıldı. İkinci bölümde, epoksi reçinenin kür kinetiği ve basıncın kürleme davranışına etkisi literatür bilgileri ışığında incelendi. Sonrasında ise kür kinetiği davranışı farklı basınç, ısıtma hızı ve sıcaklıklar altında HP-DSC ile incelendi. Bu testler reçine ve twill prepregler için yapıldı. Sonuçlar basıncın prepregde kıvrım bölgelerinde bulunan hava kabarcıkları ile proses esnasında su buharının uzaklaşması sonucu oluşan boşlukları uzaklaştırdığı, bu sayede reaksiyon yüzey alanını artırdığı ve reaksiyon entalpisinde artışa neden olduğunu ortaya koydu. Basıncın reçinede kürleşme süresini oldukça artırdığı görüldü. Moleküler hareketliliğin daha uzun sürmesini ve ısı dağılımının daha düzenli olmasını sağlayan düşük ısıtma hızında basıncın etkisinin daha belirgin olduğu gözlemlendi. Reoloji verileri B-derece prepregdeki viskozite değerlerinin reçineden daha yüksek olduğunu gösterdi. 3 ve 7 bar basınç koşulları için belirlenen iki farklı kürleme döngüsü uygulandı ve referans karakterizasyon ve mekanik test sonuçlarının başarıyla sağlandığı görüldü. Üçüncü bölümde ise UD prepregler kullanılarak ilk sisteme benzer test koşulları altında çalışıldı. Tek yönlü fiberlere sahip olan ve kıvrım bölgesi barındırmayan UD prepreglerde entalpi üzerinde basıncın etkisi gözlemlenmedi. Bununla birlikte, nano katkılı ve katkısız UD prepregler arasındaki kürlenme davranısı farklılıkları incelendi. MWCNT'nin kullanılması ile reaksiyon entalpisinde küçük artışlar görüldü ve MWCNT'nin reaksiyon yüzeyini artırdığı için kürlenme hızında artış olduğu sonucuna varıldı. MWCNT ile güçlendirilen prepregin vizkozite değeri daha yüksekti. Son olarak bu prepregler için kür döngüsü belirlendi. 3 ve 7 bar olmak üzere iki farklı basınç kullanıldı. Bu kür döngüleri ile yapılan üretime uygulanan testler sonucunda 3 bar basıncın bu sistemde referans üretim değerlerini sağlamadığı 7 bar basıncın ise sağladığı görüldü.

Acknowledgement

First, I would like to express my gratitude to Sabanci University Integrated Manufacturing Technologies Research and Application Center (SU- IMC), where I learned a lot thanks to the laboratory facilities it provides. Afterwards, I would like to thank my thesis advisor dear Assoc. Prof. Dr. Bekir Dızman for listening to my research ideas and trusting me while carrying out my studies with his support.

I would also like to thank to Asst. Prof. Dr. Serkan Ünal, who included me in his project and provided open source on every subject. I would also like to thank Prof. Dr. Mehmet Yıldız, who guided me to pursue my master's degree and gave me his moral support.

In addition, I would like to thank Dilay Serttan and Murat Tansan for their help during the manufacturing part of my thesis. One of my biggest thanks would be to Kadir Erdoğan, one of the most important members of the SU-IMC Characterization Laboratory, who contributed a lot to my learning the device I use. I would like to express my gratitude to Burak Özdemir for his help, and to Yaşar Güray, Turgay Gönül, Mehmet Olcaz and Fatih Polat for sharing their experiences with me.

I would like to thank Zeynep Şahin, Gülayşe Şahin, Büşra Nakipoğlu and Dilara Çelik for the motivation and moral support they provided me throughout my work.

I would like to thank my love Sacit Boztaş and my family members; Sevdiye Sümbül, Muhittin Sümbül, Hakan Sümbül, Merve Sümbül, Hamza Sümbül and to my second mother Nuriye Özbay who were always there for me.

I dedicate my thesis to the people who work hard for their values and who I think will be rewarded for their efforts one day and to everyone who has been discriminated agains in the world and to our precious children and women who were brutally raped an murdered since they could not make their voice heard.	st

TABLE OF CONTENTS

CHAPTER 1	1
1. Literature review	1
1.1. Scope	1
1.2. Epoxy resin	3
1.3. Carbon fiber	7
1.4. Autoclave manufacturing of carbon/epoxy composites	9
1.5. Cure cycle in autoclave manufacturing	10
1.6. Differential Scanning Calorimetry (DSC) for carbon/epoxy composites	11
1.6.1. High-Pressure Differential Scanning Calorimetry (HP-DSC 2+)	11
1.6.2. Model-Free Kinetic analysis for carbon/epoxy composites	13
1.7. Rheometer for carbon/epoxy composites	17
1.8. Dynamic Mechanical Analysis of carbon/epoxy composites	19
1.9. Composite density and constituent content for carbon/epoxy composites.	21
1.10. Interlaminar shear stress for carbon/epoxy composites	22
1.11. Tensile test for carbon/epoxy composites	23
CHAPTER 2	24
2. Cure kinetic studies and determination of cure cycles for R1 and TW-R1	24
2.1. Introduction	24
2.1.1. Cure mechanism of epoxy-amine reactions	24
2.1.2. Void formation and pressure effect in cure kinetics	25
2.1.3. T _g behavior and effect of pressure on T _g	27
2.1.4. Effect of pressure on mechanical properties	28
2.2. Experimental – HP-DSC	29
2.2.1. Dynamic test methods and sample preparation for HP-DSC tests	29
2.2.2. HP-DSC dynamic test results – R1	30
2.2.3. HP-DSC dynamic test results – TW-R1	33
2.2.4. HP-DSC dynamic test results – R1 vs. TW-R1	36
2.2.5. Model Free Kinetics (MFK) analysis – R1	36
2.2.6. Model Free Kinetics (MFK) analysis – TW-R1	39
2.2.7. Sample preparation and isothermal test methods for HP-DSC tests	40
2.2.8. HP-DSC isothermal test results – R1	40
2.2.9. HP-DSC isothermal test results – TW-R1	43
2.2.10. Model Free Kinetics (MFK) analysis results vs. isothermal test resu	
R1	47

2.2.11. Model Free Kinetics (MFK) analysis results vs. isothermal test results TW-R1	
2.3. Experimental - Rheometer	
2.3.1. Rheometer temperature sweep and gel time test methods	
2.3.2. Temperature sweep and gel time – R1	
2.3.3. Temperature sweep and gel time – TW-R1	
2.4. Experimental – Cure cycle determination	
2.4.1. Important parameters in determining cure cycle steps	
2.4.2. Cure cycle determination	
CHAPTER 3	
3. Cure kinetic studies and determination of cure cycles for UD-R2 and UD-R2-MWCNT	
3.1. Introduction	62
3.1.1. Effect of functionalized MWCNTs on cure kinetics, T _g and mechanical properties	
3.2. Experimental - HP-DSC	. 64
3.2.1. Dynamic test methods and sample preparation for HP-DSC tests	. 64
3.2.2. HP-DSC dynamic test results – UD-R2	. 64
3.2.3. HP-DSC dynamic test results – UD-R2-MWCNT	. 66
3.2.4. Model Free Kinetics (MFK) analysis – UD-R2 and UD-R2-MWCNT	. 68
3.2.5. Sample preparation and isothermal test methods for HP-DSC tests	71
3.2.6. HP-DSC isothermal test results and comparison with MFK analysis res – UD-R2	
3.2.7. HP-DSC isothermal test results and comparison with MFK analysis results and comparison with MFK analysis results are supported by the comparison with MFK analysis results are supported by the comparison with MFK analysis results are supported by the comparison with MFK analysis results are supported by the comparison with MFK analysis results are supported by the comparison with MFK analysis results are supported by the comparison with MFK analysis results are supported by the comparison with MFK analysis results are supported by the comparison with MFK analysis results are supported by the comparison with MFK analysis results are supported by the comparison with MFK analysis results are supported by the comparison with MFK analysis results are supported by the comparison with MFK analysis results are supported by the comparison with MFK analysis results are supported by the comparison with the comparison	
3.3. Experimental - Rheometer	75
3.3.1. Temperature sweep and gel time – UD-R2	75
3.3.2. Temperature sweep and gel time – UD-R2-MWCNT	77
3.4. Experimental - Important parameters for cure cycle steps and cure cycle determination	78
CHAPTER 4	
4. Conclusions	
Deferences	80

LIST OF FIGURES

Figure 1. A schematic diagram of cure kinetics and cure cycle studies	3
Figure 2. Chemical structure of an epoxy ring [7]	4
Figure 3. Ring opening reactions of DGEBA with benzyl alcohol [8]	5
Figure 4. The curing of an epoxy resin through: (a) a primary amine; (b) a secondary	
amine; (c) a hydroxyl group generated from reactions (a) and (b) [9]	5
Figure 5. Composite plate reinforced with 2x2 twill woven fabric (left) and UD fabric	
(right) with epoxy matrix	3
Figure 6. An autoclave for carbon/epoxy composite manufacturing	9
Figure 7. High Pressure Differential Calorimetry (HP-DSC) for cure kinetic studies 12	2
Figure 8. FRS 6+ and HSS 9+ HP-DSC sensors	3
Figure 9. MFK analysis steps: Dynamic curves (a), conversion curves (b), activation	
energy curve (c), conversion estimation curves for isothermal tests (d)	7
Figure 10. Rheometer for cure kinetic studies	3
Figure 11. Dynamic Mechanical Analysis (DMA) for T _g measurements	Э
Figure 12. An example of a Dynamic Mechanical Analysis curve	Э
Figure 13. ILSS test samples	2
Figure 14. Dynamic enthalpy (left) and conversion (right) curves carried out for R1	
under the pressures of 1, 3, 5.6 and 7 bar at the heating rates of 3, 5, 10 °C/min 32	1
Figure 15. Comparison of dynamic enthalpy values of R1 with respect to heating rate	
(left) and pressure (right)	2
Figure 16. Dynamic enthalpy (left) and conversion (right) curves carried out for TW-R1	L
under 1, 3, 5.6 and 7 bar pressures at the heating rates of 3, 5, 10 °C/min34	4
Figure 17. Comparison of dynamic TW-R1 enthalpy values with respect to heating rate	
(left) and pressure (right)	5
Figure 18. R1 MFK Analysis isothermal cure degree estimation curves at the	
temperatures of 80, 90, 100, 110, 120, 130 and 140 °C under the pressures of 1, 3, 5.6	
and 7 bar	7
Figure 19. TW-R1 MFK Analysis isothermal cure degree estimation curves at the	
temperatures of 80, 90, 100, 110, 120, 130 and 140 °C under the pressures of 1, 3, 5.6	
and 7 bar39	9
Figure 20. Isothermal enthalpy (left) and conversion (right) curves carried out for R1	
under the pressures of 1, 3, 5.6 and 7 bar at the temperatures of 90, 100, 110, 120 °C . 4	1

Figure 21. Isothermal enthalpy (left) and conversion (right) curves carried out for TW-
R1 under the pressures of 1, 3, 5.6 and 7 bar at the temperatures of 90, 100, 110, 120 $^{\circ}\mathrm{C}$
Figure 22. Comparison of isothermal TW-R1 enthalpy values with respect to
temperature (left) and pressure (right)
Figure 23. Comparison of isothermal TW-R1 curing times with respect to temperature
(left) and pressure (right)
Figure 24. Comparison of R1 MFK analysis estimations and isothermal curves 48
Figure 25. Comparison of TW-R1 MFK analysis estimations and isothermal curves 49
Figure 26. R1 temperature sweep (left) and gel time curves (right)
Figure 27. TW-R1 temperature sweep (left) and gel time curves (right)
Figure 28. CC1 cure cycle55
Figure 29. CC2 cure cycle
Figure 30. TW-R1 CC1 (left) and CC2 (right) interlaminar shear stress (ILSS) test
results
Figure 31. TW-R1 CC1 (left) and CC2 (right) tensile test results
Figure 32. Tensile test fracture surfaces
Figure 33. Catastrophic fracture surface
Figure 34. Dynamic enthalpy (left) and conversion (right) curves for UD-R2 under the
pressures of 1, 3, and 7 bar at the heating rates of 3, 5, 10 °C/min
Figure 35. Dynamic enthalpy (left) and conversion (right) curves carried out for UD-
R2-MWCNT under 1, 3, and 7 bar pressures at 3, 5, 10 °C/min heating rate 67
Figure 36. UD-R2 MFK Analysis isothermal cure degree estimation curves at 80, 90,
100, 110, 120, 130 and 140 °C temperatures under 1, 3, and 7 bar pressures
Figure 37. UD-R2-MWCNT MFK Analysis isothermal cure degree estimation curves at
80, 90, 100, 110, 120, 130 and 140 °C temperatures under 1, 3, 5.6 and 7 bar pressures
70
Figure 38. Isothermal enthalpy (left) and conversion (right) curves carried out for UD-
R2 under 1, 3, 5.6 and 7 bar pressures at 90, 100, 110, 120 °C temperatures72
Figure 39. Comparison of UD-R2 MFK analysis estimations and isothermal curves 73
Figure 40. Isothermal enthalpy (left) and conversion (right) curves carried out for UD-
R2-MWCNT under 1, 3, 5.6 and 7 bar pressures at 90, 100, 110, 120 °C temperatures 73
Figure 41. Comparison of UD-R2-MWCNT MFK analysis estimations and isothermal
curves

Figure 42. UD-R2 temperature sweep (left) and gel time curves (right)	. 76
Figure 43. UD-R2-MWCNT temperature sweep (left) and gel time curves (right)	. 77
Figure 44. CC3 cure cycle	. 79
Figure 45. CC4 cure cycle	. 80
Figure 46. UD-R2 CC3 (left) and CC4 (right) interlaminar shear stress (ILSS) test	
results curves	. 82
Figure 47. UD-R2 CC3 (left) and CC4 (right) tensile test results curves	. 83

LIST OF TABLES

Table 1. Dynamic cure enthalpies and onset temperatures of R1	32
Table 2. R1 dynamic cure degree with respect to temperatures	33
Table 3. TW-R1 dynamic cure enthalpies and onset temperatures	35
Table 4. TW-R1 dynamic cure degrees with respect to temperatures	36
Table 5. R1 MFK analysis estimation of cure degree versus time	38
Table 6. TW-R1 MFK analysis estimation of cure degree versus time	39
Table 7. R1 isothermal cure enthalpies	42
Table 8. R1 isothermal cure degrees with respect to time	43
Table 9. TW-R1 isothermal cure enthalpies	45
Table 10. TW-R1 isothermal cure degree with respect to time	47
Table 11. Complex viscosity of R1 temperature sweep and gel time	50
Table 12. Complex viscosity of TW-R1 temperature sweep and gel time	51
Table 13. Rheology and HP-DSC gel point comparison	52
Table 14. CC1 cure cycle conversions.	55
Table 15. CC2 cure cycle conversions.	57
Table 16. Comparison of the characterization and mechanical test results of CC1 and	d
CC2 cure cycles with CCRef-1	58
Table 17. UD-R2 dynamic cure enthalpies and onset temperatures	66
Table 18. UD-R2-MWCNT dynamic cure enthalpies and onset temperatures	67
Table 19. T_g variation according to different pressure conditions for UD-R2-MWCN	ΙΤ
	68
Table 20. UD-R2 MFK analysis estimation of cure degree versus time	69
Table 21. UD-R2-MWCNT MFK analysis estimation of cure degree versus time	70
Table 22. UD-R2 isothermal cure enthalpies	72
Table 23. UD-R2 isothermal cure degree according to time	72
Table 24. UD-R2-MWCNT isothermal cure enthalpies	73
Table 25. UD-R2-MWCNT isothermal cure degree according to time	74
Table 26. Complex viscosity of UD-R2 temperature sweep and gel time	76
Table 27. Complex viscosity of UD- R2-MWCNT temperature sweep and gel time	77
Table 28. Comparison of the characterization test results of CC3 and CC4 cure cycle	es
with CCRef-2	81
Table 29. Comparison of the mechanical test results of CC3 and CC4 cure cycles wi	th
CCRef-2	81

LIST OF SYMBOLS

 α Degree of conversion, changing from 0 to 1

Pre-exponential A Collision frequency (1/s)

 E_a Activation energy (kJ/mol)

 $f(\alpha)$ Reaction type (nth order, autocatalysis, nucleation, ...)

 $\frac{da}{dt}$ Reaction rate

 k_0 Rate constant at infinite temperature

R Universal gas constant



CHAPTER 1

1. Literature review

1.1. Scope

The cure cycle determination of an epoxy resin is considered as a key factor for maximizing the degree of epoxy resin reaction with curing agents to form a crosslinked network structure and increasing the resulting mechanical properties. The cure kinetics of an epoxy resin must be well studied for an accurate determination of its cure cycle.

The thesis focused on the cure kinetic studies of a commercial epoxy resin and carbon/epoxy prepregs and the use of the kinetic data in determining the cure cycle. The cure kinetic studies were mainly carried out using High Pressure Differential Scanning Calorimetry (HP-DSC). The HP-DSC data were then combined with the rheological data obtained using a rheometer to determine the cure cycle of the carbon/epoxy composites [1].

Differential Scanning Calorimetry (DSC) is a thermal analysis technique in which the difference in the amount of heat required to change the temperature of a sample and reference under the same conditions is measured as a function of temperature or time. HP-DSC, on the other hand, enables the measurement of the samples under precisely controlled pressures, which are obtained through the flow of a gas from the body of furnace into the DSC system. For polymers, phase changes, glass transition temperatures, specific heat capacity, transitions such as crystallization and curing can be observed for varying temperatures and enthalpy values by DSC and HP-DSC. In this study, glass transition temperatures, curing enthalpies, and conversion rates of the resins and carbonfiber reinforced epoxy-resin based prepregs were examined using dynamic and isothermal DSC tests at varying pressures by HP-DSC. Dynamic DSC tests were performed at varying heating rates. Model Free Kinetics (MFK) analysis was used to predict the kinetic behavior, more specifically the isothermal behavior (i.e., the curing temperatures and times) of the resins and prepregs. The isothermal DSC tests for resins and prepregs were performed based on the information obtained from the MFK analysis results of the dynamic DSC tests.

The following resins and prepregs were used in this study: A commercial epoxy resin (R1) and its prepreg (TW-R1) obtained by the impregnation of this resin into a 400 gsm 2x2 woven twill fabric. Furthermore, UD-R2 prepreg, obtained by the impregnation of the R2 resin, which is a modified version of R1 resin, into 200 gsm UD fabric. The main reason for the modification of the R1 resin to obtain R2 resin was to decrease the viscosity of the resin to make it more processible at relevant temperatures in its neat and nanomaterial-reinforced forms. The modification was also utilized to increase the dispersibility of the nanomaterials in the epoxy resin (only in R2) and to improve some of the final properties of the composites obtained from these prepregs such as Tg and toughness. MWCNTs carrying two different functional groups were used as nanomaterial reinforcements: MWCNT-1 and MWCNT-2. The MWCNT-1 (NCO-f2-MWCNT) was sprayed onto the UD-R2, and the MWCNT-2 (0.10% COOH-f-MWCNT) was added into R2 and UD-R2-MWCNT was obtained.

The thesis discussed the cure kinetic studies of R1, TW-R1, UD-R2 and UD-R2-MWCNT and determination of the cure cycles. Moreover, characterization and mechanical tests of the composites obtained from the prepregs were conducted to make sure that the idea behind cure cycle determination was correct. The schematic diagram of these studies is provided in **Figure 1**.

To date, no such detailed controlled studies have been conducted comparing the differences in cure kinetics between resin and prepreg, twill prepreg and UD prepreg, and UD prepreg and nano-reinforced UD prepreg, specifically considering the effect of pressure. Also, research to date has not yet determined the cure cycles using final product (prepreg) cure kinetics data nor checked its workability with different characterization and mechanical tests. The main purpose of these studies is to determine cure cycles that will provide the highest level of mechanical properties by increasing adhesion between carbon fiber and resin and minimizing void formation. The knowledge acquired in this study can be applied to other epoxy resin and prepreg systems.

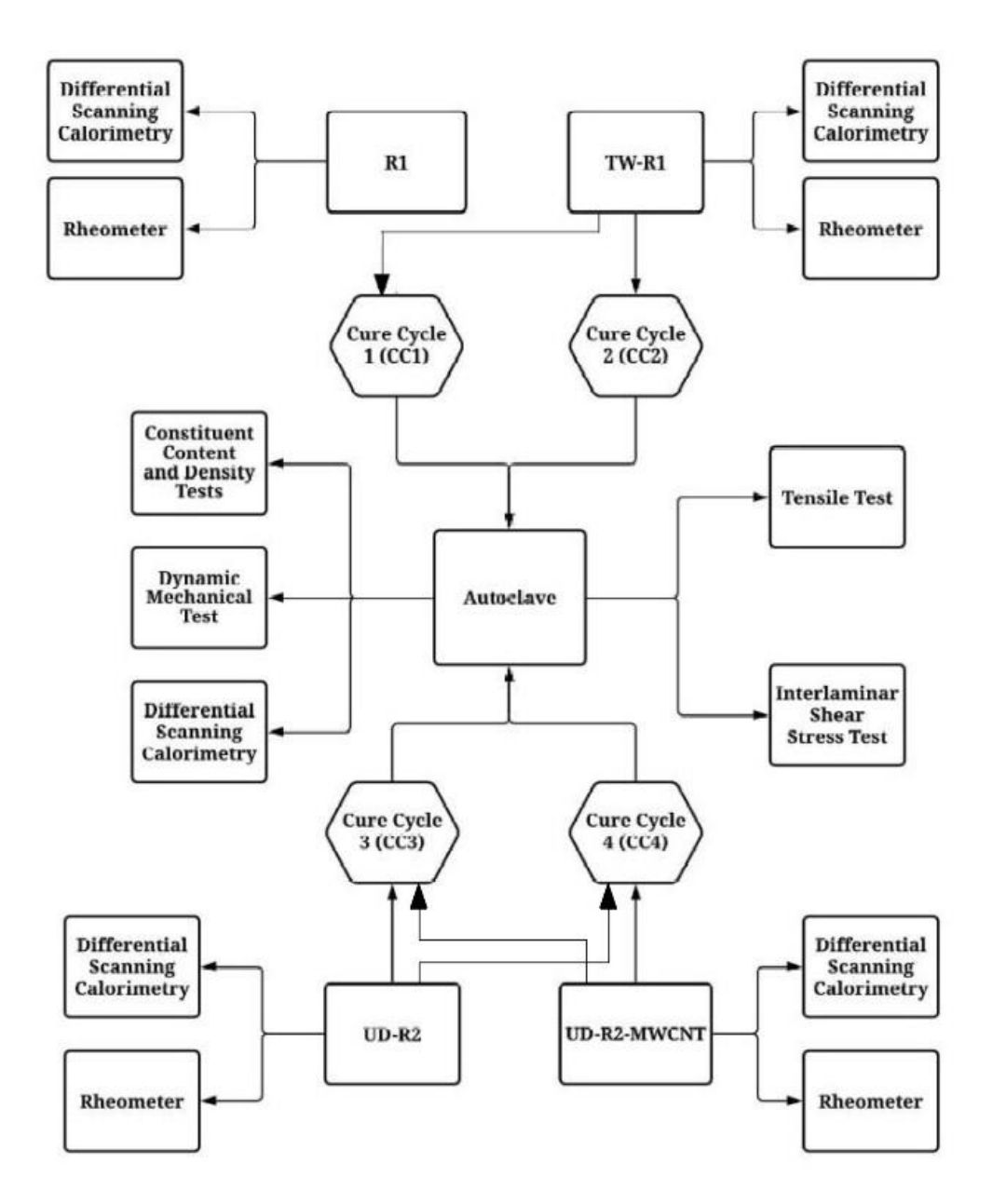


Figure 1. A schematic diagram of cure kinetics and cure cycle studies

1.2. Epoxy resin

The term resin represents the polymer or the polymer precursor and/or the chemical mixture or formulation of the polymer precursor material with various additives or reactive ingredients. The term epoxy, on the other hand, refers to the general definition of a polymer group molecules containing epoxide groups. As shown in **Figure 2**, the epoxide group carries one oxygen and two carbon atoms in the form of a ring [2,3]. Epoxy resin is a thermoset polymer, which contains one or more epoxide group and consists of oligomers that cannot be recycled after completing the formation of crosslinks. Epoxy resin contains functional groups that can react with amines, alcohols, cyanates, acids, acid

anhydrides, mercaptans and phenols and cures as a result of these reactions. In addition, the epoxy resin can self-crosslink through the epoxy group and in this way cures after the reactions are complete [2–4]. The curing stages in epoxy resins are classified as follows. A-stage is the stage where the resins do not react, B-stage is the stage where the resins are generally vitrified below the gel temperature and add workability to the system, and C-stage is the stage where the resin is fully cured [2].

The curing of the epoxy resin takes place as follows. The bonding angles of the epoxide groups in the epoxy resin enables reactive materials such as amines and acids to cause ring opening, and to be easily crosslinked [5]. Epoxy resin transforms from a low molecular weight liquid into a gel form (gelation), which creates a dense cross-linked and network structure with the effect of temperature and time, and then into a rigid solid form (vitrification) irreversibly. In the curing phase, which is an exothermic reaction, if the oxirane ring is cured with an amine in the epoxy, a high enthalpy of 103-110 kJ/mol is obtained [2,4]. Although epoxy resins can cure themselves with the aid of a catalyst, they are mostly cured with the above-mentioned hardeners. The curing speed of an epoxy resin is slower than other resins such as polyester resin due to epoxy-hardener reactions. These reactions are highly exothermic and the use of catalysts is limited as they can cause thermal decomposition in the matrix [5].

The most common epoxy resin is based on bisphenol A, which is called "diglycicidyl ether of bisphenol A" or DGEBA. Reactions with this resin can take place at room temperature or at high temperatures, depending on the type of hardener used. The reaction mechanisms of DGEBA with benzyl alcohol and amines are shown in **Figure 3** and **Figure 4**, respectively [6].

Epoxy resins are utilized in a number of different formulations due to their high strength, excellent adhesion to various substrates, good solvent resistance, low shrinkage, low toxicity, good gap-filling capabilities, good elevated-temperature resistance, effective electrical insulation, and relatively low cost. Cured epoxy resins have tensile strengths of 90 to 120 MPa, tensile modules of 3100 to 3800 MPa, and T_g values of 120 to 220 °C [6].

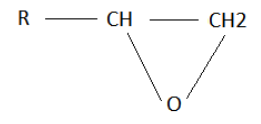


Figure 2. Chemical structure of an epoxy ring [7]

Figure 3. Ring opening reactions of DGEBA with benzyl alcohol [8]

Figure 3. Ring opening reactions of DGEBA with benzyl alcohol [8]

(a)

$$R = \begin{pmatrix} 1 & H_2 & H_3 & H_4 & H_4 & H_5 &$$

Figure 4. The curing of an epoxy resin through: (a) a primary amine; (b) a secondary amine; (c) a hydroxyl group generated from reactions (a) and (b) [9]

Epoxy resins are called high or low viscosity resins according to the form of the main structure. The low viscosity resins can wet and impregnate the fibers more easily forming the composite structure without additional assistance such as application of pressure. In high viscosity resins, wetting and impregnation are more difficult. These problems can be solved by the application of high temperatures and pressures, or through the use of various reactive diluents [2,3,5].

Epoxy resins are used as components in composite structures thanks to their adhesive properties, and as binders in metal, wood, and plastics in industries such as aerospace, dentistry, and automotive. They are used in electronics, printed circuits, owing to their thermal and electrical insulation properties and resistance to chemicals and corrosion, and can be used on floors and constructions thanks to their castability. As disadvantages, epoxy resins cannot show these properties in high temperatures and wet conditions and cause allergic reactions, and during exposure to UV rays, they can change color and deteriorate their structures [2,4,10]. However, the use of epoxy resins in carbon fiber reinforced composite materials is critical. Owing to their high adhesive properties, they keep the carbon fibers together and distribute the load on the structure homogeneously. Thanks to their resistance to chemicals and corrosion, they enable carbon/epoxy

composites to be used in many areas. With their low shrinkage coefficient, they ensure that the designed part shape is obtained without distortions.

Pressure is one of the most crucial factors in the manufacturing of carbon/epoxy composites. The pressure applied in composite materials ensures that the resin wets the fabric well, that is, increases the flow (transport), as well as enables the gas phase to be carried from one place to another with the resin, and with the help of the breather / bleeder used during production, it helps prevent the formation of voids. The pressure applied in composite materials creates the resin pressure, which changes as a function of applied pressure and depends on process materials that are used for curing, design, and reinforcement. For instance, one of the design factors affecting the resin pressure is the honeycomb and some types of foam cores used in sandwich composites. In co-cured skins, if a force is applied to the tool or bag side of the skin, resin pressure will be created, but in case the skin is thin, the resin cannot handle this pressure and flows into the cell to reduce its pressure. Therefore, this can cause quality issues with the honeycomb parts if the shells are thin, while if the skins are quite thick, it can cause resin pressure variations across the thickness. Therefore, the size of the applied pressure should be chosen considering the structural design and cure kinetics of the composite [2,3,11]. Additionally, some resin systems such as polyimides and phenolics produce some volatiles during the curing reactions. However, after the volatiles are formed, these volatiles can be removed from the system with the fluid resin with high pressure. The actual pressure on the resin, the hydrostatic pressure (the pressure for dissolving the volatiles in the resin), can be quite low since the fibers carry the load of this pressure. One of the problems encountered during the manufacturing of composite parts is that the applied pressure and the pressure transferred to the resin are not the same. This causes volatiles to come out of the solutions to form voids and to enlarge if pressure insufficiency occurs at high temperatures, that is, when the resin pressure falls below the volatile vapor pressure [3,11]. However, although they give addition reactions, volatiles are not formed as a by-product in epoxy resins. This takes epoxy resins one step ahead of other resins as they provide a significant convenience in preventing the formation of voids. However, epoxy resins are susceptible to moisture absorption due to their structure and generation of consequent water vapors during processing [12,13]. Water vapor, which is formed at high temperatures during manufacturing, causes the formation of voids. However, application of pressure prevents the composite materials from this.

1.3. Carbon fiber

Organic structures resulting from the carbonization of rayon, pitch and polyacrylonitrile (PAN) are mostly used in the production of carbon fiber. Processing techniques are difficult and complex, and produced fiber diameters generally range from 4 to 10 nm [3,14]. Carbon fibers are the most widely used performance materials with high mechanical properties, which are used along with polymer matrices. The most striking features of carbon fibers are their high specific strength and modulus, and the fact that they can maintain these properties at high temperatures. Additionally, their thermal and electrical conductivity are quite high. For instance, carbon fibers can have a tensile strength of 1000-7000 MPa depending on the source of manufacturing and processing method. They can have a tensile modulus parallel to the fiber long axis in the range of 200-750 GPa thanks to their highly anisotropic structure. Carbon fibers are classified as standard, medium, high, and ultra-high modulus carbon fibers according to their tensile modulus. Their densities vary between 1.75 and 1.90 g/cm³. At room temperature, they are not affected by humidity and are resistant to chemicals such as acids and bases. The feature that increases the performance is their molecular structure. Although they do not have a 100% crystalline structure, carbon fibers have excellent properties owing to their aligned crystal structures in fiber form, the strong interatomic and intermolecular forces, and the presence of few defects in their molecular structure that will reduce strength [3,14]. Carbon fibers can be found in continuous and discontinuous forms and both forms can be preferably used according to the part to be produced [14,15].

Carbon fibers can be utilized as woven fabrics in composite structures (**Figure 5**). The use of woven fabric form is quite common since woven fabrics can be laid more easily on the molds during production, the targeted product shape can be obtained without difficulty, and balanced mechanical properties can be obtained in every plane in the final product [16–18]. However, due to the yarn crimp in woven fabrics, properties such as high strength and rigidity of carbon fiber drop to lower levels. For example, the tensile strength of a unidirectional (UD) fabric is quite high compared to a twill fabric [16]. Woven fabrics can also show different strength and machinability properties according to the weaving method. For instance, twill and sateen fabrics offer better formable properties thanks to their less yarn crimp than plain weaves. However, their stability during laying may be lower due to yarn crimp also [5]. Furthermore, in a study, it was concluded that twill fabric gave higher strength than other types of weaving [17]. To add to all this, resin

can be impregnated to woven fabrics to obtain prepregs. Prepregs, which provide convenience in production steps such as laying and shaping, ensure correct application and minimize damage in this way, ensure that the mechanical properties of the fiber and resin of the produced part are observed at the maximum. Prepregs are also highly preferred in industries such as aviation and space [15].





Figure 5. Composite plate reinforced with 2x2 twill woven fabric (left) and UD fabric (right) with epoxy matrix

Composite structures can be obtained by combining carbon fibers with polymer matrices. The most known and applied polymer is epoxy resin. Epoxy resin is responsible for dispersing external forces as well as being an adhesive that holds the fibers together. However, due to the fact that it is a polymer, it causes the high mechanical properties of carbon fibers to decrease to a certain level. These composites are called carbon fiber reinforced polymer matrix composites (CFRP). In order for CFRPs to be successful, the direction and length of the carbon fiber, the fiber-to-resin volumetric ratio, the void content are very important. The curing of the resin that will provide them these properties must be maximized [14,19]. CFRPs can be obtained by many different methods such as hand lay-up, oven, autoclave, UV rays, vacuum bagging, pultrusion, Resin Transfer Molding (RTM), Vacuum Assisted Resin Transfer Molding (VARTM), automatic fiber laying machine (AFP) [14,19].

The most crucial point in all these productions is to determine the curing cycle, which will ensure 100% completion of the curing. Cure cycle is generally provided by the resin provider. Nevertheless, this may not always give 100% curing for different designs and sizes. Therefore, it is necessary to examine the curing behavior through parameters such as the characterization of the curing process from a viscous liquid to a rigid solid, control of exothermic energy, and the effect of pressure [19].

The use of CFRPs is increasing in engineering applications to produce large and complex parts where strength and flexibility are important at the same time. It is highly preferred in sports equipment such as fishing rods, surfboards, tennis rackets, bicycles, pressure vessels, construction reinforcement, marine industry, and automotive industry. On the other hand, the aerospace industry is more dominant as it can better cope with the cost of CFRPs. They are used in areas such as the engine cases of rockets, wings, fuselage, propellers, reinforcement and interior design elements in aircrafts, jet planes and helicopters [4,14,19–22].

1.4. Autoclave manufacturing of carbon/epoxy composites

Autoclave is a pressure vessel with an internal pressure of 20 bar and a temperature of up to 370 °C (**Figure 6**). Temperature distribution is applied with fans and heat exchangers in the autoclave. It can be used not only in the composite industry, but also in different areas depending on preference. It is a production technique where high pressure can be provided for composite materials, thus low void ratio and a homogeneous product are obtained. Besides, for thermoset resins, productions are made at temperatures up to 120-180 °C, and it is an indispensable production technique for industries such as the aerospace industry due to its production quality. Since high temperatures are reached with the autoclave, nitrogen gas is used as the atmosphere that will create pressure by removing oxygen from it. In this way, it is ensured that the materials do not undergo any thermal decomposition or burnout [3,11,15,22].



Figure 6. An autoclave for carbon/epoxy composite manufacturing

The composite material is autoclaved after certain processes. On the fabrics or prepregs laid in the desired direction, consumables such as peel ply, release film, and

bleeder/breather are placed on them. Then, air is vacuumed by laying the vacuum bag and closing the edges tightly. In production, where negative atmospheric pressure is applied, the layers of material are compressed along its thickness against the mold. Later, in the vacuum bag process, the part is autoclaved, and the curing cycle recipe determined according to the resin type is entered into the system. The viscosity of the resin decreases and wetting of the fibers become more homogeneous with the increase in temperature and pressure. All along the viscosity is low, the gases between and inside the layers are removed by vacuum through the breather/bleeder, which helps evacuate the gases together with the resin. In this way, the formation of voids is prevented, and with the increase in temperature and the passage of time, cross-links form in the epoxy resin and turn into a network structure. As the crosslinking increases, the viscosity of the resin increases, and gelation occurs. After the gel point, the effect of pressure decreases on the part and after a while, the curing process is completed. The part is cooled slowly to prevent shrinkage due to the resin characteristic and the autoclave is closed at around 50 °C and the part is left to cool to room temperature [3,11,15,22–24].

1.5. Cure cycle in autoclave manufacturing

Cure cycle stages are determined based on the type of epoxy matrix used. In general, there are two steps in the cure cycle, in which isothermal holding is performed. The first isothermal hold is applied to decrease the resin viscosity, help resin wet the fibers homogeneously, show the effect of pressure, evacuate the volatiles, and reduce the void ratios. At this stage, some exothermic reactions take place, which are helpful in avoiding the large exothermic heats in the second step. The second isothermal hold stage is carried out to allow the resin to cure 100% and to achieve a high adhesion with the fibers. The heating rates are crucial to achieve the first and second isothermal holding stages since sufficient time must be allowed for the reactions to occur and homogeneous heat distribution must be provided. Therefore, low heating rates should be preferred. Besides, due to the large volume of the autoclave, the heating rate of the autoclave will be the same as the heating rate written in the production recipe simultaneously, only at slow heating rates. The control of the cooling after the second isothermal holding stage is as important as the heating rates. In this way, distortion caused by the shrinking of epoxy resin is avoided during cooling [3,15,22,23].

1.6. Differential Scanning Calorimetry (DSC) for carbon/epoxy composites

Differential Scanning Calorimetry (DSC) is a thermo-analytical technique in which the difference in the amount of heat flux required to increase or decrease the temperature of a material is measured as a function of temperature or time. DSC examines the variation of the heat capacity (C_p) of a material with temperature. Thermal transitions of materials are studied by heating or cooling a sample of known weight and reference material and measuring changes in heat capacity. In other words, DSC is a technique in which a solid or liquid sample, which undergoes a physical change due to chemical reactions, is heated more or less in order to increase or decrease its temperature at the same rate as the reference, and the thermal behavior of the material is found by giving endothermic or exothermic thermal transitions [25–28].

Two basic approaches exist in DSC: dynamic and isothermal approaches. In dynamic DSC approach, a material can be heated and cooled at a constant rate. In the isothermal approach, the material is heated to the desired temperature quickly and kept at this temperature for long periods of time. DSC analysis is useful in determining the glass transition, crystallization, and melting temperatures of polymeric materials. In addition, many parameters such as initiation of curing, curing temperature, maximum curing speed, and degree of curing can be obtained in terms of cure kinetics [29,30].

HP-DSC can be used to better understand the dependence of curing behavior on pressure. This relation needs to be understood well because high pressures are often used during the manufacturing and processing of materials. HP-DSC devices can reach pressure values of 1 GPa [31].

1.6.1. High-Pressure Differential Scanning Calorimetry (HP-DSC 2+)

Cure kinetic studies can be carried out on Mettler Toledo brand High-Pressure Differential Scanning Calorimetry (HP-DSC 2+), which is shown in **Figure 7**. Dynamic and isothermal tests on the device and Model Free Kinetics (MFK) analyses can be performed using STAR^e Software. The module of the device is a differential scanning calorimeter that can reach high pressures, which includes a measuring cell and a stainless-steel pressure cylinder. With this device, the temperature can be adjusted from room temperature up to 700 ° C and the highest working pressure of 10 MPa. The furnace and the HP-DSC sensor, which enables to reach these values, constitute the main components of the measuring cell. The furnace surrounds the sensor and reference crucible for

measuring. The furnace body, the heating plate, the furnace cover, and the thermal resistance are the components of the furnace, and the furnace power is 400 Watt. The thermal conductivity of the furnace, which is made of pure silver and provides good heat conduction between them by pressing the furnace parts together with the spring furnace assembly, is very high [32].



Figure 7. High Pressure Differential Calorimetry (HP-DSC) for cure kinetic studies In the device, temperature-controlled heating and cooling are precisely monitored by the cell temperature, which is measured by the temperature sensor in the furnace body. The HP-DSC sensor is attached to a ceramic disc that fits into the furnace body, which ensures good and homogeneous heat conduction, and is based on the proven Boersma or heat flux principle by generating the accurate measurement signal. Differential heat flow between the sample and the reference is measured directly from the sample and reference crucible positions with star-shaped thermocouples. Beside this, the furnace is insulated with glass wool and in this way there is no temperature gradients and reproducible baselines are obtained even under high pressure conditions [32].

The HSS 9+ (High-sensitivity sensor) ceramic sensor used for the HP-DSC module is a type of sensor that gives very accurate and sensitive results (**Figure 8**). The temperature measurement range of the HSS 9+ ceramic sensor is -150 °C to 700 °C and has \pm 0.2 K temperature accuracy, \pm 0.02 K temperature precision and \pm 0.1 K temperature repeatability. The resolution value is 0.01 μ W. The thermocouple number is 120 (AuAuPd) and it is arranged in three layers. Its star-shaped structure and double-multiple T_0 measurement allow the net heat flow between the sample and the reference to be measured separately. These sensors are very good at measuring small sample weights,

low heating rates, very small ΔC_p values, low energy transitions such as solid to solid and dilute solutions such as used in biology [32].

The gas supplied to the device to provide pressure can be in different types such as dry air and N_2 , and it enters the gas inlet in the device, passes through the furnace body and flows to the sample in a manner that has gained cell temperature. The rupture disc and sealing system in the device ensure that the pressure values remain at the set level [32].



Figure 8. FRS 6+ and HSS 9+ HP-DSC sensors

1.6.2. Model-Free Kinetic analysis for carbon/epoxy composites

Molecular mobilities formed during the polymerization reactions of the epoxy resin give the reaction kinetics of this system. The proportions and rates of chemical processes can be determined by reaction kinetics. Reaction kinetics can be explained as the time-dependent rates of chemical reactions. Chemical reactions take place by collisions of molecules with a minimum level of kinetic energy. This energy, which changes according to each reaction, is the activation energy (E_a). Therefore, the reaction rate depends on E_a . If E_a is high, the intermolecular collision is fewer, and the reaction rate is low. However, some factors affect the E_a . The higher the concentration of the reactants, the more collisions will result, which increases the reaction rate. In addition, if reactant molecules exist in two separate phases, then the reaction rate will be related to the surface area, and the reaction rate will increase with increasing surface area. An important parameter in the reaction rate is temperature. Since the temperature will increase the kinetic energy, the collisions increase and therefore the reaction rate increases. However, with the help of a catalyst, alternative reaction routes can be created, and the reaction rate can be increased.

The reason for making kinetic calculations is to accurately predict the reaction transformation (α) at a desired isothermal temperature or heating rate. The rate of a reaction depends on the temperature or the rate of unreacted substance (or conversion). These molecules, which gain energy with heat in the HP-DSC device, gain activation

energy (E_a) and react. By increasing the temperature, molecules with higher E_a react more and the reaction rate increases. This situation is generally described by the Arrhenius equation [33,34].

$$\frac{d\alpha}{dt} = Aexp\left(\frac{-E_a}{RT}\right)f(\alpha) \tag{1}$$

 α : Degree of conversion, changing from 0 to 1

Pre-exponential A: Collision frequency (1/s)

 $\boldsymbol{E_a}$: Activation energy (kJ/mol)

 $f(\alpha)$: Reaction type (nth order, autocatalysis, nucleation, ...)

 n^{th} order kinetic estimates can be made for a simple model with this main equation. In this analysis method, E_a is considered constant and the rate decreases towards zero during the reaction. In this analysis, estimates of time-dependent conversion or iso-conversion can be made using a single heating rate [35].

Based on this basic equation, two different approaches as Model-free and Model-based have been put forward. In the model-free approach, the reactions are A (reactant) \rightarrow B (product) reactions that do not contain intermediate steps, and the approach analyzes based on this. Since the intermediate steps of the reaction are not taken into account, only one E_a can be analyzed with this approach. The Arrhenius equation, which can be established on systems with the same total area under the peak or the total weights and having reaction steps in only one direction (endo or exo), is as follows in this approach [35,36].

$$\frac{d\alpha}{dt} = A(\alpha) \exp\left(\frac{-E_a(\alpha)}{RT}\right) f(\alpha) \tag{2}$$

 $E_a(\alpha)$ and $A(\alpha)$ are unknown and $A(\alpha)$ can only be found by estimating, $f(\alpha)$. $E_a(\alpha)$ and $A(\alpha)$ depend on the value of α . In this case, Model-free kinetic analysis can be defined from two estimations. One is that only one kinetic equation can be obtained for α , and the other is that the reaction rate at a constant conversion value is only a function of temperature.

In this analysis method, when the maximum points of the peak are taken from the curves of at least 3 different heating rates and the points on the graph drawn with the Arrhenius equation are combined $E_a(\alpha)$ are found with the slope of the line. However, systems with more than one E_a can be analyzed with the multi-points model free method [35,36].

In addition to MFK analysis, advanced model-free kinetics analysis (AMFK) can also be performed. Estimations can be made with the advanced mathematical procedure over isothermal and combined curves, as well as estimations made on dynamic curves [35]. However, chemical reactions are processes that are too complex to be just one step, and intermediate steps are an important parameter that changes the reaction kinetics because of causing different E_a to occur. Based on this situation, a Model-based analysis approach has been developed and can be used according to preference [36].

Curing conversions in simple and complex reactions can be estimated without the need for reaction modeling thanks to model-free kinetic analysis. Conversion, iso-conversion, and activation energy plots can be obtained from this analysis. STAR^e Software calculates these transformations with the Vyazovkin method. According to the Vyazovkin method, E_a is constant only for a certain transformation, unlike the nth order kinetic estimation. Besides, the Arrhenius equation remains valid on account of the rate coefficient is related to temperature [35,36].

$$\frac{da}{dt} = k_0 \cdot e^{\frac{E(\alpha)}{R.T}} \cdot f(\alpha) \tag{3}$$

 $\frac{da}{dt}$: Reaction rate

 k_0 : Rate constant at infinite temperature

 $f(\alpha)$: Reaction model

 E_a : Activation energy as a function of the conversion α

R: Universal gas constant

$$\beta. g(\alpha) = k_0 \int e^{\frac{-E(\alpha)}{R.T}} dT$$
 (4)

where: $g(\alpha) = \int \frac{1}{f(\alpha)} d\alpha$

with $\frac{2R.T}{E(\alpha)} \ll 1$ we get:

$$\beta. g(\alpha) = k_0. \frac{RT^2}{E(\alpha)} e^{\frac{-E(\alpha)}{R.T}}$$
(5)

Separating the variables in the velocity equation and integrating them with respect to t also gives $g(\alpha)$. In another way, $g(\alpha)$ can be expressed as.

$$\frac{d\alpha}{dt} = k(T)f(\alpha) \tag{6}$$

$$g(\alpha) = \int_{0}^{\alpha} \frac{1}{f(\alpha')} d\alpha' = \int_{t_{0}}^{t_{\alpha}} k dt$$
 (7)

with the addition of $\beta = \frac{dT}{dt}$ and the Arrhenius equation:

$$g(\alpha) = \frac{k_0}{\beta} \int_{0}^{T_{\alpha}} exp\left(-\frac{E(\alpha)}{RT}\right) dT$$
 (8)

$$\int_{0}^{T_{\alpha}} exp\left(-\frac{E(\alpha)}{RT}\right) dT : I(E_{\alpha}, T_{\alpha, \beta})$$
(9)

 $g(\alpha)$ is assumed to be independent of β . From the curves obtained as a result of different heating rates, β_1 solves the following equation (Vyazovkin):

$$g(\alpha) = \frac{k_0}{\beta_1} I(E_{\alpha}, T_{\alpha, \beta_1}) = \frac{k_0}{\beta_2} I(E_{\alpha}, T_{\alpha, \beta_2}) = \dots = \frac{k_0}{\beta_n} I(E_{\alpha}, T_{\alpha, \beta_n})$$
(10)

Last of all, the application of the MFK analysis is as follows. Dynamic tests are performed at least at 3 different heating rates. As shown in **Figure 9**, conversion curves are found through the software taking the integral of the areas under the dynamic curves. MFK analysis is applied to conversion curves via STAR^e Software and activation energy (E_a) curve is obtained. Using E_a curve, the conversion or iso-conversion plot curve is drawn with the MFK analysis. With the conversion curve, isothermal test estimations are made, and the time required for the desired conversion at the desired temperature is found [37,38].

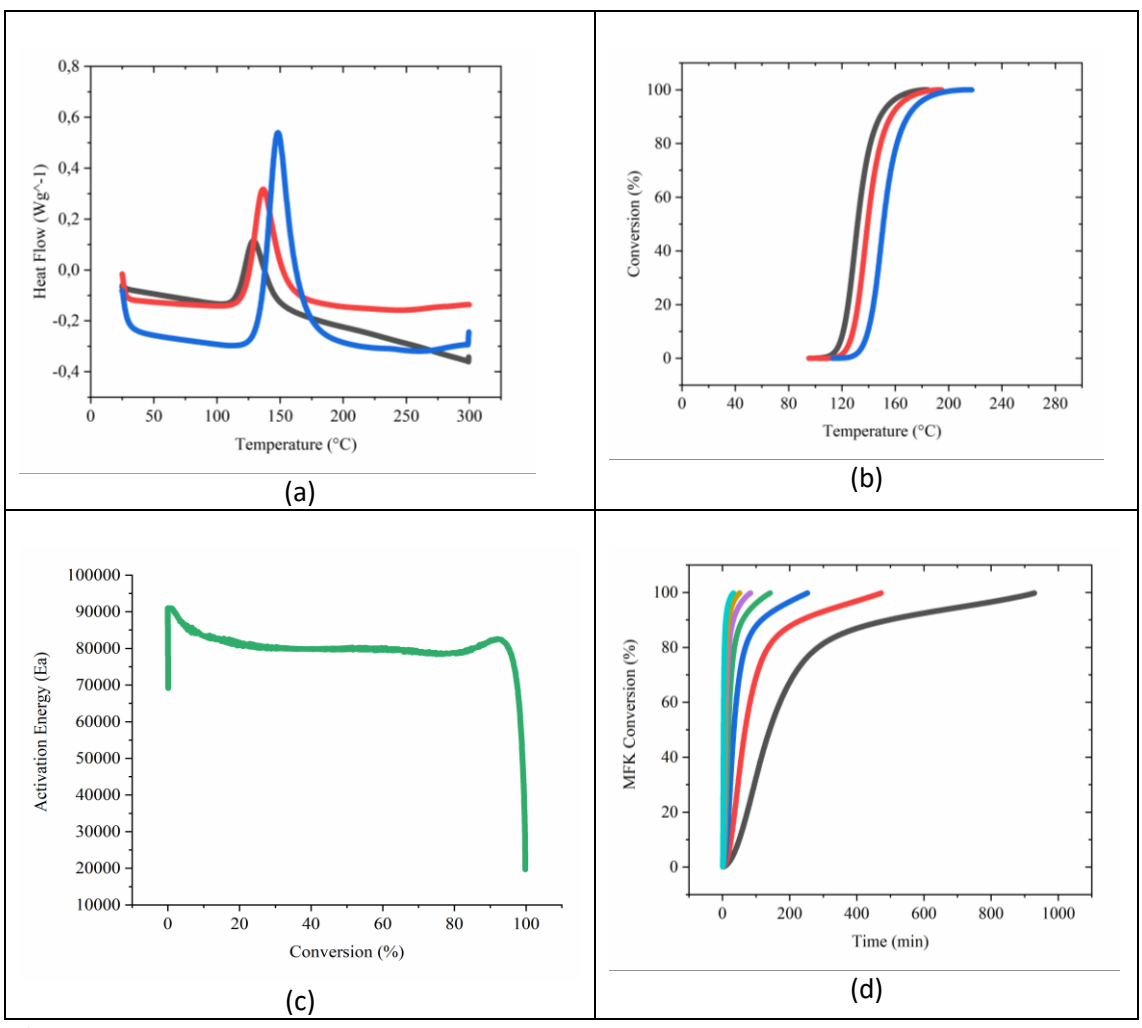


Figure 9. MFK analysis steps: Dynamic curves (a), conversion curves (b), activation energy curve (c), conversion estimation curves for isothermal tests (d)

1.7. Rheometer for carbon/epoxy composites

In an ideal viscous fluid, the deformation energy occurs in the form of heat, while the applied forces are not recovered when released (Newton's Law), whereas in an ideal elastic solid, the solid returns to its original state (Hooke's Law) when the applied forces are removed. Nevertheless, polymers with entangled chains of varying lengths behave like a viscoelastic material when softened or melted. That is, they behave somewhere between the viscous behavior of the liquid and the elastic behavior of the solid when force is applied [39].

Rheology is concerned with the deformation and flow of materials under the influence of stresses caused by the application of these forces to a material by continuously increasing and decreasing in a certain frequency range. Application in rheology tests can be done in two ways. In the first, torque (stress) command is given, and angular displacement (strain) result is obtained. In the second, the angular displacement (strain) command is given, and

the torque (stress) is measured. Rheometer measures the rheological behavior of materials by calculating the phase difference between shear strain (γ) and shear stress (τ). In a material with ideal elastic behavior, stress and strain are directly proportional and are in the same phase at 0°, while a material with ideal viscous behavior is in different phases with a 90° difference between the phases. These two phases are seen in polymers, which are viscoelastic materials. The molecular weight of the polymer, the entangled chains, the size of the branches in these chains and the bonds between the chains affect the viscosity in polymers. Therefore, as the molecular weight of the polymer increases, the viscosity increases [39,40].

The rheometer measures the elastic stress to strain ratio, that is, the storage modulus (E'), which gives the material's capacity to store energy elastically, and the loss modulus (E"), which is the energy dissipation measure of the material, which is the ratio of viscous stress to strain (**Figure 10**). The complex modulus (E*) is the material's resistance to deformation and can be found briefly at the cross section of points of the storage and loss modulus [40].



Figure 10. Rheometer for cure kinetic studies

The mobility of molecules can be measured as a function of temperature or time by rheological measurements. In thermoset polymers, these changes in molecular mobility are responsible for the viscosity differences due to crosslinking. In this type of polymer, with the increase in temperature, the van der Waals forces are ended, and the viscosity decreases up to a certain point. After this point, polymerization reactions take place and

the molecular chains begin to grow and expand, and cross-links are formed. As this situation restricts mobility, the complex viscosity increases [39,41,42]. At these stages, voids may occur in the structure due to volatile release from organics or water [41].

Anton-Paar Modular Compact Rheometer is one of the devices where rheology tests can be performed. This rheometer device contains a highly sensitive EC motor made of airbearing with fine-pored carbon to minimize friction. Rheometer can apply normal force up to -70 N to 70 N and torque up to 0.5 nNm to 230 mNm. TruStrain™, TruRate™ and TruGap™ sample-adaptive controllers are available in the device. In this way, it provides instantaneous feedback during the measurement and adapts itself. For instance, TruGap™ measures the gap and returns itself to the position set at the beginning of the test by controlling the expansion in the sample caused by the temperature generated in the sample. The tool that will apply the force is easily mounted on the system and the system automatically recognizes the mounted tool and transfers the necessary parameters to the software [43]. By applying the deformation mode to the material with the rheometer, the force produced can be measured and the stress and strain values are calculated, or the deformation in the material can be measured by applying the force mode [39].

1.8. Dynamic Mechanical Analysis of carbon/epoxy composites

In thermosetting resins, Dynamic Mechanical Analysis (DMA) is generally used to study the T_g behavior and to determine transitions corresponding to other molecular motions (**Figure 11**). The elasticity or shear modulus found is qualitative and does not reflect the actual results due to the anisotropy of the analyzed sample and the analysis characteristics of the DMA equipment [41]. T_g behavior in DMA is measured as follows. In the softening behavior of cured composite materials, the storage modulus is considerably reduced and there is a rapid increase in the loss modulus, and this phase shift can be examined over $\tan \delta$ and the T_g value can be determined with high precision [44].

T_g behavior is also examined by DSC. However, DMA is believed to give more accurate results. This is due to the fact that stiffness and damping properties occur more dramatically than heat capacity or thermal expansion and are more easily determined. Additionally, DMA measures macroscopic gelation instead of molecular gelation, and small samples of DSC heat up faster, thus more accurate results can be obtained by DMA [44,45].



Figure 11. Dynamic Mechanical Analysis (DMA) for T_g measurements

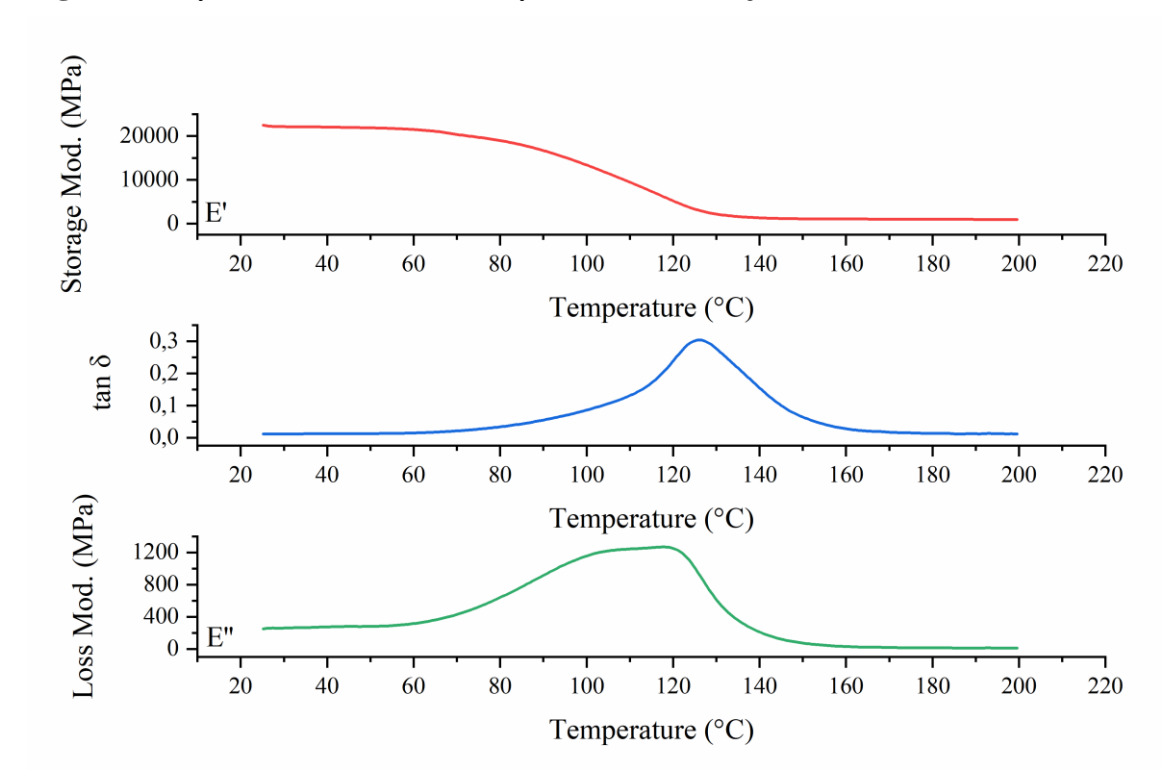


Figure 12. An example of a Dynamic Mechanical Analysis curve

The Mettler Toledo SDTA861^e Dynamic Mechanical Analysis (DMA) instrument is a device in which a sinusoidal acting force is applied to the materials at a certain frequency and measures the dynamic mechanical behavior of the material, that is, the deformation, as a function of temperature. DMA curves can be seen in **Figure 12**. DMA can be applied to thermoset, thermoplastic and elastomeric polymers, ceramics, and metal materials. Bending, shear, tensile and compression tests can be performed according to the module installed with DMA. The raw data obtained from these measurements are used to

calculate desired material properties such as the force and displacement amplitudes, F_a and L_a , and the phase shift (δ) of these data. These properties are complex modulus (M^*): modulus of elasticity, Young's modulus (E) or shear modulus, G^* : proportional to the elastically and reversibly stored energy storage modulus, M': loss modulus proportional to the energy converted into heat and M'': irreversibly lost, and $\tan \delta$: the loss factor (the ratio M'' to M'). To determine the T_g temperature of the materials, in general, the temperature $\tan \delta = G'' / G'$ is taken. If a dynamic force is applied to the material, elastic materials respond immediately to the force and do not experience any phase shift, while fully viscous materials respond to the displacement in a late time, which causes a phase shift and for viscous materials, this shift is 90° at $\tan \delta$. For viscoelastic materials, this shift is from 0 to infinity ($\delta=90^\circ$). The displacement measurement is made in a very wide range with nanometer resolution with the LVDT (linear variable differential transformer) sensor, which only measures the deformation of the sample [46].

1.9. Composite density and constituent content for carbon/epoxy composites

Different methods can be used to determine the density of composite materials reinforced with polymer matrix fibers. Liquid and gas pycnometer are among them. Liquid pycnometer allows the determination of the density of the composite by measuring the density difference of the sample in air and water, based on the Archimedes principle. It is accepted that the sample placed in the liquid pycnometer causes the displacement of the sample, as well as the volume of the sample, and the density of the composite is found by dividing the weight of the sample in air by its volume. ASTM D792 standard is one of the standards used for this measurement. It is important to make sure that the edges and surfaces of the sample are smooth while making the measurements so that false measurements due to the tendency to catch air bubbles are prevented. However, immersed fibers may not be completely wetted in most cases. Therefore, since the wet weight will be low, the fiber density will be low, which may result in high fiber volume ratio and low epoxy volume ratio due to low fiber density. Helium (gas) pycnometer can avoid this problem [44,47].

Knowing the fiber-resin ratio in the composite material is a kind of production quality control method and is frequently used. In this method, according to the matrix type, the matrix is dissolved in a solvent (hot nitric acid for epoxies), the fiber-resin weight ratios are calculated over the previously known epoxy and carbon fiber density, then this can

be converted to the volumetric ratio and the void ratio can be found since all values are known. These test conditions are applied using the ASTM D3171 standard. However, negative values can be seen from time to time in the void ratio. This is due to the abovementioned problems with measuring fiber density, and even a small measurement error causes significant differences for void ratio calculation [44,47].

1.10. Interlaminar shear stress for carbon/epoxy composites

In composite materials reinforced with polymer matrix fibers, the ability to carry transverse forces, that is, the shear strength between layers, is measured through a test called the short beam test, which can be carried out within the framework of the most common standard, ASTM D2344. A displacement occurs along the interface plane between two layers by the applied shear forces in composite materials with this test [3]. In composite laminates, the load transfer between these layers at the interface is very important and high strength can be achieved only with the strong adhesion between the carbon fiber and the matrix. If the bond between the fiber and the matrix is strong, failure can be prevented as the matrix will spread the incoming force between the fibers. Therefore, a correctly applied cure cycle of the matrix is very important to increase adhesion and prevent the number of voids, and carbon fiber fabrics must be laid very carefully and protected from wrinkles during the laying process. Otherwise, premature delamination errors will occur due to stresses caused by material mismatch with the incoming load [3,48–50].



Figure 13. ILSS test samples

In the test applied according to the ASTM D2344 standard used in the Instron - 100 kN Universal Electromechanical Test Machine, the ratio of the support span length to the sample thickness should be 4 and this test should be carried out over the 3-point loading fixture and continued until shear and distortion occur in the central plane. In this way, pure interlaminar shear failure will be achieved. For instance, if the test is performed with a thin plate without complying with this ratio, the damage that will occur during the compression force is applied may occur around the support spans and this will affect the

test result in the wrong direction [51–53]. To summarize, the fixture on which this test is applied is very important. The spacing of the spans on the fixture should be adjusted very carefully and in the center to comply with the standards and should not be accommodated in order to prevent any damage, indentation, and deformation on their surfaces [49,51,52].

1.11. Tensile test for carbon/epoxy composites

Tensile test is a test method in which composite materials are exposed to tensile forces in one axis. The tensile test results are used as data in the parts to be designed, and at the same time as a quality control. As a result of this test, parameters such as yield stress, ultimate tensile stress, Young, Chord modulus, Poisson ratio and maximum elongation values can be obtained. One of the most important properties of composite materials is the excellent performance of the fibers in the tensile direction. This test can be performed on the Instron - 100 kN Universal Electromechanical Test Machine using the ASTM D3039 standard. A minimum of 6 specimens cut from a composite laminate in the form of dog bones are attached to the lower and upper jaws in the Instron device after the tab process, and the tensile is started at a certain speed, with the lower jaw stable and the upper jaw moving. During the tensile test, elongations and forces are measured in the axial direction very precisely, from strain gauges on the sample or from the outside with attachments such as video extensometer. The data is reflected to the computer through the software and calculated as the tensile stress and elastic modulus [17,20].

Since various damage mechanisms occur, the composite structure causes catastrophic irreversible damage after a certain strength. One of these damage mechanisms is propagation through fibers. It is known that the fibers have very high tensile strength, but they are also quite rigid and can break easily. The matrix is a more ductile material. During the test, when the force comes on, the fibers will cause high shear stresses in the matrix-fiber surface area as they are the side close to rupture due to their rigidity, these stresses will be transferred to other regions and these shear stresses may cause a crack to propagate, which may spread to other regions and cause damage [3]. However, damages such as fiber breakage or pull-out may occur due to damages caused by the gaps remaining in the composite structure or the fiber-matrix interface is not strong, that is, the adhesion is not good [3,4].

CHAPTER 2

2. Cure kinetic studies and determination of cure cycles for R1 and TW-R1

2.1. Introduction

Chapter 2 presents the findings of the HP-DSC and rheology test results of R1 and TW-R1, focusing on enthalpy and cure degree (conversion). Besides, cure cycle is determined, and carbon/epoxy composite laminate's characterization and mechanical tests are performed.

2.1.1. Cure mechanism of epoxy-amine reactions

Epoxy-amine curing reaction involves different steps depending on the type of amine used as curing agent. During the epoxy-amine curing reaction, primary amine reacts with one of the epoxide group, leading to the generation of secondary amines that can react with another epoxide group. The hydroxyl groups generated upon reaction of epoxide group with primary and secondary amine groups are involved in the formation of ether linkages. This etherification reaction competes with the epoxy-amine curing reaction. Etherification reaction might take place after depletion of amine hydrogens if epoxide groups are in excess [19]. The utilization of multifunctional epoxides and amines result in crosslink points. The curing reaction proceeds with the addition polymerization reactions. This reaction is diffusion controlled at lower temperatures [54,55]. As the temperature increases, the kinetic energies of molecules and molecular chains increase, and the reactions are accelerated. The reaction rate continues to increase rapidly with autocatalytic acceleration. The diffusion effect is lost because the increasing energies of the molecules easily allow for high molecular mobility. As the molecular mobility and crosslink density increase, the epoxy resin reaches the gel point, in this case the viscosity starts to increase and the molecular chains that do not have enough space for movement can usually only continue their local movements. If it is desired to go beyond their local mobility, greater energies should be given. Therefore, after this stage, the rate of motion becomes very low and the mechanism turns back to diffusion [41,54–58].

Molecular mobility, which increases with rising temperature, determines the rate of the reaction. Therefore, as the temperature rises, the reaction rate increases and the reactions are completed in a short time [54,58].

2.1.2. Void formation and pressure effect in cure kinetics

The void formation in composites occurs as follows. Air bubbles can be mechanically entrapped inside the fabric itself or generated during resin mixing process and as a result of the release of volatiles as by-products of the reactions (apart from epoxy resin) with the increase of temperature. Additionally, voids in the prepreg can be formed as a result of the evaporation of water present in the micro-voids of the prepreg and attached to the polar groups in the cross-linked network of the resin or the evaporation of free water with the increase in temperature. As soon as high temperatures are reached in prepregs that contain moisture, the high internal void pressure caused by the water vapor pressure is the source of the gaps to grow [59]. The moisture absorbed in the prepreg, which occupies an important place in the resin due to its high molar percentage, does not only cause the formation of voids, the moisture absorbing fiber does not expand, but the polymer matrix expands and creates an internal stress caused by dimensional changes [42,44,59,60].

The voids formed in composites give rise to many problems that will directly reduce the mechanical properties of the composite material. They cause a significant decrease in tensile, compression, bending and interlayer shear strengths. For this reason, the acceptable void content in composites is 1% in the aviation industry, and around 3-5% in industries with less critical standards. However, it should be known that the amount of void around 1-3% can reduce the mechanical properties of the composite up to 20% [44,59].

In order to prevent the formation of voids or to maintain the stability of the void, the manufactured parts are exposed to vacuum and pressure. The reverse pressure applied by vacuuming before the composite part is placed in the autoclave is carried by the component that is fluid (resin) in the prepreg. Excess resin also bleeds with pressure and the thickness of the composite decreases in this way, and the resin bleed stops after a certain point and the pressure begins to be carried by the fibers. Air bubbles trapped in the resin or fabric geometry also diffuse into the resin with vacuum and exit the system as the resin bleeds. If the air bubbles are far from the vacuum applied area, for instance, if they are close to the mold, the size of the ellipsoid shaped air bubbles decreases with the pressure in accordance with the ideal gas law principle. In this way, the void rate decreases. However, with this method, the void rate can only be reduced up to 10%. For this reason, the autoclave pressure must be activated, and the cavity volumes are reduced considerably with this pressure. With the pressure applied to the part, the gaps caused by

water vapor are eliminated as follows. After being placed in the autoclave, the water vapor formed with high temperature spreads to the resin whose viscosity has not yet increased with pressure faster than the spaces in the prepreg. The trapped water vapor does not dissolve in the resin, it is compressed and reduced in the system, or the system can be taken out with the flowing resin. Moisture prevents the completion of Van Der Waals bonds between polymer chains and causes resin plasticization. Moisture in micro voids or voids in free volume also damages the bond at the fiber and matrix interface and therefore causes a decrease in tensile strength. In addition, the high void ratio means that the resin is not fully impregnated into the fibers and these voids will cause cracks and interfaces where they will cause their progress. However, fibers that remain resin-free wear, break, and become damaged [44,59,61,62].

Considering all this, the application of high pressure in composite parts lowers the void ratio in the part to very low levels, provides bonding between layers, increases the fluidity of resins with high viscosity and helps some reactions take place in this way [23,63].

The amount of the pressure applied is also important. Different studies have been conducted on this. If the amount of pressure is insufficient, assuming that the internal and external pressures are equal in the low viscosity resin, it causes the internal pressure to equalize by expanding the volume. Nevertheless, it has previously been observed that as the pressure increased from 0.1 MPa to 0.7 MPa, a significant decrease in the void ratio was found, but no significant differences between 0.7 MPa and 1 MPa were reported by Olivier et al. [61]. Boey et al. also conducted similar studies for higher pressures and examined the effects of pressure between 100 MPa and 7000 MPa, and in this case, the gap reduction increased with pressure up to 400 MPa, although after this pressure amount the rate of void reduction was decreased [64]. However, existing research recognizes the critical role played by different type of resin system. It was observed that the effect of pressure can vary from system to system. A pressure of 0.69 MPa reduces the void ratio more in one resin system, while with the same amount of pressure the decrease is less in the other resin systems [44]. Moreover, it has been noticed that after a certain critical value at low pressures such as 3 and 7 bar, the gap reduction ratio does not have to increase in direct proportion to the rise in pressure. Sometimes, in cases where the pressure increases, no significant change can be seen [44,59,61,64].

2.1.3. T_g behavior and effect of pressure on T_g

 T_g is a property that is directly related to the matrix structure in composite materials. T_g value of a composite material changes as a function of the curing degree, chain structure of the resin, and crosslink density. T_g is a very crucial parameter. The composite structure exhibits a viscoelastic behavior at temperatures above T_g , decreasing its mechanical properties, and at temperatures below T_g , it behaves like a glass phase and exhibits its mechanical properties at the highest level. Therefore, a high T_g value is important as it will increase the working range of the composite structure. In the literature, it is recommended to set a temperature tolerance of 28 °C as a safety parameter while choosing the carbon/prepreg composite material in accordance with the temperature it will be exposed to in the area where it will be used [3,64].

Researchers have examined the factors affecting T_g and found that the impurities present in the resin used may cause a decrease in Tg temperatures up to 40 °C [18]. Humidity in the composite structure has also caused a decrease in Tg [13]. However, the failure of the resin reactions to occur homogeneously causes scattering in T_g values [11,18]. More importantly, the T_g behavior is determined by the cure kinetics applied to the material. The heating rate, the degree of cure, and holding time at a certain temperature affects the T_g behavior [11,18]. If these conditions are adjusted to give 100% curing, the pressure under which the reactions are carried out becomes important. Several theories on the behavior of T_g have been proposed. Brandrup and Immergut concluded that pressure up to 4 MPa applied during the cure cycle does not have a significant effect on Tg [10]. WenjunLi observed T_g variation in two different resin systems in his study when he performed the tests with a DSC. WenjunLi, in two studies, reduced the pressure from 0.69 MPa to 0.31 MPa in the first resin system and observed a 1.6% increase in the T_g temperature. However, when he reduced the pressure value from 0.31 MPa to 0.1 MPa in the same resin system, no change was visible in T_g behavior. Even though, the pressure was lowered in the second resin system from 0.69 MPa to 0.31 MPa, it was found that the T_g temperature increased by 0.5%. Then, when the pressure was lowered from 0.69 MPa to 0.31 MPa in the second resin system, it was seen that the T_g temperature increased by 1.9%. The conclusion of this study is that it is possible to observe different behaviors with the application of varying pressures in different resins. However, while performing these tests on a DMA device, differences were found to be insignificant [44]. Furthermore, another study was conducted by Olivier et al. With the increase of pressure from 0.1 MPa

to 0.69 MPa, the cure degree increased from 97% to 98% and the T_g value increased 5 °C [12]. In addition to all these, Nakamae et al. experienced a decrease of 20-30 °C in T_g when the pressure value increased to as high as 1000 MPa. The reason for this decrease is that pressure significantly restricts molecular diffusion and mobility, slowing or preventing the rate at which reactions take place [63]. The pressure effect varies considerably according to the resin system. However, unless very high pressures are used, no difficulties to prevent 100% curing will be met, but the crosslink density will change [65].

2.1.4. Effect of pressure on mechanical properties

The void ratio reduction with pressure significantly affects the mechanical properties. Many diverse studies have been done on this subject and the results are as follows. Olivier et al. showed the change of longitudinal tensile strength in carbon/epoxy laminates made of unidirectional fabric. In their study, as the void ratio increased from 0.3% to 10.3%, the longitudinal tensile strength decreased by 12%, but the tensile modulus did not change. Transverse tensile strength was more sensitive to the void ratio and decreased by 30%. The transverse tensile module has also changed significantly in this case. However, the interlaminar shear strength (ILSS) decreased by 15% when the void ratio increased from 0.3% to 6.8%. However, these results refer to a specific region in the produced plate. Since the void distribution and the dimensions of the void in the plate are not homogeneous, different results can be obtained in diverse regions of the plate [61].

WenjunLi tested the effect of increasing the number of voids on mechanical properties for two different resin systems. An 8% reduction in tensile modulus was observed when the pressure was reduced from 0.69 MPa to 0.31 MPa for the first resin system. In the second resin system, the tensile modulus dropped by 1.8%. The tensile modulus of the first resin system decreased by 1.3% when WenjunLi reduced the pressure from 0.31 MPa to 0.1 MPa. In the second resin system, the tensile modulus decreased by 10.8% [44].

In the study conducted by Hoda Koushyar et al. the amount of pressure was reduced from 552 kPa to 276 kPa. However, the decrease in pressure did not cause an increase in the void content so as to affect the mechanical properties [66]. However, in the study of Vasileios Drakonakis et al., an increase in flexural modulus from 448 MPa to 522 MPa was observed when pressure was increased from 0 psi to 30 psi. Also, the pressure increases from 30 psi to 50 psi increased the flexural modulus to 547 psi, and the pressure

increase from 50 psi to 70 psi increased the flexural modulus to 613 MPa. Moreover, it can be seen that the rate of increase in flexural modulus slowed down even though the pressure increased after the initial situation where the pressure increased to 30 psi [22].

These results show that the amount of applied pressure affects the mechanical properties in different ways. The increase in pressure does not always cause significant increases in mechanical properties. However, pressure affects the diverse mechanical properties such as tensile and compressive differently. Pressure effect varies depending on the type of resin. In one resin system, high pressure can provide high mechanical properties, while in another resin system, low pressure can provide high mechanical properties. It can be concluded that there is a pressure range that works best for each resin and the effect of pressure should be examined when determining the cure cycle.

2.2. Experimental – HP-DSC

2.2.1. Dynamic test methods and sample preparation for HP-DSC tests

Sample preparation for HP-DSC tests was carried out as follows. Resin samples stored at -18 °C were let to reach room temperature and 7 to 10 mg of samples were placed in aluminum pans in the sample chamber next to the empty aluminum pan used as reference sample in the device. The device was tightly closed, and the testing continued under atmospheric conditions. If the test was carried out under pressure, the device was pressurized with N₂ gas from outside and the pressure value was controlled digitally and analogously. Tests were conducted under two conditions: dynamic and isothermal. Tests were carried out once. However, residual cure scans were carried out on several samples from each set in order to find the enthalpy value in the system, and tests were repeated if necessary. The most appropriate results were included in the shared tables. The thermal transitions of the test were monitored through STAR^e Software.

TW-R1 prepregs with 42% resin content in the same ambient conditions as the resin were prepared in the range of 17 to 24 mg by weight.

The temperature was increased from 25 °C to 300 °C with heating rates of 3, 5 and 10 °C/min under 1 (atmospheric pressure), 3, 5.6 and 7 bar pressures in the dynamic HP-DSC tests. Additionally, some tests were carried out as 3 cycles to examine the presence of residual cure. For this, after the first heating the temperature was cooled to 25 °C from

300 °C with 10 °C/min and again temperature was raised from 25 °C to 300 °C with a heating rate of 10 °C/min. EN6041 standard was used for the dynamic HP-DSC tests.

2.2.2. HP-DSC dynamic test results – R1

Cure kinetics behavior of the resin (R1) was examined in this section through dynamic DSC tests. Curing and conversion curves obtained in dynamic tests are shown in **Figure 14**. Enthalpy and conversion values are provided in **Table 1** and **Table 2**. The normalized enthalpy values were taken into consideration while interpreting the test results. The enthalpy values were compared among each other and the cure degrees corresponding to the temperatures were found.

Firstly, when the graphs in the left column of **Figure 14** were examined, it was observed that while the curing reactions took place in the resin, it created an upward exothermic peak. When the graphs in the right column of **Figure 14** were examined, the following information was obtained regarding the rate of curing reactions (it can be called also conversion or cure degree). The molecules in the epoxy resin first started to give reactions by diffusion after gaining a certain amount of heat energy with the increase in temperature. Therefore, the reaction rate in the beginning was slow. Then, with the increasing temperature, the kinetic energy of the molecules increased, and an autocatalytic mechanism was activated. The crosslink density increased rapidly with this mechanism. The reaction rate slowed down with the increase in cross-linking degree due to the decrease in the number of molecules that would react, the decrease in the mobility of the long molecular chains and the restrictions on each other's movements. Reactions whose rate slowed down started to react by diffusion again and curing reactions were completed after a certain time. This curing mechanism was observed in **Section 2.2.3-2.2.8-2.2.9-3.2.2-3.2.3-3.2.6-3.2.7** in the same way.

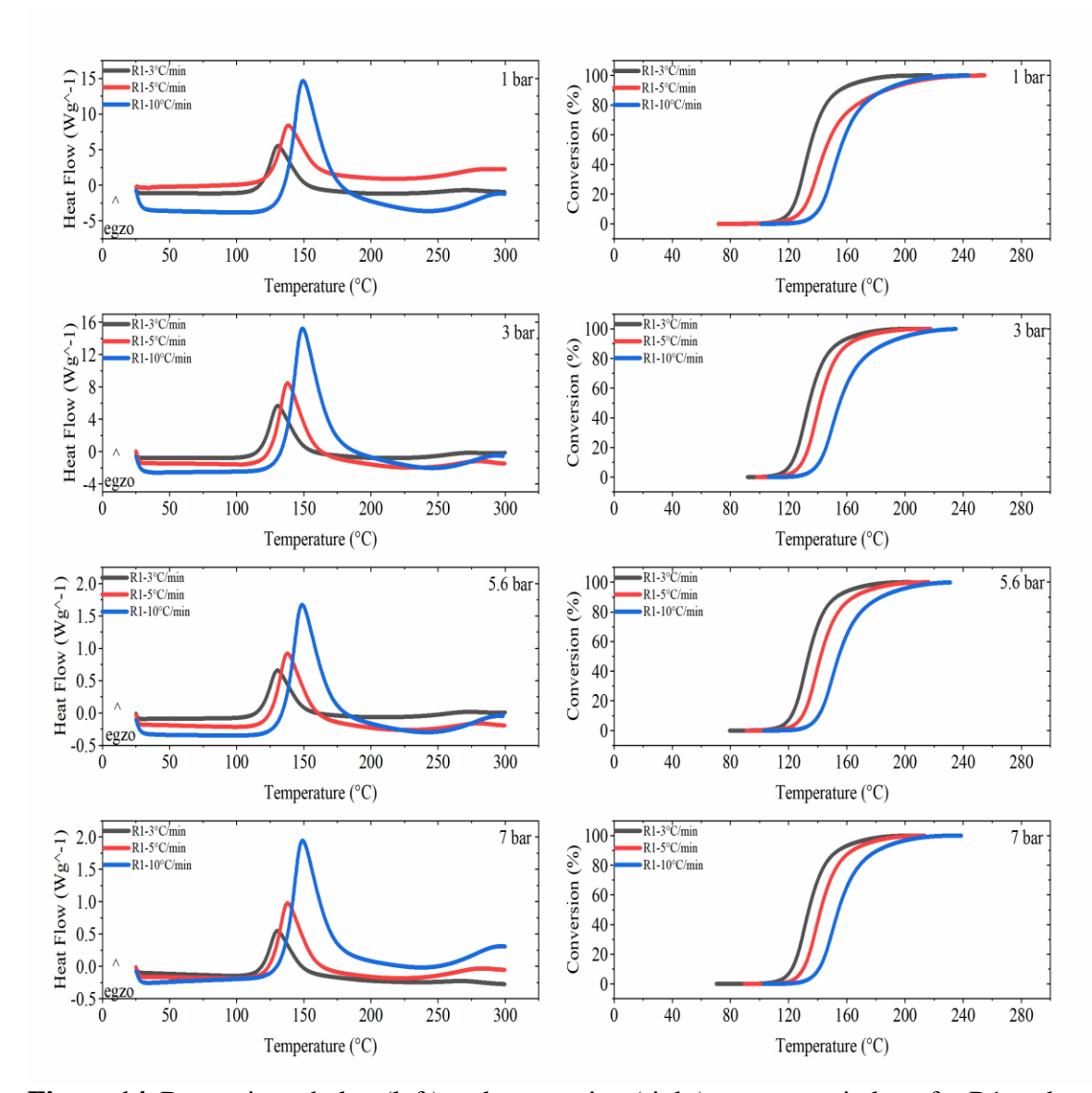


Figure 14. Dynamic enthalpy (left) and conversion (right) curves carried out for R1 under the pressures of 1, 3, 5.6 and 7 bar at the heating rates of 3, 5, 10 °C/min

The dynamic DSC test results for R1 are presented in **Table 1** and **Figure 15**. The normalized enthalpy values are in the range of 341-350 J/g. As expected, enthalpy values did not change at different heating rates. Residual cure tests were completed at one heating rate for four different pressure conditions and no residual cure was observed. In this way, the enthalpy value range of the system was finalized. The enthalpy values are shown in **Table 1**, demonstrating that the curing reactions were completed in each system.

The results showed that with increasing heating rate, onset and endset temperatures shifted to the right and sharper-peaks were observed as the reactions occurred more rapidly (**Figure 14**).

Table 1. Dynamic cure enthalpies and onset temperatures of R1

Pressure (bar)	Heating Rate (°C/min)	Normalized Enthalpy (Jg^- 1)	Onset Temperature (°C)
	3	349.88	118.28
1	5	344.55	125.70
	10	342.52	135.80
	3	343.57	118.00
3	5	343.79	125.26
	10	343.08	135.65
	3	344.67	117.79
5.6	5	350.51	125.11
	10	347.54	135.23
	3	341.95	118.07
7	5	344.66	125.31
	10	353.80	135.49

The results obtained for the R1 resin at various pressures have also shown that the pressure has no effect on curing enthalpy. The results obtained in this system, which is in the form of bulk resin without any woven fabric or fiber, show that the reactions could be performed via molecule and chain motions without any physical or chemical obstacles thanks to the increased surface area. Besides, molecule and chain motions did not require pressure effect to complete the reactions thanks to the low void content and low amount of moisture.

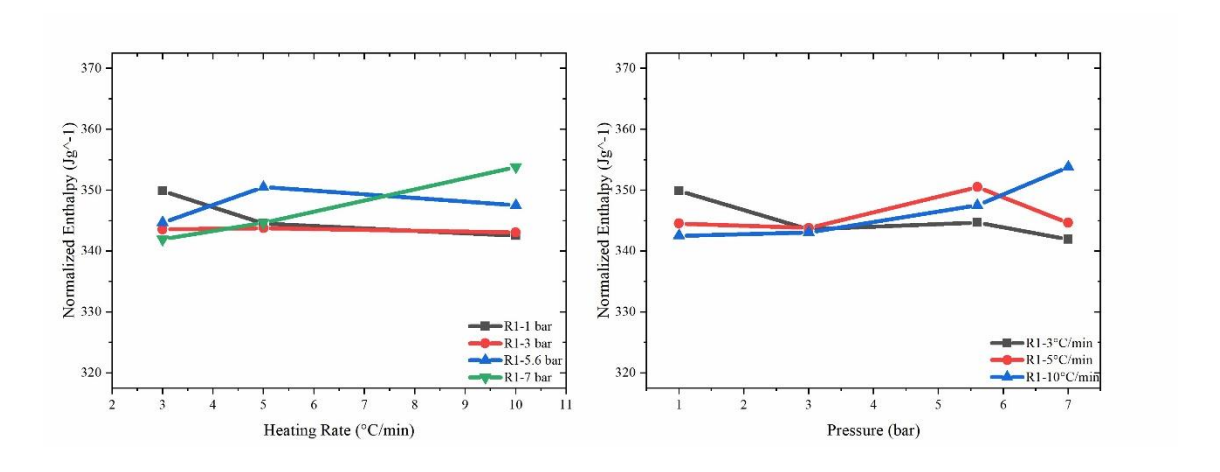


Figure 15. Comparison of dynamic enthalpy values of R1 with respect to heating rate (left) and pressure (right)

Table 2 shows the cure degrees corresponding to certain temperatures. The results show that the temperature to reach 100% cure degree under the same heating rate increases with pressure. The increase in curing temperature with pressure could best be observed at a

heating rate of 3 °C/min. The mobility of the molecules was relatively limited by the consolidation effect of the pressure, causing the reactions to be completed later.

To sum up, it is clear that the pressure had no effect on the enthalpy energy resulting from the reactions in the resin, so this must be considered while determining the cure cycle steps.

Table 2. R1 dynamic cure degree with respect to temperatures

Pressure (bar)	sure (bar) Conversion (%) Temperature (°C)				
, ,	, ,	3 °C/min	5 °C/min	10 °C/min	
	90	153.41	171.38	187.14	
1	95	162.98	184.42	200.88	
1	99	179.81	204.09	214.35	
	100	195.65	225.11	221.65	
	90	153.93	161.64	186.80	
3	95	164.50	172.56	200.73	
3	99	183.33	193.30	214.29	
	100	208.66	218.04	221.56	
	90	152.78	164.83	183.64	
5.6	95	163.01	176.23	196.87	
3.0	99	181.55	188.37	217.57	
	100	206.26	195.01	241.46	
	90	154.20	163.88	181.17	
7	95	165.09	174.93	193.54	
1	99	183.94	193.67	213.77	
	100	209.80	214.06	238.93	

2.2.3. HP-DSC dynamic test results – TW-R1

TW-R1 prepreg dynamic DSC tests were carried out using the same methods as R1 resin. Curing and conversion curves obtained as a result of dynamic tests are shown in **Figure 16**. Enthalpy and conversion values are provided in **Table 3** and **Table 4**. As shown in **Table 3**, the cure enthalpies in the prepreg samples are in the range of 82-93 J/g, 90-93 J/g, 94-104 J/g, 90-109 J/g under 1 bar, 3 bar, 5.6 bar and 7 bar pressures, respectively. As in R1, it was concluded that when the heating rate is increased, the cure onset and endset temperatures increase.

The TW-R1 prepreg was reinforced with 2x2 twill woven fabric and had an epoxy matrix that is in the B-stage cure. The average enthalpy value of the resin is 346 J/g and theoretically expected enthalpy value from prepreg is 145 J/g on average since resin percentage is 42% in the prepreg. However, it is known that a certain amount of curing takes place during the B-stage cure; therefore, enthalpy values would be less than 145 J/g in prepregs. The crucial thing about the TW-R1 is that the prepreg contains air bubbles

due to the twill weave fabric and these air bubbles cause voids. Besides, as a result of the evaporation of the moisture in the prepreg with the temperature, voids may occur. Therefore, these voids and fibers create physical barriers to molecular mobility.

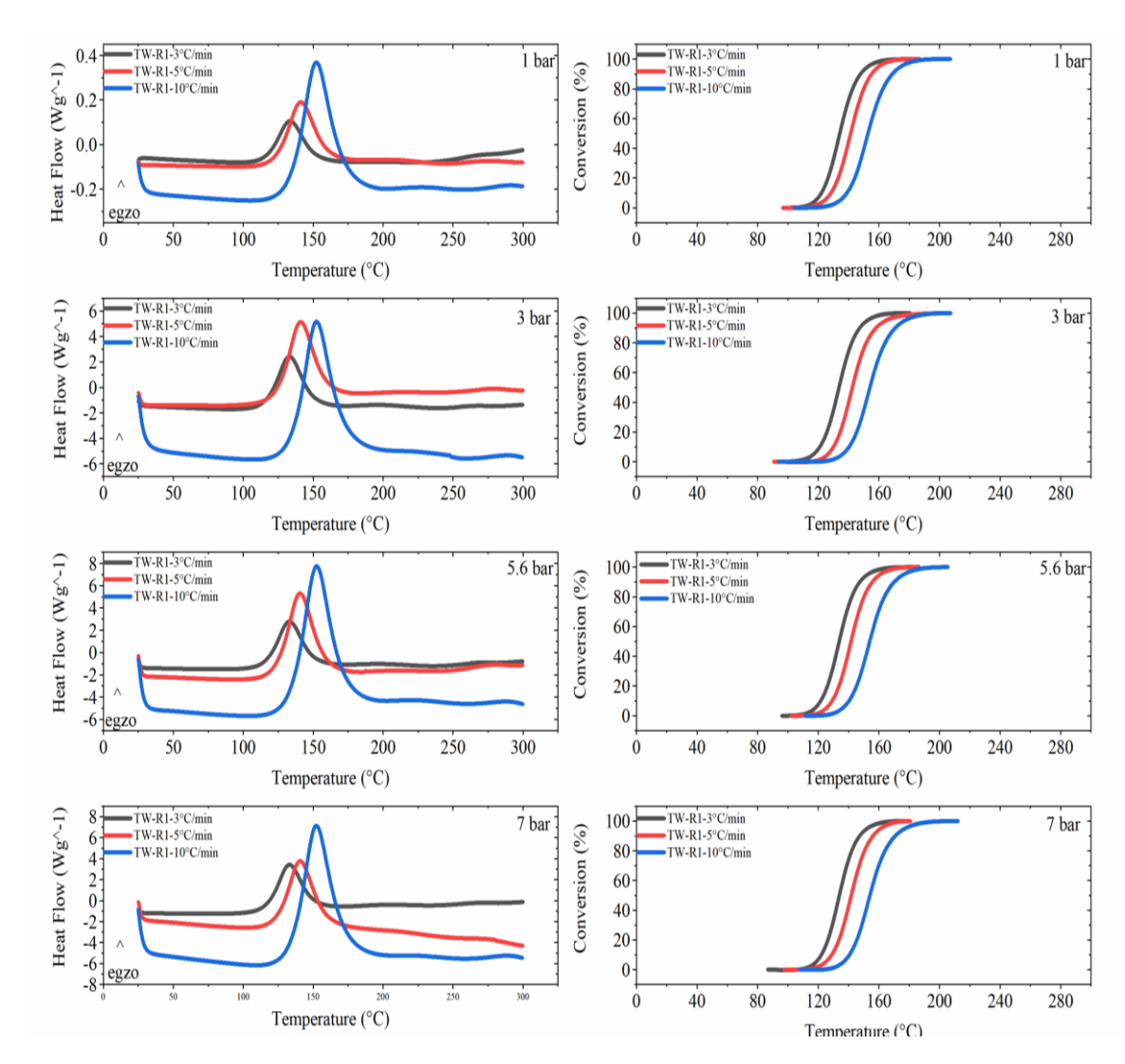


Figure 16. Dynamic enthalpy (left) and conversion (right) curves carried out for TW-R1 under 1, 3, 5.6 and 7 bar pressures at the heating rates of 3, 5, 10 °C/min

If the effect of pressure on enthalpy is examined for TW-R1 from **Table 3**, it can be noticed that it is more difficult to understand the effect of pressure on enthalpy values at high heating rates since the molecules react so fast and pressure could not affect the crosslink density. If the effect of pressure at a low heating rate of 3 °C/min is examined, small increases in enthalpy values with rising pressure can be noticed. These results may be explained by the fact that the size of the voids decreases with pressure or voids can be removed with resin and they do not become physical obstacles. Due to the decrease in void content, surface area for the reactions increases, and molecular mobility occurs at every point in the prepreg. Additionally, better dissipation of heat is observed in the

prepreg as a result of increased heat transfer and molecules have more time to react with slow heating rate. Therefore, the collusion possibility of molecules, the molecular mobility and cross-link density can increase and therefore, enthalpies can increase [11,65].

Table 3. TW-R1 dynamic cure enthalpies and onset temperatures

Pressure (bar)	Heating Rate (°C/min)	Normalized Enthalpy (Jg^-1)	Onset Temperature (°C)
	3	85.78	116.76
1	5	81.54	123.55
	10	92.64	133.93
	3	93.21	116.59
3	5	90.53	124.49
	10	93.21	135.34
	3	94.19	116.62
5.6	5	104.00	124.00
	10	97.91	134.70
	3	108.9	117.06
7	5	90.58	124.19
	10	98.72	134.87

However, when **Table 3** was examined, it can be noticed that the enthalpy values under the same pressure are in a certain range. This can be confusing when examining the effect of pressure on enthalpy values. Nevertheless, the important point is that the effect of pressure shows an upward trend at low heating rate as can be seen in **Figure 17**, and it is explained above why the effect of pressure is seen at low heating rate. Besides, supporting information was also obtained from the isothermal and UD prepreg test results analyzed in the following sections. With all that claimed, the point to focus on here is the pressure as evidenced by other studies discussed in **Section 2.1.2**. It is known that voids are entrapped inside the woven fabric and pressure and temperature are used as a manufacturing parameter to eliminate voids. Additionally, in the same studies, the effect of pressure is confirmed by characterization and mechanical tests. For this reason, it can be said that the use of pressure is mandatory in the production of composite parts. Besides, since the pressure has an effect on the prepreg rather than the resin, it was taken into account that the curing kinetic results of the prepreg tests should be used when determining the cure cycle.

Additionally, it was seen that the cure degrees corresponding to temperatures have not changed with pressure.

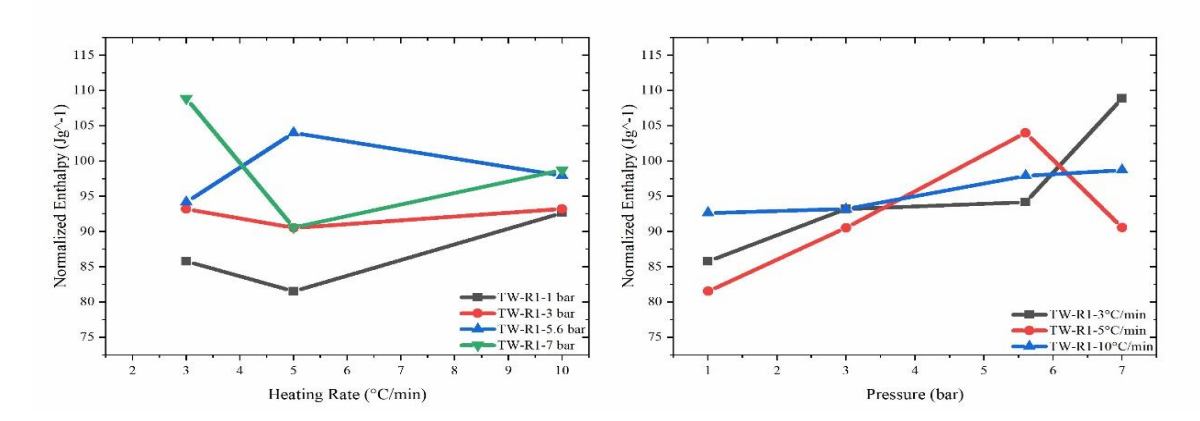


Figure 17. Comparison of dynamic TW-R1 enthalpy values with respect to heating rate (left) and pressure (right)

Table 4. TW-R1 dynamic cure degrees with respect to temperatures

Pressure (bar)	Conversion (%)		Temperature (°C	C)
,		3 °C/min	5 °C/min	10 °C/min
1	99.90	176.48	176.93	203.74
3	99.90	161.42	200.43	218.39
5.6	99.90	174.14	181.96	200.97
7	99.90	176.58	177.34	207.67

2.2.4. HP-DSC dynamic test results – R1 vs. TW-R1

Firstly, when the starting points of cure temperatures of the resin were compared with the prepreg, it was observed that they were the same since the molecular mobility and bonding potential were high at the beginning of the reaction both in resin and prepreg. However, this mechanism was different when comparing the temperatures at which R1 and TW-R1 reached 100% cure. Resin samples were in bulk form, while prepreg samples contained both resin and fiber. Therefore, it was predicted that the crosslink formation and density in the prepreg would be less than the bulk resin due to physical barriers such as the fibers and the voids in them and their surface area restrictions. In the resin, on the other hand, since the crosslink density was higher than the prepreg, this would cause the molecular mobility to be highly restricted after the gelation point. In this case, the resin would require greater energies for chain mobility, and this will cause the %100 cure temperature to shift to the right compared to prepreg.

2.2.5. Model Free Kinetics (MFK) analysis – R1

The MFK analysis, that gives estimations about the cure degrees of reactions in isothermal tests by using the activation energies obtained at different heating rates in dynamic DSC tests, enables the examination of reaction mechanisms rapidly (**Figure 18**). Besides, MFK analysis reduces the number of tests and facilitates the manufacturing

processes through process optimization allowing the cure degrees to be known quickly. As a result of the analysis, the manufacturing time to reach the desired degree of cure at the desired temperature can be estimated.

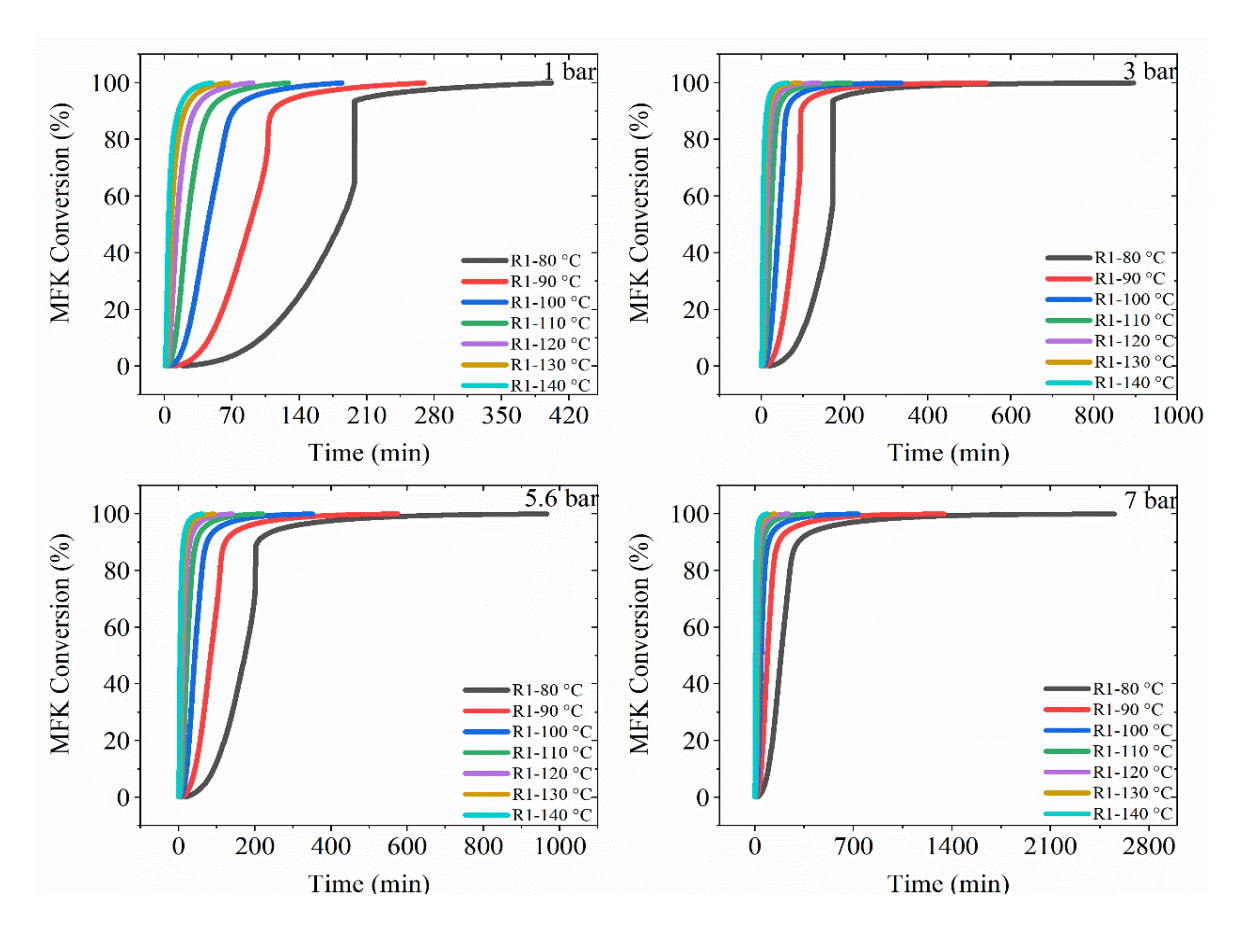


Figure 18. R1 MFK Analysis isothermal cure degree estimation curves at the temperatures of 80, 90, 100, 110, 120, 130 and 140 °C under the pressures of 1, 3, 5.6 and 7 bar

MFK extrapolations were applied to R1 resin system at varying temperatures in addition to isothermal test temperatures. Thus, observations could be made about the reaction kinetics. For instance, in the MFK analysis of the R1 resin, the times corresponding to the cure percentages such as 10, 50, 99% were found at 80, 90, 100, 110, 120, 130 and 140 °C temperatures. MFK analysis was investigated under pressures of 1, 3, 5.6 and 7 bar and the results were shown in **Table 5.** To exemplify, 99.90% curing at 120 °C under 1 bar pressure appears to occur in 91 minutes. Additionally, it can be observed that the same cure degrees were achieved in longer periods with the rising pressure specially for low temperature. For instance, 99.9% cure was achieved in 269 minutes at 90 °C under 1 bar pressure, while this time was 540 minutes at 3 bar.

Table 5. R1 MFK analysis estimation of cure degree versus time

			1 bar				
Conversion		MFK Co	onversion at	Different T	emperature	es (min)	
(%)	80 °C	90 °C	100 °C	110 °C	120 °C	130 °C	140 °C
10	100.82	46.78	22.62	11.36	5.91	3.17	1.76
50	181.81	88.54	44.81	23.50	12.74	7.11	4.09
75	197.42	106.28	59.11	33.89	19.99	12.10	7.51
90	197.62	112.66	71.66	46.67	31.06	21.10	14.60
95	214.00	138.13	91.27	61.63	42.45	29.79	21.26
97	257.37	167.22	111.16	75.49	52.28	36.88	26.45
99	340.92	223.18	149.49	102.25	71.30	50.62	36.53
99.90	401.94	269.29	184.33	128.70	91.51	66.18	48.62
			3 bars				
Conversion		MFK Co	onversion at	Different T	emperature	es (min)	
(%)	80 °C	90 °C	100 °C	110 °C	120 °C	130 °C	140 °C
10	92.19	43.30	21.17	10.75	5.65	3.06	1.71
50	164.72	81.09	41.50	21.99	12.03	6.78	3.93
75	172.10	93.76	52.78	30.63	18.28	11.19	7.01
90	172.46	95.13	61.24	40.37	27.17	18.65	13.04
95	192.03	123.94	81.88	55.28	38.08	26.72	19.07
97	252.60	162.16	106.60	71.63	49.11	34.31	24.39
99	421.02	265.18	171.23	113.12	76.32	52.51	36.78
99.90	894.87	540.97	335.97	213.91	139.36	92.74	62.94
			5.6 bar	rs			
Conversion		MFK Co	onversion at	Different T	emperature	es (min)	
(%)	80 °C	90 °C	100 °C	110 °C	120 °C	130 °C	140 °C
10	92.52	43.21	21.02	10.62	5.55	3.00	1.67
50	173.81	84.34	42.55	22.24	12.02	6.70	3.84
75	201.48	106.02	57.72	32.45	18.78	11.17	6.81
90	207.96	122.84	74.66	46.57	29.75	19.44	12.96
95	277.41	168.00	104.51	66.65	43.49	28.98	19.70
97	363.97	220.08	136.71	87.06	56.73	37.76	25.63
99	574.59	344.85	212.71	134.55	87.12	57.64	38.90
99.90	966.39	573.87	350.43	219.57	140.89	92.41	61.87
			7 bars				
Conversion		MFK Co	onversion at			, ,	1
(%)	80 °C	90 °C	100 °C	110 °C	120 °C	130 °C	140 °C
10	95.85	44.53	21.55	10.84	5.64	3.03	1.68
50	183.99	88.21	43.97	22.74	12.16	6.71	3.81
75	236.66	120.27	63.38	34.53	19.4	11.22	6.66
90	307.40	168.36	95.36	55.64	33.35	20.51	12.91
95	488.06	268.82	152.86	89.53	53.88	33.25	21.01
97	697.75	381.39	215.31	125.24	74.88	45.93	28.85
99	1220.32	659.5	368.38	212.11	125.61	76.35	47.54
99.90	2553.61	1344.49	732.65	412.09	238.67	142.03	86.67

2.2.6. Model Free Kinetics (MFK) analysis – TW-R1

The MFK extrapolations obtained for TW-R1 prepreg applied with the same method as the R1 were quite short compared to the resin results **Figure 19**. For instance, **Table 6** shows that, for TW-R1 99.90% cure degree occurs in 50 minutes at 120 °C under 3 bars while for resin this time is 139 minutes. However, the effect of pressure did not show a clear trend in TW-R1 MFK estimations.

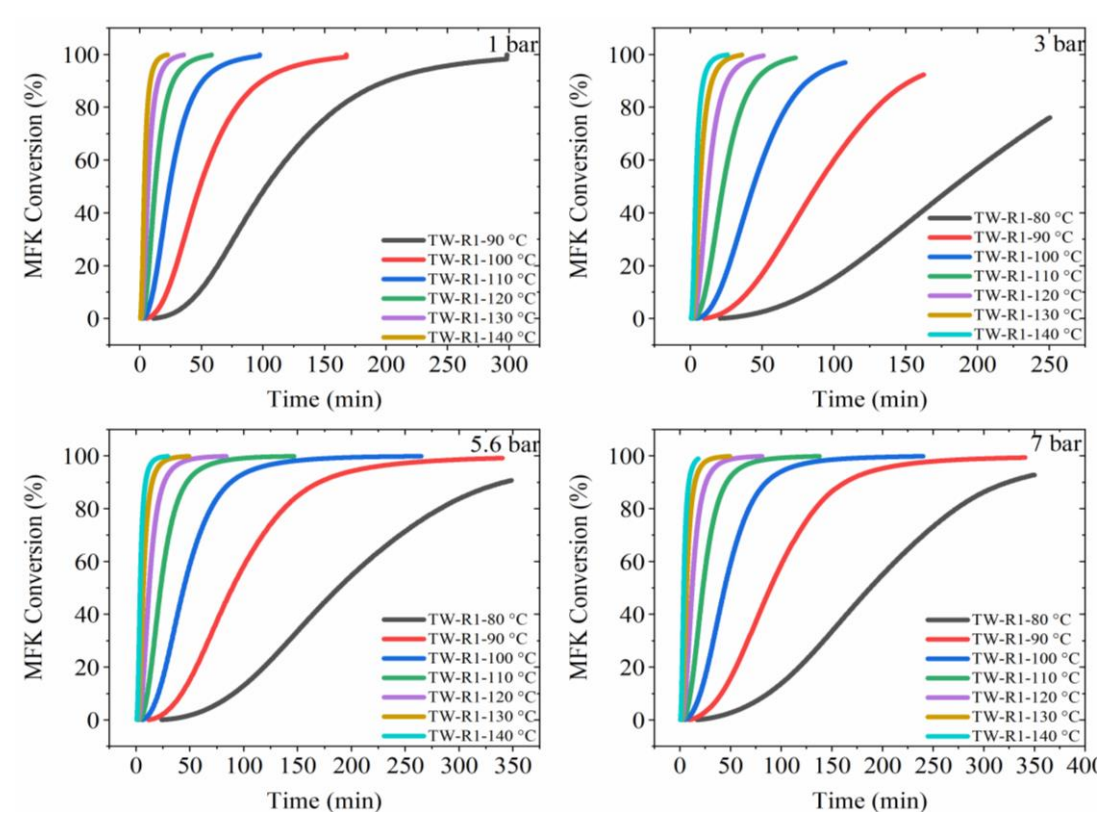


Figure 19. TW-R1 MFK Analysis isothermal cure degree estimation curves at the temperatures of 80, 90, 100, 110, 120, 130 and 140 °C under the pressures of 1, 3, 5.6 and 7 bar

Table 6. TW-R1 MFK analysis estimation of cure degree versus time

1 bar								
Conversion		MFK Conversion at Different Temperatures (min)						
(%)		90 °C	100 °C	110 °C	120 °C	130 °C	140 °C	
10		47.67	21.81	10.40	5.15	2.64	1.40	
50		102.46	48.58	23.95	12.24	6.46	3.52	
75		148.55	71.40	35.66	18.45	9.86	5.43	
99.9		298.26	167.71	97.18	57.89	35.39	22.15	
			3 bars	S				
Conversion		MFK C	onversion a	t Different T	Temperature	es (min)		
(%)	80 °C	90 °C	100 °C	110 °C	120 °C	130 °C	140 °C	
10	83.87	39.93	19.78	10.17	5.40	2.97	1.67	
50	183.24	87.76	43.73	22.59	12.07	6.65	3.78	
75	247.02	121.23	61.81	32.64	17.80	10.01	5.79	
90	250.42	153.45	81.82	45.08	25.61	14.96	8.97	
99.9	250.52	162.52	107.9	73.18	50.63	35.67	25.56	

	Table 6 continued								
5.6 bars									
Conversion (%)		MFK Conversion at Different Temperatures (min)							
	80 °C	90 °C	100 °C	110 °C	120 °C	130 °C	140 °C		
10	90.35	42.22	20.55	10.39	5.43	2.94	1.63		
50	188.05	89.29	44.14	22.63	12.00	6.57	3.70		
80	282.04	137.05	69.23	36.25	19.61	10.93	6.27		
90	341.47	169.95	87.82	46.97	25.93	14.74	8.61		
99.9	-	ı	264.7	146.38	83.43	48.89	29.41		
			7 bars	S					
Conversion		MFK C	conversion a	t Different T	Temperature	es (min)			
(%)	80 °C	90 °C	100 °C	110 °C	120 °C	130 °C	140 °C		
10	91.9	42.61	20.58	10.33	5.36	2.88	1.59		
50	184.73	88.16	43.77	22.54	12.01	6.60	3.73		
75	228.81	111.56	56.53	29.68	16.10	9.00	5.18		
90	278.84	144.92	77.98	43.35	24.83	14.62	8.83		
99.9	319.77	197.32	124.95	81.04	53.73	36.35	25.07		

2.2.7. Sample preparation and isothermal test methods for HP-DSC tests

The sample preparation method for isothermal HP-DSC tests was the same as the sample preparation method for dynamic HP-DSC tests.

The isothermal test methods were as follows for R1 and TW-R1. Throughout performing DSC tests, firstly, 90, 100, 110 and 120 °C temperatures were raised with 130, 150, 170 and 190 °C/min heating rates, respectively, from 25 ° C, preventing reactions to occur in 0.30 seconds. Also, all tests were conducted under 1, 3, 5.6 and 7 bar pressures. The temperatures and times required for 100% curing were determined in the light of MFK analysis predictions. In order to check the accuracy of the MFK analysis estimations, the longer durations were used. Tests were carried out once. However, residual cure scans were carried out on one sample from each pressure set in order to find the enthalpy value in the system and the tests were repeated if necessary. The most appropriate results were included in the shared tables. The thermal transitions of the test were monitored through STARe Software.

2.2.8. HP-DSC isothermal test results – R1

MFK data taken into account when deciding on isothermal test times of resin, it was evaluated that the tests must be carried out for a very long time in order to reach 100% curing percentage at 90 °C and 100 °C. To exemplify, if it is desired to test at 90 °C under 7 bar pressures, a test time of 540 minutes was predicted. The possibility of data usage about these temperatures in the cure cycle was evaluated and it was decided that there is no need to reserve a long time for these tests. On the other hand, in order to examine the

cure kinetics of the resin at these temperatures and to compare with the prepreg, the time the prepregs reached 100% cure degree was also applied to these tests. Besides, heating was continued for the time estimated by the analysis for 110 and 120 °C.

In the light of all this, curing and conversion curves obtained in dynamic tests are shown in **Figure 20**. Enthalpy and conversion values are provided in **Table 7** and **Table 8**. It can be seen that when the test results for 120 °C were examined, the enthalpy values are in the range of 337-344 J/g. Besides, enthalpy values were in the same range including diverse pressure conditions and R1 dynamic tests. It was understood from this, which is also confirmed by residual cure tests, that the curing at 120 °C was 100% completed. Based on verified enthalpy values, if the enthalpy values at 90 and 100 °C temperatures are evaluated, cure degrees between 70-80% were observed in the R1. Nevertheless, the TW-R1 samples reached 100% cure degree at the same time **Section 2.2.9**. Additionally, it was observed that although the test was continued during the times suggested by the MFK analysis, 100% cure percentage could not be reached at 110 °C. Cure degrees varied between 85-94% at 110 °C. However, if the onset times of the curing was interpreted, as expected it was observed that the onset cure time decreased as the temperature increased from 90 °C to 120 °C.

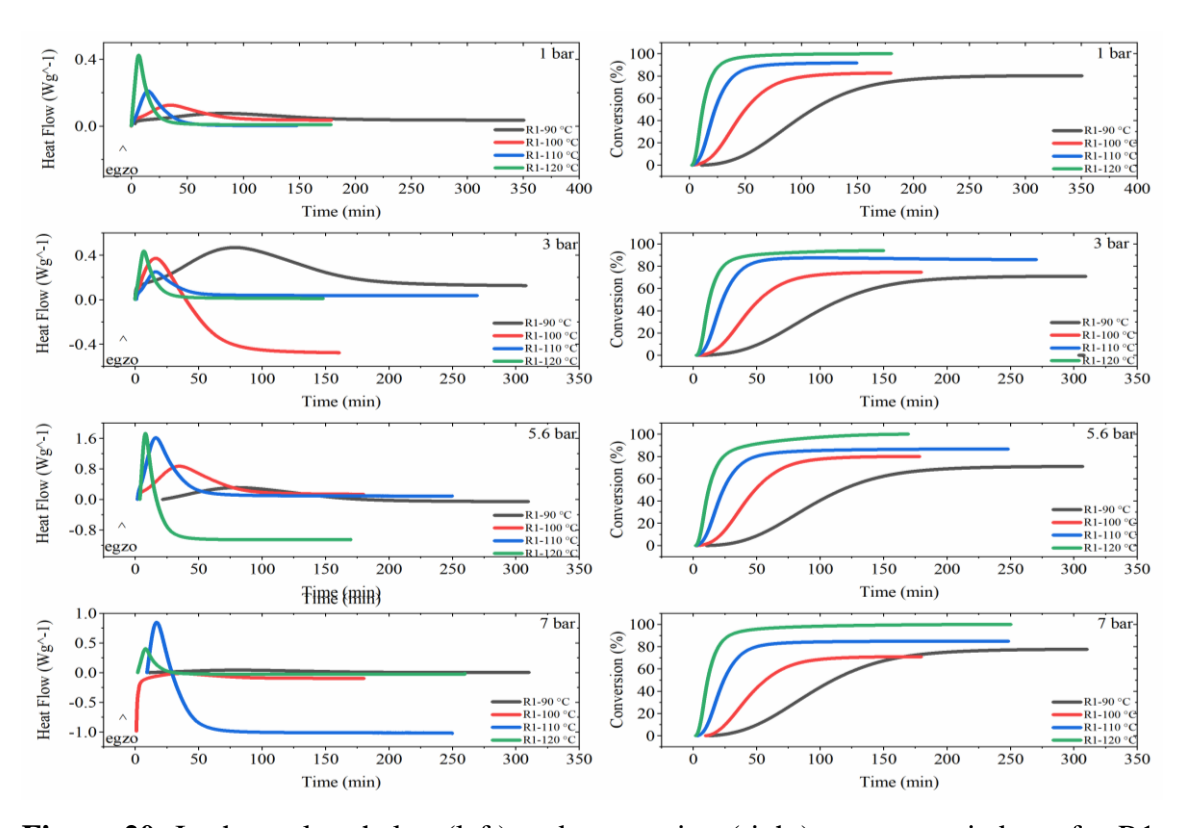


Figure 20. Isothermal enthalpy (left) and conversion (right) curves carried out for R1 under the pressures of 1, 3, 5.6 and 7 bar at the temperatures of 90, 100, 110, 120 °C

Table 7 showed that pressure had no effect on enthalpy as in dynamic tests, while the effect of pressure on enthalpy was examined. On the other hand, with the rising of pressure, the cure times increased considerably. The increase in curing times with pressure especially occurred after the gel point (**Table 8**). To give an illustration, 50% cure degree at 120°C was reached between 11-12 minutes under four different pressure conditions. Nevertheless, 76, 149, 169 and 249 minutes were required for 1, 3, 5.6 and 7 bar pressures, respectively to reach 100% curing at 120 °C. This is due to the consolidation effect of the pressure relatively on the bulk resin, which has low molecular mobility after the gel point and requires more energy for chain mobility and causing further limitation of chain mobility.

Table 7. R1 isothermal cure enthalpies

Pressure (bar)	Temperature (°C)	Normalized Enthalpy (Jg^-1)	Pressure (bar)	Temperature (°C)	Normalized Enthalpy (Jg^-1)
	90	265.01		90	243.25
1	100	281.28	5 6	100	273.61
1	110	312.56	5.6	110	295.57
	120	337.83		120	340.84
	90	242.92		90	264.01
3	100	254.07	7	100	244.46
3	110	312.56	/	110	289.96
	120	343.38		120	344.59

In addition to all these, it was noticed that the enthalpy values of a bulk resin are quite high to autoclave production since the high amount of exothermic heat, which may vary according to the size of the part, has the possibility of endangering the production environment. Therefore, this parameter was taken into account in the cure cycle determination.

In the end, the results of R1 isothermal study indicated that pressure cause long time periods to %100 cure degree and excess exotherm heat. Thus, it is critical to note that in resin systems, pressure negatively affects the duration and occupational health and safety from the manufacturer's point of view.

Table 8. R1 isothermal cure degrees with respect to time

	1 bar						
90 °C (350	0 Min)	100 °C (18			110 °C (150 Min)		0 Min)
Conversion	Time	Conversion	Time	Conversion	Time	Conversion	Time
(%)	(min)	(%)	(min)	(%)	(min)	(%)	(min)
50	110.35	50	50.03	50	22.82	50	11.80
60	128.80	60	59.03	60	26.63	60	13.76
70	156.15	70	71.99	70	31.70	70	16.35
80	280.06	80	106.80	80	39.70	80	20.12
		82	137.40	90	71.98	90	27.38
				91	90.71	95	37.42
						98	57.52
						99	76.96
			31	bar			
90 °C (310	0 Min)	100 °C (18	0 Min)	110 °C (27	0 Min)	120 °C (15	0 Min)
Conversion	Time	Conversion	Time	Conversion	Time	Conversion	Time
(%)	(min)	(%)	(min)	(%)	(min)	(%)	(min)
50	116.98	50	52.32	50	23.30	50	12.72
60	142.20	60	63.48	60	27.27	60	15.04
70	224.99	70	85.63	70	32.69	70	18.29
70.5	245.55	74.5	146.3	80	42.03	80	23.82
				85	54.28	90	47.54
				87	71.79	94	149.88
			5.6	bar			
		100 °C (180 Min)		110 °C (250 Min)			
90 °C (31	· ·	,	,	· ·		120 °C (17	
Conversion	Time	Conversion	Time	Conversion	Time	Conversion	Time
Conversion (%)	Time (min)	Conversion (%)	Time (min)	Conversion (%)	Time (min)	Conversion (%)	Time (min)
Conversion (%) 50	Time (min) 110.35	Conversion (%) 50	Time (min) 50.03	Conversion (%) 50	Time (min) 23.67	Conversion (%) 50	Time (min) 12.16
Conversion (%) 50 60	Time (min) 110.35 128.80	Conversion (%) 50 60	Time (min) 50.03 59.03	Conversion (%) 50 60	Time (min) 23.67 28.27	Conversion (%) 50 60	Time (min) 12.16 14.60
Conversion (%) 50 60 70	Time (min) 110.35 128.80 156.15	Conversion (%) 50 60 70	Time (min) 50.03 59.03 71.99	Conversion (%) 50 60 70	Time (min) 23.67 28.27 34.92	Conversion (%) 50 60 70	Time (min) 12.16 14.60 18.05
Conversion (%) 50 60	Time (min) 110.35 128.80	Conversion (%) 50 60 70 80	Time (min) 50.03 59.03 71.99 106.80	Conversion (%) 50 60 70 80	Time (min) 23.67 28.27 34.92 49.53	Conversion (%) 50 60 70 80	Time (min) 12.16 14.60 18.05 24.00
Conversion (%) 50 60 70	Time (min) 110.35 128.80 156.15	Conversion (%) 50 60 70	Time (min) 50.03 59.03 71.99	Conversion (%) 50 60 70 80 85	Time (min) 23.67 28.27 34.92 49.53 89.36	Conversion (%) 50 60 70 80 90	Time (min) 12.16 14.60 18.05 24.00 43.95
Conversion (%) 50 60 70	Time (min) 110.35 128.80 156.15	Conversion (%) 50 60 70 80	Time (min) 50.03 59.03 71.99 106.80	Conversion (%) 50 60 70 80	Time (min) 23.67 28.27 34.92 49.53	Conversion (%) 50 60 70 80 90 95	Time (min) 12.16 14.60 18.05 24.00 43.95 75.55
Conversion (%) 50 60 70	Time (min) 110.35 128.80 156.15	Conversion (%) 50 60 70 80	Time (min) 50.03 59.03 71.99 106.80	Conversion (%) 50 60 70 80 85	Time (min) 23.67 28.27 34.92 49.53 89.36	Conversion (%) 50 60 70 80 90 95 99	Time (min) 12.16 14.60 18.05 24.00 43.95 75.55 126.78
Conversion (%) 50 60 70	Time (min) 110.35 128.80 156.15	Conversion (%) 50 60 70 80	Time (min) 50.03 59.03 71.99 106.80 137.40	Conversion (%) 50 60 70 80 85 86.5	Time (min) 23.67 28.27 34.92 49.53 89.36	Conversion (%) 50 60 70 80 90 95	Time (min) 12.16 14.60 18.05 24.00 43.95 75.55
Conversion (%) 50 60 70 80	Time (min) 110.35 128.80 156.15 280.06	Conversion (%) 50 60 70 80 82	Time (min) 50.03 59.03 71.99 106.80 137.40	Conversion (%) 50 60 70 80 85 86.5	Time (min) 23.67 28.27 34.92 49.53 89.36 178.30	Conversion (%) 50 60 70 80 90 95 99 100	Time (min) 12.16 14.60 18.05 24.00 43.95 75.55 126.78 169.01
Conversion (%) 50 60 70 80 90 °C (310	Time (min) 110.35 128.80 156.15 280.06	Conversion (%) 50 60 70 80 82	Time (min) 50.03 59.03 71.99 106.80 137.40 71	Conversion (%) 50 60 70 80 85 86.5 110 °C (25	Time (min) 23.67 28.27 34.92 49.53 89.36 178.30 0 Min)	Conversion (%) 50 60 70 80 90 95 99 100	Time (min) 12.16 14.60 18.05 24.00 43.95 75.55 126.78 169.01
Conversion (%) 50 60 70 80 90 °C (310 Conversion	Time (min) 110.35 128.80 156.15 280.06	Conversion (%) 50 60 70 80 82 100 °C (18 Conversion	Time (min) 50.03 59.03 71.99 106.80 137.40 71.00 Min) Time	Conversion (%) 50 60 70 80 85 86.5 110 °C (25 Conversion	Time (min) 23.67 28.27 34.92 49.53 89.36 178.30 0 Min) Time	Conversion (%) 50 60 70 80 90 95 99 100 120 °C (26 Conversion	Time (min) 12.16 14.60 18.05 24.00 43.95 75.55 126.78 169.01 0 Min) Time
Conversion (%) 50 60 70 80 90 °C (310 Conversion (%)	Time (min) 110.35 128.80 156.15 280.06 0 Min) Time (min)	Conversion (%) 50 60 70 80 82 100 °C (18 Conversion (%)	Time (min) 50.03 59.03 71.99 106.80 137.40 71.60 Min) Time (min)	Conversion (%) 50 60 70 80 85 86.5 Dar 110 °C (25 Conversion (%)	Time (min) 23.67 28.27 34.92 49.53 89.36 178.30 0 Min) Time (min)	Conversion (%) 50 60 70 80 90 95 99 100 120 °C (26 Conversion (%)	Time (min) 12.16 14.60 18.05 24.00 43.95 75.55 126.78 169.01 0 Min) Time (min)
Conversion (%) 50 60 70 80 90 °C (310 Conversion (%) 50	Time (min) 110.35 128.80 156.15 280.06 D Min) Time (min) 110.39	Conversion (%) 50 60 70 80 82 100 °C (18 Conversion (%) 50	Time (min) 50.03 59.03 71.99 106.80 137.40 71 100 Min) Time (min) 57.03	Conversion (%) 50 60 70 80 85 86.5 Conversion (%) 50	Time (min) 23.67 28.27 34.92 49.53 89.36 178.30 0 Min) Time (min) 24.19	Conversion (%) 50 60 70 80 90 95 99 100 120 °C (26 Conversion (%) 50	Time (min) 12.16 14.60 18.05 24.00 43.95 75.55 126.78 169.01 Time (min) 11.4
Conversion (%) 50 60 70 80	Time (min) 110.35 128.80 156.15 280.06 0 Min) Time (min) 110.39 129.86	Conversion (%) 50 60 70 80 82 100 °C (18 Conversion (%) 50 60	Time (min) 50.03 59.03 71.99 106.80 137.40 71.60 Min) Time (min) 57.03 70.58	Conversion (%) 50 60 70 80 85 86.5 20 110 °C (25 Conversion (%) 50 60	Time (min) 23.67 28.27 34.92 49.53 89.36 178.30 0 Min) Time (min) 24.19 28.69	Conversion (%) 50 60 70 80 90 95 99 100 120 °C (26 Conversion (%) 50 60	Time (min) 12.16 14.60 18.05 24.00 43.95 75.55 126.78 169.01 0 Min) Time (min) 11.4 13.39
90 °C (310 Conversion (%) 50 60 70 80	Time (min) 110.35 128.80 156.15 280.06 0 Min) Time (min) 110.39 129.86 161.23	Conversion (%) 50 60 70 80 82 100 °C (18 Conversion (%) 50 60 70	Time (min) 50.03 59.03 71.99 106.80 137.40 71 60 Min) Time (min) 57.03 70.58 118.20	Conversion (%) 50 60 70 80 85 86.5 Conversion (%) 50 60 70	Time (min) 23.67 28.27 34.92 49.53 89.36 178.30 0 Min) Time (min) 24.19 28.69 35.19	Conversion (%) 50 60 70 80 90 95 99 100 120 °C (26 Conversion (%) 50 60 70	Time (min) 12.16 14.60 18.05 24.00 43.95 75.55 126.78 169.01 0 Min) Time (min) 11.4 13.39 16.04
90 °C (310 Conversion (%) 50 60 70 80 90 °C (310 Conversion (%) 50 60 70 75	Time (min) 110.35 128.80 156.15 280.06 D Min) Time (min) 110.39 129.86 161.23 199.23	Conversion (%) 50 60 70 80 82 100 °C (18 Conversion (%) 50 60	Time (min) 50.03 59.03 71.99 106.80 137.40 71.60 Min) Time (min) 57.03 70.58	Conversion (%) 50 60 70 80 85 86.5 110 °C (25 Conversion (%) 50 60 70 80	Time (min) 23.67 28.27 34.92 49.53 89.36 178.30 0 Min) Time (min) 24.19 28.69 35.19 49.97	Conversion (%) 50 60 70 80 90 95 99 100 120 °C (26 Conversion (%) 50 60 70 80	Time (min) 12.16 14.60 18.05 24.00 43.95 75.55 126.78 169.01 Time (min) 11.4 13.39 16.04 20.00
90 °C (310 Conversion (%) 50 60 70 80	Time (min) 110.35 128.80 156.15 280.06 0 Min) Time (min) 110.39 129.86 161.23	Conversion (%) 50 60 70 80 82 100 °C (18 Conversion (%) 50 60 70	Time (min) 50.03 59.03 71.99 106.80 137.40 71 60 Min) Time (min) 57.03 70.58 118.20	Conversion (%) 50 60 70 80 85 86.5 Conversion (%) 50 60 70	Time (min) 23.67 28.27 34.92 49.53 89.36 178.30 0 Min) Time (min) 24.19 28.69 35.19	Conversion (%) 50 60 70 80 90 95 99 100 120 °C (26 Conversion (%) 50 60 70 80 90	Time (min) 12.16 14.60 18.05 24.00 43.95 75.55 126.78 169.01 Time (min) 11.4 13.39 16.04 20.00 28.54
90 °C (310 Conversion (%) 50 60 70 80 90 °C (310 Conversion (%) 50 60 70 75	Time (min) 110.35 128.80 156.15 280.06 D Min) Time (min) 110.39 129.86 161.23 199.23	Conversion (%) 50 60 70 80 82 100 °C (18 Conversion (%) 50 60 70	Time (min) 50.03 59.03 71.99 106.80 137.40 71 60 Min) Time (min) 57.03 70.58 118.20	Conversion (%) 50 60 70 80 85 86.5 110 °C (25 Conversion (%) 50 60 70 80	Time (min) 23.67 28.27 34.92 49.53 89.36 178.30 0 Min) Time (min) 24.19 28.69 35.19 49.97	Conversion (%) 50 60 70 80 90 95 99 100 120 °C (26 Conversion (%) 50 60 70 80 90 95	Time (min) 12.16 14.60 18.05 24.00 43.95 75.55 126.78 169.01 0 Min) Time (min) 11.4 13.39 16.04 20.00 28.54 44.54
90 °C (310 Conversion (%) 80 90 °C (310 Conversion (%) 50 60 70 75	Time (min) 110.35 128.80 156.15 280.06 D Min) Time (min) 110.39 129.86 161.23 199.23	Conversion (%) 50 60 70 80 82 100 °C (18 Conversion (%) 50 60 70	Time (min) 50.03 59.03 71.99 106.80 137.40 71 60 Min) Time (min) 57.03 70.58 118.20	Conversion (%) 50 60 70 80 85 86.5 110 °C (25 Conversion (%) 50 60 70 80	Time (min) 23.67 28.27 34.92 49.53 89.36 178.30 0 Min) Time (min) 24.19 28.69 35.19 49.97	Conversion (%) 50 60 70 80 90 95 99 100 120 °C (26 Conversion (%) 50 60 70 80 90	Time (min) 12.16 14.60 18.05 24.00 43.95 75.55 126.78 169.01 Time (min) 11.4 13.39 16.04 20.00 28.54

2.2.9. HP-DSC isothermal test results – TW-R1

Isothermal tests were performed for TW-R1 based on the MFK estimation results, however, with a longer time period to confirm the MFK estimations. Curing and conversion curves obtained in dynamic tests are shown in **Figure 21**. Enthalpy and conversion values are provided in **Table 9** and **Table 10**. The curing enthalpies under 1,

3, 5.6 and 7 bar pressure values are in the range of 85-95 J/g, 100-120 J/g, 100-110 J/g, 110-115 J/g, (see **Table 9**) respectively. In addition, when the TW-R1 isothermal test results and dynamic test results were compared and the residual cure test results for some samples were evaluated, it was assumed that 100% cure degree were achieved in the isothermal tests.

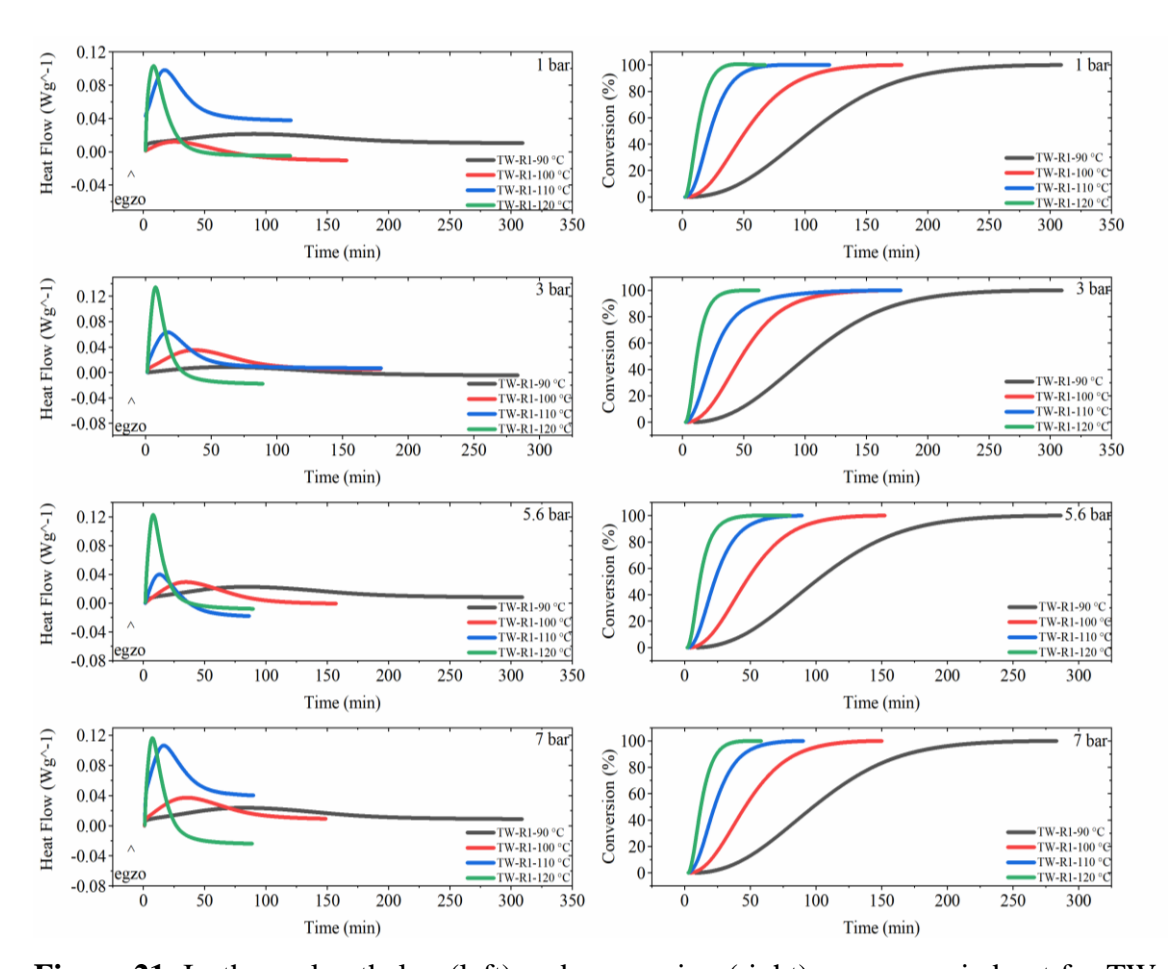


Figure 21. Isothermal enthalpy (left) and conversion (right) curves carried out for TW-R1 under the pressures of 1, 3, 5.6 and 7 bar at the temperatures of 90, 100, 110, 120 °C If the isothermal and dynamic test results under 3 bar pressure were compared, it could be seen that the isothermal curing enthalpy value under 3 bar pressure is higher than the dynamic test result performed under 3 bar pressure. It was thought that the pressure increases the cross-link density by being more effective than dynamic tests in reducing the amount and size of voids and overcoming physical obstacles such as fiber and increasing surface area to react in the long time period during the isothermal test. Additionally, **Table 3** and **Table 9** provided the data that the isothermal curing enthalpy value under 3 bar pressure is higher than the isothermal enthalpy value under 1 bar pressure. The reason for this is attributed to increase in the cross-link density by

increasing the molecular collisions by minimizing the effect of the void and fiber, as explained in **Section 2.2.3**.

Continuing to interpret the effect of pressure on enthalpy, it was seen that enthalpy values under 5.6 bar pressure are higher than isothermal enthalpy values under 1 bar pressure and 5.6 bar dynamic pressure. The reason thought to be similar to the one described previously for 3 bar pressure effect. However, it was observed that the enthalpy values at 5.6 bar are lower when compared to the enthalpy values of the isothermal curves at 3 bar pressure. This may give information about that enthalpy does not always increase under conditions of rising pressure, and it is necessary to find the reaction conditions in which the reaction works best. That is, effective pressure amount can change according to resin type.

Table 9. TW-R1 isothermal cure enthalpies

Pressure (bar)	Temperature (°C/dk)	Normalized Enthalpy (Jg^-1)	Pressure (bar)	Temperature (°C/dk)	Normalized Enthalpy (Jg^-1)
	90	87.99		90	104.97
1	100	92.33	5.6	100	107.67
1	110	95.82	3.0	110	102.32
	120	92.65		120	107.89
	90	100.24		90	106.74
3	100	114.25	7	100	100.87
3	110	115.30	7	110	116.94
	120	117.26		120	115.93

If the effect of 7 bar pressure on isothermal tests was examined, it could be seen that the enthalpy values are higher than the dynamic curves under 7 bar pressure and 1 bar isothermal curves. However, when the enthalpy values under 7 bar were compared with the enthalpy values of the isothermal curves under 3 and 5.6 bar pressure, similarities and differences were observed. This can be attributed to the reasons in the above sections where the effects of pressure on molecular mobility under 3 and 5.6 bar pressure conditions were mentioned. The increase trend in enthalpy values under the mentioned different pressures can be observed on **Figure 22**.

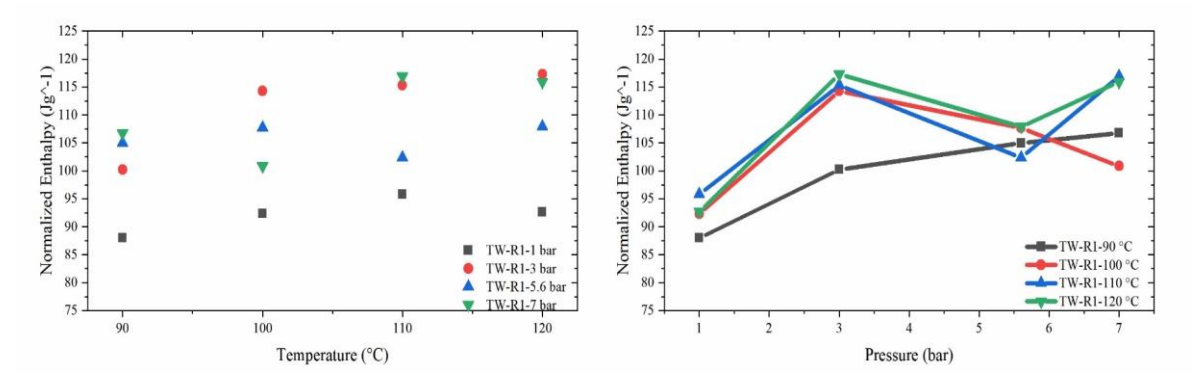


Figure 22. Comparison of isothermal TW-R1 enthalpy values with respect to temperature (left) and pressure (right)

Figure 23 and **Table 10** presents the curing times corresponding to cure degree under diverse pressures and at different temperatures. When the test results were interpreted, it was concluded that the effect of pressure could be observed more regularly at 90 °C, which is the lowest temperature and has the longest test period to cure. The reason for this can be explained as in **Section 2.2.3**. On the other hand, while a decrease in curing time was observed when the pressure at 90 °C, a significant increase in curing time was observed when the pressure was increased from 1 bar to 3 bar at 120 °C.

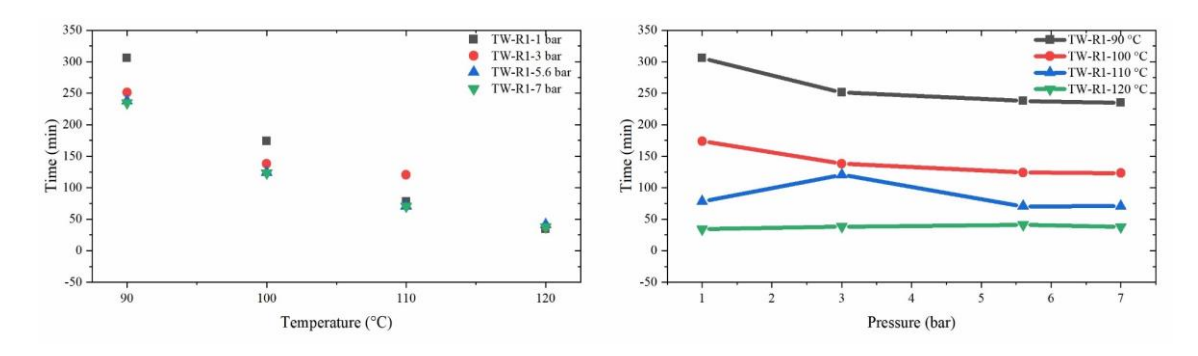


Figure 23. Comparison of isothermal TW-R1 curing times with respect to temperature (left) and pressure (right)

In essence, it was investigated that although the main effect of pressure is seen as reducing the void ratio and providing homogeneous distribution during production, it is believed that the effects of pressure on cure kinetics and cure enthalpy were also observed in this study. It should be remembered that the tested sample was prepreg and when considering molecular mobility, it should be taken into account that the fibers and void content can hinder reactions since they restrict the reaction surface area. In addition, another parameter that affects the enthalpy values is the time given to the curing reactions. Only if cure time is longer, the pressure can show its effect through the mentioned parameters.

Table 10. TW-R1 isothermal cure degree with respect to time

1 bar							
90 °(C	100 °		110 °	C	120 °	C
Conversion	Time	Conversion	Time	Conversion	Time	Conversion	Time
(%)	(min)	(%)	(min)	(%)	(min)	(%)	(min)
98	245.69	98.05	133.84	98	60.32	98	32.28
99	285.69	99.53	153.84	99	65.88	99	34.46
99.99	305.69	99.98	173.84	100	78.05	100	37.98
			31	oar			
90 °C	C	100 °	C	110 °	C	120 °	C
Conversion	Time	Conversion	Time	Conversion	Time	Conversion	Time
(%)	(min)	(%)	(min)	(%)	(min)	(%)	(min)
50	102.31	50	48.25	50	24.87	50	11.68
60	115.97	60	55.3	60	29.21	60	13.43
70	131.28	70	63.49	70	34.71	70	15.6
80	150.06	80	74.01	80	42.75	80	18.56
90	178.14	90	90.76	90	58.81	90	23.45
95	203.44	95	106.8	95	77.76	95	28.21
98	232.84	98	126.07	99	120.56	99	38.22
99	251.32	99	138.27	100	178.21	100	53.34
				bar			
90 °C	_	100 °		110 °C		120 °C	
Conversion	Time	Conversion	Time	Conversion	Time	Conversion	Time
(%)	(min)	(%)	(min)	(%)	(min)	(%)	(min)
50	99.4	50	46.58	50	22.6	50	11.4
60	112.62	60	53.35	60	26.18	60	13.26
70	127.42	70	61.14	70	30.5	70	15.58
80	145.45	80	70.93	80	36.19	80	18.78
90	171.99	90	85.82	90	45.35	90	24.23
95	195.3	95	99.26	95	54.03	95	29.69
99	237.68	98	114.56	98	64.15	99	41.02
100	286.34	99	123.95	99	70.39	100	52.12
				par			
90 °C		100 °		110 °		120 °	
Conversion	Time	Conversion	Time	Conversion	Time	Conversion	Time
(%)	(min)	(%)	(min)	(%)	(min)	(%)	(min)
50	97.87	50	45.95	50	22.65	50	12.32
60	110.85	60	52.69	60	26.17	60	14.21
70	125.36	70	60.47	70	30.4	70	16.49
80	143.01	80	70.3	80	35.98	80	19.51
90	169.08	90	85.28	90	44.97	90	24.28
95	192.2	95	98.75	95	53.64	95	28.69
98	218.58	99	123.07	99	70.83	99	37.49
99	234.81	100	150.09	100	90.08	100	50.08

2.2.10. Model Free Kinetics (MFK) analysis results vs. isothermal test results – R1

The MFK analysis and isothermal test results were compared for R1 for different temperatures **Figure 24.** The compatibility of the conversions against time was quite low at 90 and 100 °C. However, as the temperature increases, it was seen that compatibility increases slightly. For instance, at 120 °C the MFK analysis prediction times and the time of isothermal tests were quite compatible with each other. Nevertheless, incompatibilities

in the cure times of nearly 100% conversion degrees were also observed. It was interpreted that the formation of cross-links and in which regions they are intense and how restrictive this is for molecular mobility cannot be predicted by MFK analysis for resin. However, it was believed to be an analysis method that the manufacturer should not give up in terms of giving information about test times at the desired temperatures.

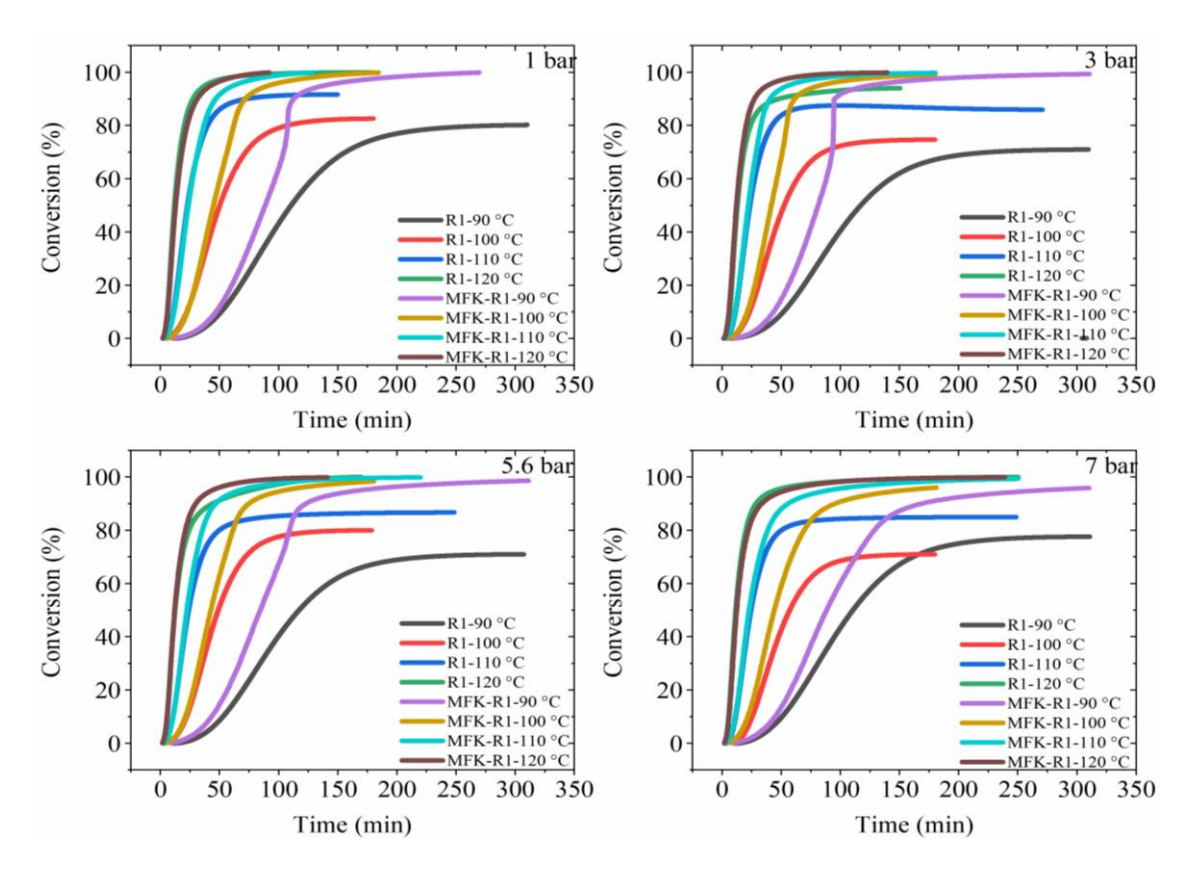


Figure 24. Comparison of R1 MFK analysis estimations and isothermal curves

2.2.11. Model Free Kinetics (MFK) analysis results vs. isothermal test results – TW-R1

Comparing the MFK estimation and isothermal test results of the TW-R1 prepreg, it was seen that they were in high agreement (**Figure 25**). In this way, the benefits of performing MFK analysis for the producer were confirmed. It will be possible to obtain information about time which needs to pass to achieve 100% cure degree at the desired temperature. Besides, the information can be obtained about cure degrees during cure cycle steps. The better working mechanism of the analysis in the final product (prepreg) was taken into account in the studies to determine the cure cycle.

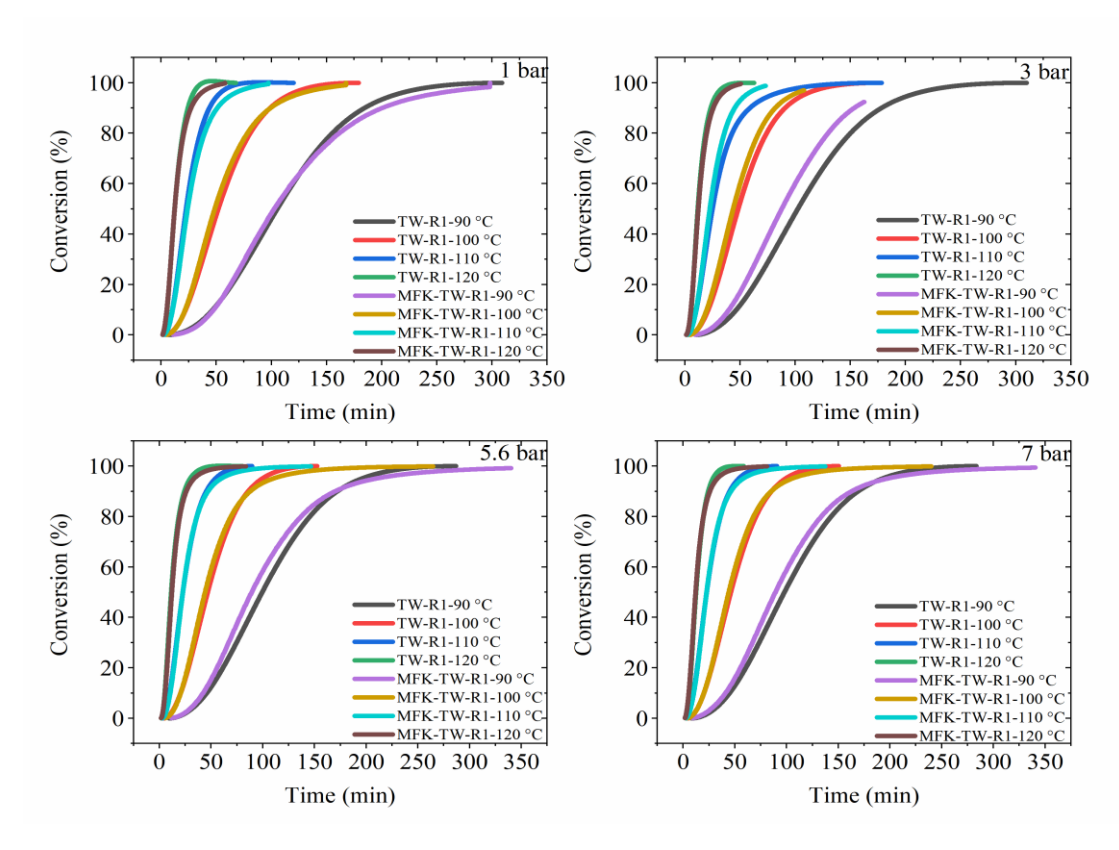


Figure 25. Comparison of TW-R1 MFK analysis estimations and isothermal curves

2.3. Experimental - Rheometer

2.3.1. Rheometer temperature sweep and gel time test methods

Temperature sweep and gel time tests were carried out with the Anton-Paar MCR 302 Rheometer device while the other studies on cure kinetics were conducted on the HP-DSC device. The test methods were based on EN6043 A for temperature sweep and EN6043 B for gel time. Measurements were made in shear strain mode and amplitude gamma 10% and angular frequency omega 10 rad/s, and gap ranged from 0.50 to 0.70.

Temperature sweep was tested between the temperatures of 50-200 °C. Gel time tests were performed for 90 and 120 °C according to the information obtained from the temperature sweep. The same test methods were applied for R1 and TW-R1 and the results were compared on complex viscosity indicating the total resistance to deformation of a material against temperature.

2.3.2. Temperature sweep and gel time – R1

The **Figure 26** and **Table 11** illustrates complex viscosity test results obtained from temperature sweep and gel time tests. Temperature sweep test start with 72.44 Pa.s complex viscosity at 50 °C and it decreased to 2.70 Pa.s at 120 °C. The gel time and

temperature, which are found by taking the point where the loss modulus (E') and storage (E") modulus crossing, are 39.082 min and 127.66 °C, respectively, and the complex viscosity value at gel point is 1342.4 Pa.s.

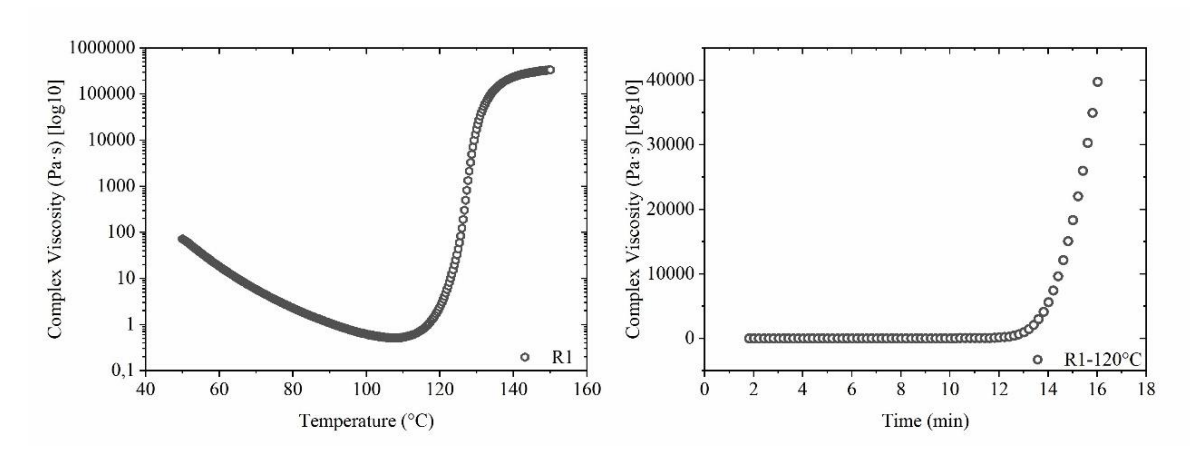


Figure 26. R1 temperature sweep (left) and gel time curves (right)

In the gel time test performed at 120 °C, the complex viscosity value first seen at 120 °C in the 5th minute is 0.25 Pa.s and the complex viscosity value is 2960.54 Pa.s with the gelation taking place in 12.00 minutes.

Table 11. Complex viscosity of R1 temperature sweep and gel time

	Temperature Sweep							
Time (min)	Temperature (°C)	Complex Viscosity (Pa·s)						
1.394	50.02	72.44						
6.411	60.10	18.21						
18.95	85.17	1.52						
21.46	90.19	1.07						
36.51	120.29	2.70						
Gel Time (39.082 min)	127.66	1,342.40						
	Gel time							
Time (min)	Temperature (°C)	Complex Viscosity (Pa·s)						
5.019	120.00	0.25						
Gel Time (12.033 min)	120.00	2,960.40						

2.3.3. Temperature sweep and gel time – TW-R1

The **Figure 27** and **Table 12** illustrates complex viscosity test results obtained from temperature sweep and gel time tests. The complex viscosity values obtained from temperature sweep test are 4807.9 Pa.s at 50 °C and 678.98 Pa.s at 120 °C. Besides, the gel time, temperature, and complex viscosity are 36.32 min, 122.31 °C and 3207.3 Pa.s, respectively. In addition to this information, from the temperature sweep curve in **Figure 27**, temperatures at which viscosity drops can be seen. These temperatures will be important throughout determining the dwell temperature (first isothermal stage) in the cure cycle.

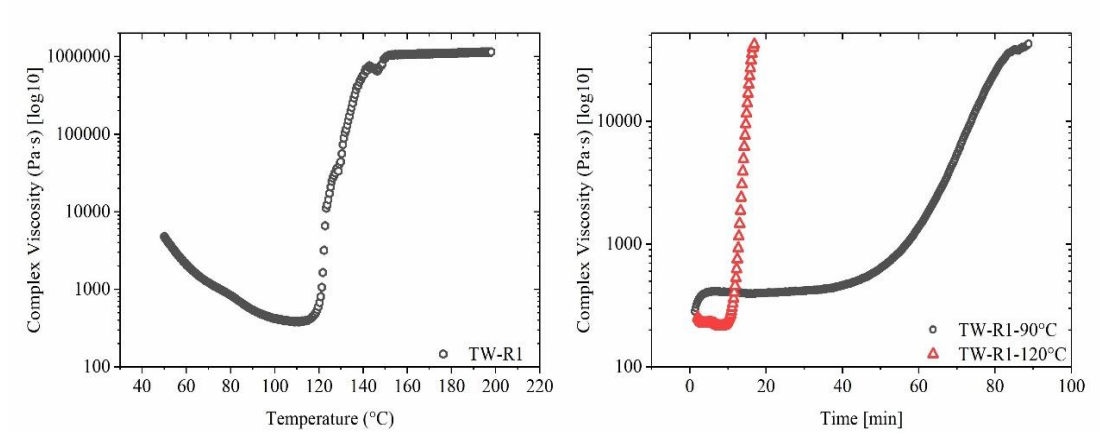


Figure 27. TW-R1 temperature sweep (left) and gel time curves (right)

A gel time test was conducted at 90 °C, firstly. The complex viscosity value first seen at 90 °C in the 4.20 min is 402.27 Pa.s. The complex viscosity value reached after 74.3 minutes at 90 °C is 12,817 Pa.s.

Second gel time test was conducted at 120 °C. The complex viscosity value first seen at 120 °C in the 4.80 min is 229.75 Pa.s. The gel time at 120 °C is 12.9 min and the complex viscosity value is 7,705.5 Pa.s. Data from **Table 12** compared the results between 90 °C and 120 °C gel time tests and it was seen that the gel time at 90 °C took quite a long time and the complex viscosity value is much higher than that obtained at 120 °C. It can be concluded that the molecular mobility at 90 °C is more controlled and homogeneous, and the crosslink density are higher and therefore complex viscosity is higher than the 120 °C. As mentioned in **Section 2.2.3**, the rate of molecular mobility at low temperatures changes the crosslink structure more and ensures the traceability of the changes.

Table 12. Complex viscosity of TW-R1 temperature sweep and gel time

Temperature Sweep				
Time (min)	Temperature (°C)	Complex Viscosity (Pa·s)		
1.447	50.02	4,807.9		
6.464	60.10	2,083.7		
19.01	85.18	665.97		
21.51	90.20	539.36		
36.326	120.30	678.98		
Gel Time (36.326 min)	122.31	3,207.30		
Gel time				
Time (min)	Temperature (°C)	Complex Viscosity (Pa·s)		
4.261	90.00	402.27		
Gel Time (74.336 min)	90.00	12,817.00		
Gel time				
Time (min)	Temperature (°C)	Complex Viscosity (Pa·s)		
4.853	120.00	229.75		
Gel Time (12.933 min)	120.00	7,705.50		

In addition to all of these, if the gel time curves are examined on **Figure 27**, it is possible to follow that time of the viscosity remains constant at that temperature and also these times are crucial when determining the dwell time in the cure cycle.

Table 13. Rheology and HP-DSC gel point comparison

	Temperature (°C)	Gel Time (min)	HP-DSC Conversion (%)
R1	90	114.50	50
	100	45.60	46
	110	23.57	50
	120	13.84	60
	90	74.36	30
TW-R1	100	48.60	53
	110	25.35	60
	120	14.20	60

The complex viscosity value of R1 under the same conditions is very low compared to TW-R1. It can make inferences two for that. The first one is that the resin in the prepreg is in the B-stage, resulting in a certain amount of cross-link structure in it. Moreover, the fibers in the prepreg also have a reaction to the incoming shear force and the force they transmit to the resin decreases when the test is performed on the device. If the curve profiles are examined on **Figure 26**, it can be observed that the behavior of the resin progresses in a certain order, conversely the situation is not the same for prepregs due to the fibers.

As an additional information, the times corresponding to the gel points of TW-R1 and R1 were found in the HP-DSC isothermal test results and matched with the cure degrees corresponding to these times. In HP-DSC tests, it was seen that the point where the cure degree, which increased rapidly with time, slowed down, coincided with the gel point obtained from the rheology test. Thus, these two results confirmed each other. It can be concluded that if the values are found where curing slows down, it can provide estimation about gel points. In the designed cure cycles, suitable time can be found so that the resin can be distributed homogeneously without reaching the gel point, and the maximum time to be kept at a constant temperature to achieve %100 cure degree can be determined, and a relevant time calculation can be made with HP-DSC test results. However, it is believed that supporting determination cure cycle with rheology tests will give more consistent results for providing workability to cure cycle.

2.4. Experimental – Cure cycle determination

2.4.1. Important parameters in determining cure cycle steps

Various parameters were considered while determining the cure cycle to produce carbon/epoxy composite laminate. For this purpose, it is necessary to maximize the mechanical and thermal properties of the matrix with the cure cycle in order not to experience losses in the mechanical properties of the composite. However, the energy expended with the cure time should be kept in an optimum amount to reduce the cost [67].

Contribution of the pressure used during the cure cycle is quite critical. It reduces the amount of void to less than 1% by carrying the fluid resin and being bleed. It allows the excess resin to be bleed and thus, it has a high fiber ratio of 55-60% by volume, which brings high mechanical properties. Another important issue in the cure cycle is the temperatures to be applied. First, the viscosity of the resin should be reduced by rising temperature where it wet the fabric thoroughly, enter the gaps and provide homogeneous distribution with the pressure nevertheless, without any gelation (dwell time). Thus, with the pressure, time is allowed for the air bubbles and water vapor in the structure to come out. The next step is the temperature that will allow the resin to cure. This temperature must be high enough for the resin to cure in a short time and not to cause great exothermic temperatures and a fire. However, the time between these steps also needs attention. Time should be allowed for reactions to occur during heating and enough time should be allowed to avoid shrinkage in the epoxy during cooling. Additionally, when holding at the curing temperature, enough time should be allowed to achieve 100% cure degree in composite part, however, this period should not be long enough to cause excessive energy [41,42,67-72].

2.4.2. Cure cycle determination

Based on all these assumptions and test results, the cure cycle estimation was made. The cure kinetic results of prepreg were taken as a source while specifying the temperatures and times of the cure cycle. The rigid barriers that restrict the mobility and interactions of the molecular chains such as the void content caused by weave of the fabric and tendency to absorb moisture from the environment exist in prepreg and owing to this, especially the effect of pressure, were seen more clearly in HP-DSC test results can be given as the reason behind this. Beside this, it is more correct to manufacture from an

input with a process history. Therefore, the final product form to manufacture was the prepreg and prepreg cure kinetics results were used while determining cure cycle.

Overall, these results suggest that the cure cycles can be examined on Figure 28 and Figure 29. The temperature to be used as dwell time was determined as follows. It was observed that when the TW-R1 prepreg temperature sweep test results were examined, the first temperature range of the complex viscosity with the lowest value is around 90 °C. This temperature provides that the resin will be homogeneously distributed with a minimum amount of cure reaction. Therefore, it was evaluated as the first target temperature. The ramp to reach this target was determined as 3 °C/min, where the effect of temperature and pressure, which gives the most balanced behavior in the test results, was seen the most. The time to hold at the first target temperature provides the resin to diffuse homogeneously and allow the voids to evacuate from the system or to reduce their volumes. It can be seen that from Figure 27, dwell time can be determined by checking the point where the slope starts to increase, that is, the viscosity gradually increases. Dwell time was determined based on the rheology test results performed at 90 °C as the 20th minute, which is the first point of viscosity increase. Cure degrees up to these processes in the cure cycle were calculated based on the conversions of the dynamic and isothermal test results. These values can be seen from **Table 14** and **Table 15**.

The next step in the cure cycle was stated to be 120 °C, which will give 100% cure within a reasonable time and found as the gelation temperature in the temperature sweep test. The hold time at this temperature was specified as 53 minutes based on the results of the isothermal test conversion carried out on the HP-DSC device in specific pressure amount. Cure degrees in the other steps were neglected due to the lower cure degrees when calculating the total cure degree and choosing hold time.

Finally, the cooling ramp was determined as 3 °C/min thus, as not to cause distortion of the produced plate because of the shrinkage in the resin. The cured composite structure was kept under pressure and vacuum in the autoclave up to a temperature of 50 °C. It was taken from the autoclave by releasing the pressure and left to cool at room temperature since after this temperature it will not affect the structure of the composite.

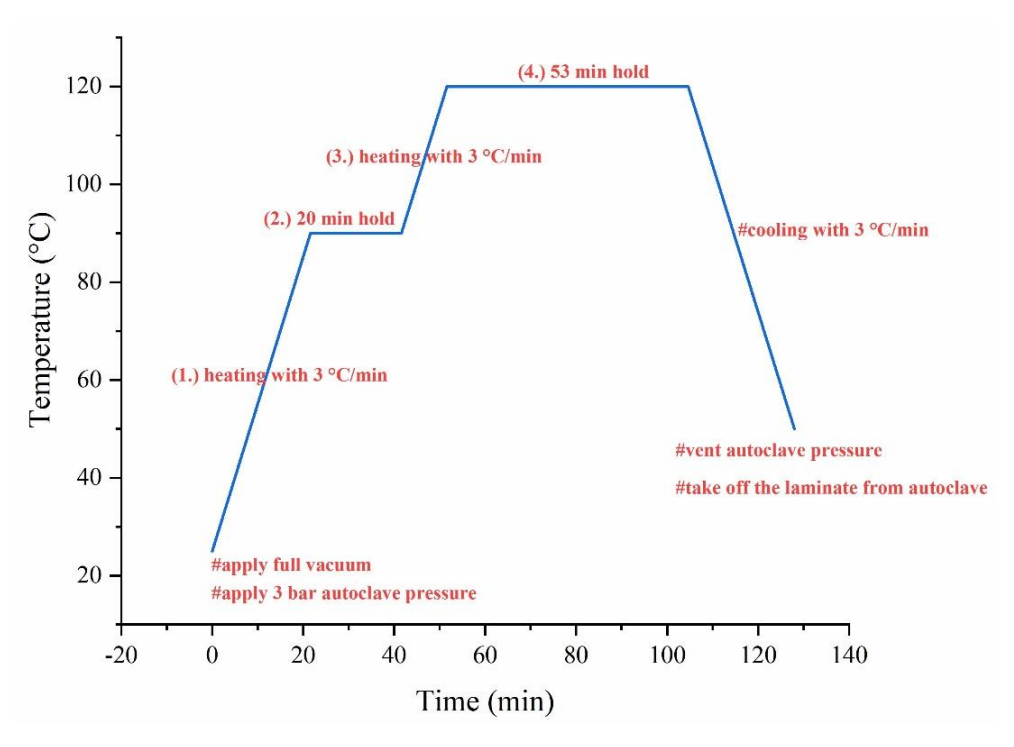


Figure 28. CC1 cure cycle

Table 14. CC1 cure cycle conversions

Cure Cycle Step	Conversion (%)
1	0.5
2	1.5
3	20
4	100

The amount of pressure to be applied in all these stages was chosen as 3 bar. This cure cycle will be referred to as CC1 (**Figure 28**). Especially, the isothermal test results were examined, it can be seen for this system that the amount of pressure did not affect so much the cure kinetics and 3 bar was the good candidate to achieve good mechanical properties. In other words, there was not much difference between 3 bar and 5.6 and 7 bar in terms of effect on the system. Therefore, the amount of pressure was chosen as 3 bar due to the energy consumption. On the other hand, it was desired to make a production test for the 7 bar pressure used in many productions in the literature and industry. This cure cycle will be referred to as CC2 (**Figure 29**). Considering all this, the amount of the effect of pressure during production and how it would make a difference over the characterization and mechanical tests were observed. The test times and temperatures were rearranged according to the dynamic and isothermal test results made under 7 bar pressure and the production was carried out.

The cure cycle specification steps can be determined by the size of the part to be produced, whether it has a complex shape-curved structure, the desired production time, and the

amount of energy to be consumed. Based on the dynamic-isothermal and rheology test results were made, it has been seen that cure cycle can be adapted. To exemplify, for the laminate having a larger surface area, the holding time for homogeneous distribution and void control at 90 °C can be increased to 30-40 minutes by checking the complex viscosity curve. Additionally, curing can be completed quickly around 35 minutes by choosing 130 °C instead of 120 °C.

Besides all this, some characterization and mechanical tests was done to check if the cure cycle is working. All mentioned parameters can be checked via **Table 16**. DSC tests were done in order to control the residual cure of the carbon/epoxy composite laminate, DMA tests were done according to EN6032 standards in order to control the cure degree and cross-link density through T_g behavior. Composite laminate density measurement was made according to the ASTM D792 method, the fiber-resin-void ratio was learned via ASTM D3171 standard. In addition to the characterization test, ASTM D3039 tensile test and ASTM D2344 interlaminar shear stress (ILSS) tests were applied to control its mechanical properties. The ability of working of the cure cycle was checked by comparing the results of the CC1 and CC2 cure cycles with the same test results of the composite laminates produced by the cure cycle obtained from the resin manufacturer. This cure cycle will be referred to as CCRef-1.

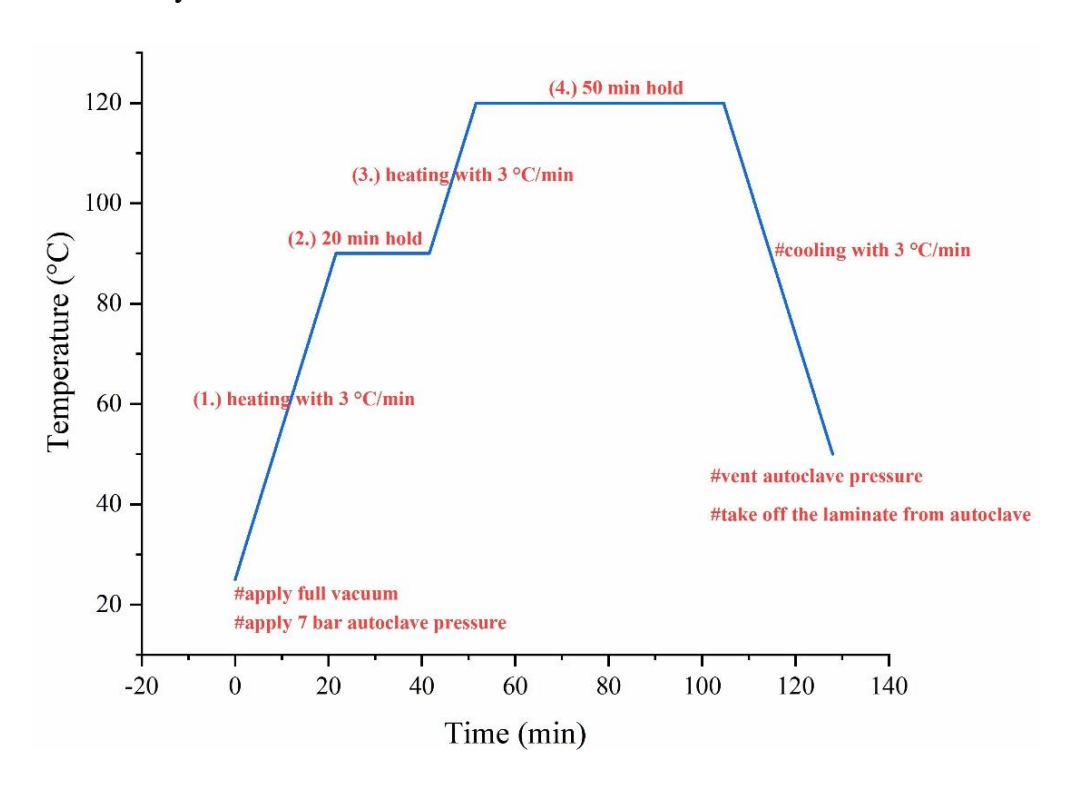


Figure 29. CC2 cure cycle

Table 15. CC2 cure cycle conversions

Cure Cycle Step	Conversion (%)
1	0
2	1.5
3	20
4	100

Residual curing test was performed on the DSC device to check the percentage of curing in the composite laminate produced with the CC1 cure cycle. According to the test results, the residual cure amount is 0.23 J/g. In other words, it can be concluded that the cure degree is 100%. According to the composite density test performed, the composite density is 1.48 g/cm³. This density is the same as produced with CCRef-1. In the constituent content determination test conducted, percentage of resin weight in composite laminate W_{m} (%), percentage of fiber weight in composite W_{r} (%) and void content V_{v} (%) are 42.98, 57.02 and -0.07, respectively. These values are very close to CCRef-1 production results, which are 41.64, 58.35 and -2.5, respectively. However, the initial content of resin in the prepreg was 42% and considering the resin ratio by weight in the composite laminate, it was seen that this value is 42%. It was concluded that there was no loss of resin due to pressure or dwell time, and the fiber-resin ratios were properly maintained and air bubbles or water vapor because of moisture were successfully removed. Additionally, although the pressure value is less, the void ratio was very low so that it did not reduce the mechanical properties and remains at the aviation standards. The reason for the negative test result is that no specific test has been performed for each batch of resin purchased from the manufacturer, and constituent content determination calculations have been made using the reference value given by the manufacturer. In addition, studies are carried out in the literature to cope with negative values because of the test procedures [47]. Since the reference resin density value was used, the reflection of the differences on the result caused the negative value. Nevertheless, it is certain that the void content is not more than 1%.

As the last characterization test, the DMA test results provided information about the T_g value and the degree of cure. The tan δ value obtained in CCRef-1 cure cycle is 142.01 °C and the value obtained from CC1 cure cycle is 148.03 °C. It was concluded that all the curing reactions were completed, and the crosslink density was quite high.

Table 16. Comparison of the characterization and mechanical test results of CC1 and CC2 cure cycles with CCRef-1

	CCRef-1	CC1	CC2
Residual Cure Enthalpy (J/g)		0.23	0.25
Pycnometer density (g/cm ³)	1.51	1.48	1.48
Percentage of resin weight in composite W _m (%)	41.64	42.98	41.86
Percentage of fiber weight in composite W_r (%)	58.35	57.02	58.14
Void Content V _v (%)	-2.5	-0.07	0.04
DMA tan δ T _g	142.01	148.03	145,29
Tensile Strength (MPa)	918.97	944.068	920.2
Tensile Modulus (GPa)	63.73	60.104	58.622
Short Beam Strength (MPa)	59.4	58.325	61.923

After the characterization tests were completed, the tensile test was first applied to composite laminate which product with CC1, and its tensile strength is 944 MPa and tensile modulus is 60.10 GPa. The tensile test results of CCRef-1 are 918.97 MPa and 63.73 GPa, respectively. Secondly, ILSS test was applied to composite laminate, and the short beam strength found as 58.32 MPa for CC1 and 59.4 MPa for CCRef-1. As can be seen from these results, the mechanical properties are very high in tensile strength and short beam strength. It was understood from all these results that the cure cycle works quite well despite the pressure value of 3 bar.

The test results of the cure cycle with 7 bar pressure were examined and the residual cure amount was found as 0.25 J/g according to DSC test results. It can be interpreted that the curing was completed as %100. Additionally, the composite density was found as 1.48 g/cm³. This density is the same as produced with CCRef-1 and CC1. The constituent content determination test results gave that percentage of resin weight in composite W_m (%), percentage of fiber weight in composite W_r (%) and void content V_v (%) are 41.86, 58.14 and 0.04, respectively. It can be seen from these results that, with increasing pressure towards 7 bar or due to dwell time, no resin loss was encountered, and fiber-resin ratios were preserved in a way to give high mechanical properties. However, compared to the CC1 cycle, the pressure value did not create a positive change on the void ratio, even if it is taken into account, it caused an increase in the void ratio, albeit very small.

The DMA test result is 145.29 °C and it showed that the reactions were completed, and the cross-link density is quite high. As mentioned earlier, the increase in the amount of pressure may cause a decrease in the degree of cure or crosslinking ratio in some resin systems. On the other hand, the findings can be interpreted from the DMA and residual

cure test results that this resin system works quite well under two pressure conditions, 3 bar and 7 bar pressures.

The tensile strength and modulus of the composite laminate are 920.20 MPa 58.62 GPa, respectively for CC2. Additionally, the short beam strength was also found as 61.92 MPa. To sum up, the investigation has shown that the cure cycle works quite well. It is known that there may be some resin systems only giving maximum mechanical properties at certain pressure values. However, it can be seen that this is not the case for this type of resin system, very high mechanical strengths can be obtained for both, 3 bar and 7 bar pressures.

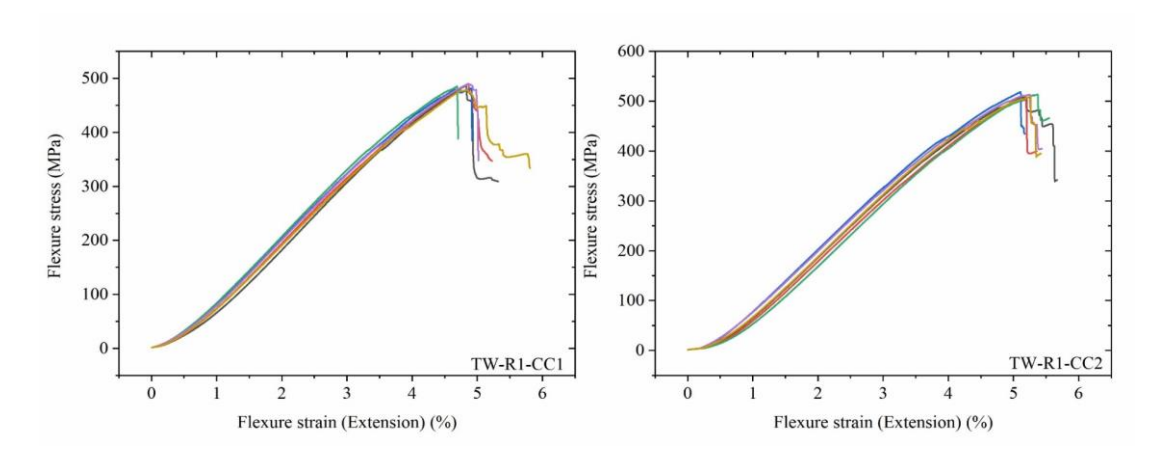


Figure 30. TW-R1 CC1 (left) and CC2 (right) interlaminar shear stress (ILSS) test results

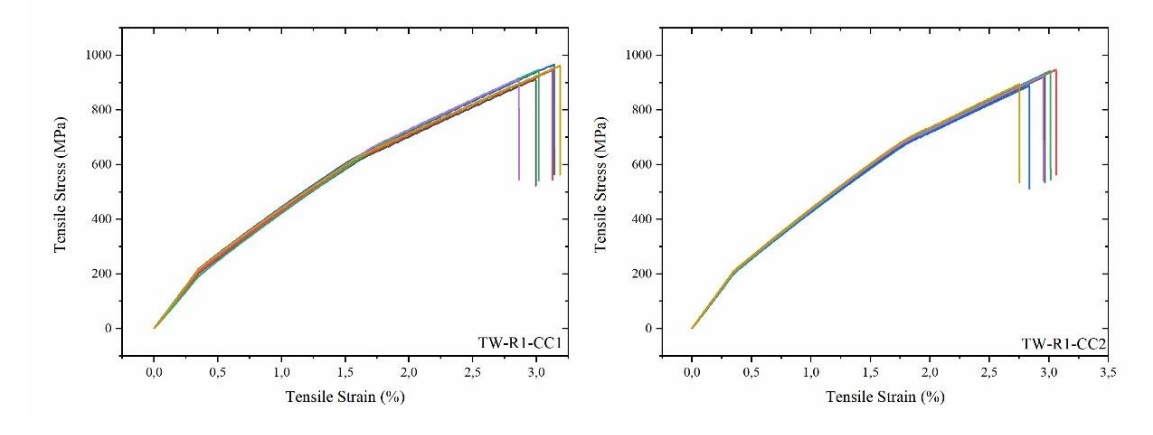


Figure 31. TW-R1 CC1 (left) and CC2 (right) tensile test results

Apart from all these, after the mechanical tests were completed, some failures on the tensile and shear test curves were taken attention and further research were made on this. **Figure 30** and **Figure 31** present the tensile test results for CC1 and CC2 that the slope of the curve that progresses linearly in the elastic region changes at the very beginning of the test. This caused the ultimate tensile strength to decrease. Similarly, some early damage was seen in the ILSS test results. This is due to a failure to the composite part.

The damage types and diverse case were investigated, it was concluded that failure was caused by the cracking of the matrix at the micro level. However, since this damage is small and the main load is carried on the fibers, it is understood that slope of curve did not drop too much and did not cause great decreases in ultimate tensile strength at this stage.



Figure 32. Tensile test fracture surfaces

The mechanism of matrix cracking error is as follows. It is stated that the hardness ratio between carbon fiber and polymer is 5-6. When the fiber and matrix interface is exposed to tensile and shear forces, micro-debonding occurs due to the difference in the transverse stiffness of the fiber and the matrix. After debonding, this can spread to the matrix and combine with other cracks or defects in the matrix. [16,73].

Another explanation for matrix cracking can be made as follows. Matrix damage first starts in fill tow in crimp zones and then continues to occur in warp tows and matrix pockets close to it as the load increases. Although this damage in the matrix is so much that it covers the entire matrix, the load carrying ability continues for a while since the main load is carried by the fibers in the composite structure. After a certain time, while the test is continued the fiber breaks, and catastrophic failure occurs in the composite structure. Fiber damage generally occurs in warp tows and crimp zones and moves in the tow transverse direction in a direction perpendicular to the loading direction. In other words, fibers at the cross-over point are exposed to higher loads and are more prone to breakage. Crimp-zones cause early damage and cause linear behavior to change and reduce ultimate strength [17,18].



Figure 33. Catastrophic fracture surface

In addition to all this, the damage mechanism followed by Acoustic Emission (AE) has been referred to as matrix damage also in another study. Transverse cracks in the matrix caused the stiffness of the material to decrease and the ultimate strength to decrease. This failure has proven by this study with AE. Other damage mechanisms occur in the composite structure, which continues for a certain period of time and interacts with the shear discontinuities caused by the transverse cracks and causes a further decrease in strength and this is also verified by AE. These accumulated damages finally caused complete rupture in the composite structure with the failure of the fiber [34]. In another study, optic nondestructive test method was used together with Acoustic Emission. In this study, matrix cracking occurs and as the load increases in the composite structure, delamination is triggered, and matrix cracks accumulate while spreading at the 0°/90° interface [35]. Similarly, in another study, matrix cracking for initial slope reduction and fiber tow rupture damage for final fracture were observed in microscopic examinations [36].

CHAPTER 3

3. Cure kinetic studies and determination of cure cycles for UD-R2 and UD-R2-MWCNT

3.1. Introduction

In Chapter 3, the cure kinetic behaviors of the UD-R2 and UD-R2-MWCNT systems were investigated, and cure cycles were suggested. The purpose of the current study in Chapter 3 is to determine the effect of the nanomaterial on the cure kinetics specifically through the pressure effect.

R1 resin was modified in order to increase its mechanical properties and T_g , and most importantly to reduce its viscosity in order to increase nano-material distribution in the resin, thus R2 resin was obtained. Furthermore, the twill fabric was replaced with UD fabric and the effect of the weave geometry on the cure kinetics was investigated as an additional parameter. This new system will be referred to as the UD-R2. Besides all this, the crucial thing is that UD-R2 was reinforced with 0.10% COOH-f-MWCNT nanomaterial which was added to resin and NCO-f-MWCNT nanomaterial was sprayed on the prepreg. This new system will be referred to as UD-R2-MWCNT.

The test methods to be applied to the UD-R2 and UD-R2-MWCNT were decided in line with the inferences from Chapter 2. In this regard, the test methods were determined and applied that had an effect on the cure kinetics and the cure cycle.

3.1.1. Effect of functionalized MWCNTs on cure kinetics, T_g and mechanical properties

MWCNT nano-material is used to reinforce different resin and prepreg systems as stateof the art. MWCNTs can be used as a reinforcer as received or can be functionalized with
different acid or amine groups before reinforcement. MWCNT nanomaterials were added
to the resin or prepreg as a reinforcer in order to increase the mechanical properties
Besides, they inherently change the cure kinetics of the resin also. To exemplify, COOHfunctionalized MWCNTs affect the cure kinetics. Nucleophilic addition reactions of
epoxy accelerate and shortens the cure time and increases their reactivity to epoxy groups
thanks to the difference in the catalytic effects of hydroxyl groups (–OH). Besides, the
reaction enthalpy increases due to the presence of surface functional groups. Studies have
been carried out to show that functionalized MWCNTs cause self-crosslinking and reduce
the curing peak in dynamic curves according to the size of specific surface areas and

aspect ratios. Additionally, more rapid reactions can be obtained at lower temperatures with MWCNTs [54,57,74–76].

With all this, there may be mechanisms where nano-cages form from time to time and chain mobility is restricted [1]. Similarly, mechanisms where -COOH groups cause a decrease in volume and restrict segmental movements related to their homogeneity in distribution have been reported. Besides, in this study, it is mentioned that the effect of MWCNT on changing the cure mechanism can be seen in isothermal DSC tests. In addition, this effect can only be seen if MWCNT is homogeneously dispersed in the resin it is added to. However, it has been stated that not every functional group will have an effect on changing the cure mechanism [4]. Some researchers found that the amine groups with high nucleophilic properties on the functionalized surfaces of MWCNTs caused ring opening of epoxy groups to accelerate curing and quickly bonded with the oxygen atom to form a secondary amine, thereby accelerating the curing reaction, and operating various cross-linking mechanisms, and this inspected with a shoulder in the DSC curve [2].

It has also been reported that changes in the mechanical properties of composites were seen when reinforced with nanomaterials. Functionalized MWCNTs, which react with the epoxy ring and form strong covalent bonds or physical interactions, increase the interfacial adhesion, thus improve the mechanical properties as the load distribution is better provided especially in bending and shear forces [57,58,76].

Diverse observations have been made regarding the effect of MWCNTs on T_g . In some studies, it has been commented that the epoxy reacts with the amine groups on the MWCNT surface, and crosslink structures that restrict the T_g behavior, which is manifested by chain mobility or free space mobility, are formed and this causes increase T_g . On the other hand, in some studies, observations have been made that the cross-links could not be completed due to the accelerated reactions if MWCNT was added, and the branching on the MWCNT surface decreased T_g due to the increase in length or the decrease in the density of the cross-links. However, it should be known that these mechanisms need to be investigated further, with no clear judgments on this issue [57,58,77,78].

3.2. Experimental - HP-DSC

3.2.1. Dynamic test methods and sample preparation for HP-DSC tests

UD-R2 and UD-R2-MWCNT prepreg samples were left outside to reach room temperature from their storage temperature of -18 °C. Prepregs with a resin ratio of 37% were placed in aluminum pans with a weight of 19 to 27 mg, and the pans were placed in the chamber where the device will take measurements under atmospheric pressure. Additionally, the pressure at the desired values is given to the system as N₂ gas from the outside with a system integrated into the device.

The tests were carried out once. However, after the tests performed at different heating rates under each pressure condition, the total enthalpy value of the system was found by performing residual cure tests with at least for one heating rate. Test repetitions were made when necessary. The most appropriate results were shared in the table. HP-DSC dynamic tests were carried out by increasing the temperature from 25 °C to 300 °C with heating rates of 3, 5 and 10 °C/min. However, the tests that follow the residual cure were performed as 3 cycles. The samples are cooled from 300 °C to 25 °C with 10 °C/min and then heated again from 25 °C to 300 °C with a heating rate of 10 °C/min. Pressure values were determined as 1 (atmospheric pressure), 3 and 7 bars in the results obtained from **Chapter 2**. The reason for choosing the 3 bar pressure was that it had a greater effect on cure kinetics than other pressure values in the studies conducted in Chapter 2 and that the CC1 cure cycle which was conducted under 3 bar pressure provided the characterization and mechanical test results with high agreement. However, as it will be explained in the following sections, since the 3 bar pressure condition did not cause certain change in the cure kinetics, it was desired to examine whether the high pressure amount would cause a change in the system, and the 7 bar pressure condition was added to the test methods.

The thermal transitions in the tests were monitored via STAR^e Software. The EN6041 standard was used in the test methods.

3.2.2. HP-DSC dynamic test results – UD-R2

In this section, the normalized enthalpy values were examined and compared with each other and the cure degrees corresponding to the temperatures were interpreted. Curing and conversion curves obtained as a result of dynamic tests can be checked via **Figure**

34. Enthalpy values are provided in **Table 17**. Curing enthalpies were determined to be in the range of 118-123 J/g, 120-126 J/g, 117-124 J/g under 1 bar, 3 bar and 7 bar pressures, respectively. It was observed that the curing onset and endset temperatures increase as the heating rate is increased. As expected, the increase in heating rate did not cause any change on the enthalpy value in the system.

It was observed that increase occurred in enthalpy values with the modified R2 resin. This was thought to be since it was modified with various crosslinking agents. It was also observed that T_g value of the R1 resin obtained from the DSC device increased from 108 °C to 126 °C under 1 bar pressure after it was modified with crosslinking agents to obtain the R2 resin. However, as can be seen in **Table 23**, the curing times increased compared to the curing times of TW-R1 (**Table 10**). In this case, it was thought that the crosslink agents caused to more crosslink in the structure and more crosslinking was related to the relative restriction of each other's molecular movements.

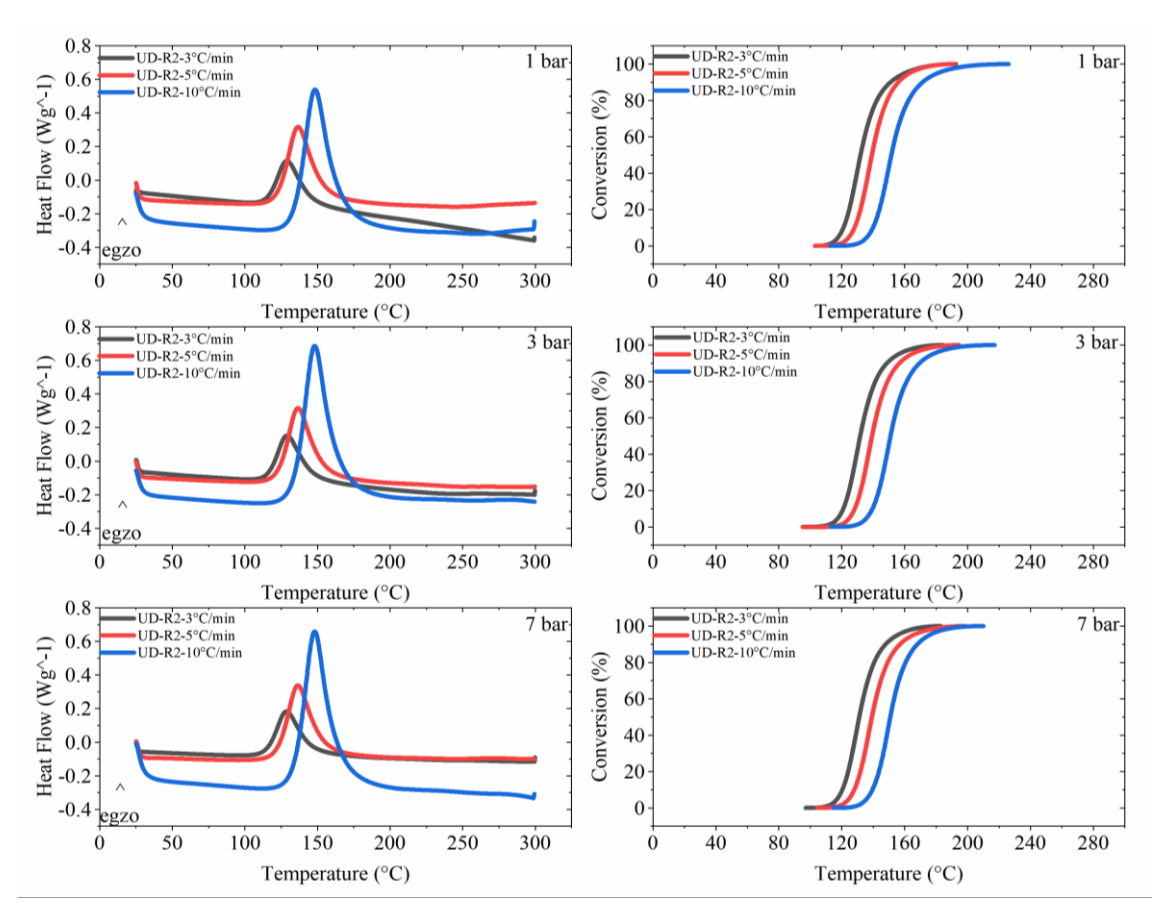


Figure 34. Dynamic enthalpy (left) and conversion (right) curves for UD-R2 under the pressures of 1, 3, and 7 bar at the heating rates of 3, 5, 10 °C/min

Table 17 presents that the enthalpy values are very close to each other under different pressures, unlike the TW-R1 prepreg, and no trend was observed among the results. The

reason for that could be attributed to the fact that UD prepreg is not woven fabric like twill fabric, so there is a difference in geometry between fabrics. The possibility of void formation in laid in only 0° direction is much less than the 2x2 twill woven fabric. It could be concluded that the application of pressure does not affect the parameters of this system such as reaction direction, time, and density with the removal of physical barriers and increasing reaction surface area that restrict molecular mobility during curing. In addition, there was no pressure-induced trend in the cure degrees when it is examined.

Table 17. UD-R2 dynamic cure enthalpies and onset temperatures

Pressure (bar)	Heating Rate (°C/min)	Normalized Enthalpy (Jg^-1)	Onset Temperature (°C)
	3	123.25	115.74
1	5	123.44	122.84
	10	118.94	134.50
	3	122.82	115.94
3	5	120.56	123.10
	10	126.85	134.31
	3	117.51	115.31
7	5	119.06	122.75
	10	124.14	134.59

3.2.3. HP-DSC dynamic test results - UD-R2-MWCNT

The results obtained from UD-R2-MWCNT prepregs reinforced with nanomaterials were examined, it was observed that the curing enthalpies in this system are in the range of 124-131 J/g, 125-135 J/g, 127-132 J/g at pressures of 1 bar, 3 bar and 7 bar, respectively. Curing and conversion curves obtained in dynamic tests are shown in **Figure 35**. Enthalpy values are provided in **Table 18**. It was also seen in these results that the cure onset and endset temperatures increased with the rise in heating rate. **Table 18** illustrates that the enthalpy values were higher in the system reinforced with nanomaterials compared with UD-R2. The reason for that can be explained as follows. Functionalized MWCNTs also participate in the reactions and form the crosslink structure, and therefore the extra reaction enthalpy occurs.

Closer inspection of the **Table 18** showed that the molecular mobility was not affected by the pressure due to the fabric geometry, as in the UD-R2 prepreg, and it did not induce any change in the reaction energy.

Besides all this, the results obtained from the effect of nano-material on T_g presented that the midpoint T_g value of UD-R2 increased from 126.41 °C to 136.51 °C under 1 bar pressure. Nevertheless, the same increase was not observed under 7 bar pressure. The T_g

value of UD-R2 under 7 bar pressure is 127.94 $^{\circ}$ C. These test results were obtained from the 3rd cycle dynamic test results performed at 10 $^{\circ}$ C/min.

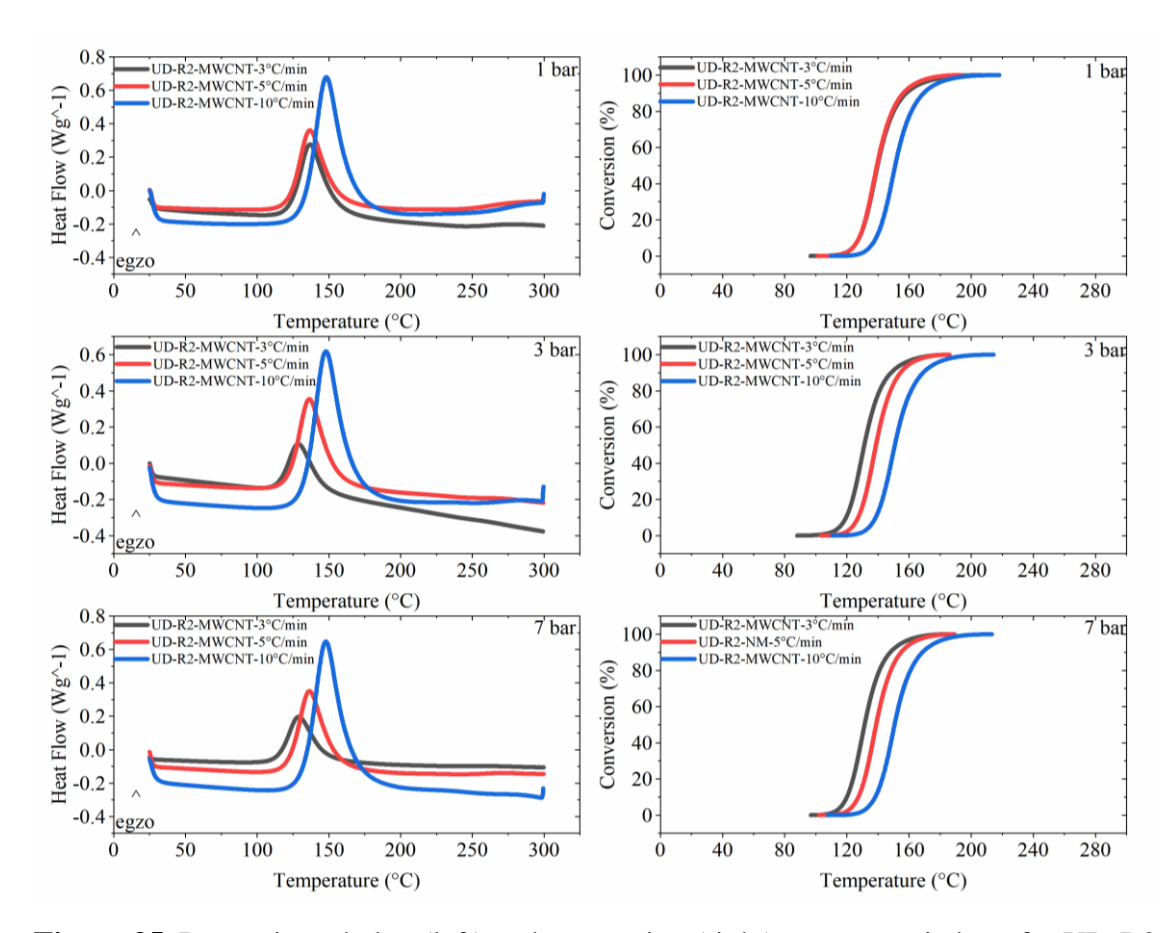


Figure 35. Dynamic enthalpy (left) and conversion (right) curves carried out for UD-R2-MWCNT under 1, 3, and 7 bar pressures at 3, 5, 10 °C/min heating rate

Table 18. UD-R2-MWCNT dynamic cure enthalpies and onset temperatures

Pressure (bar)	Heating Rate (°C/min)	Normalized Enthalpy (Jg^-1)	Onset Temperature (°C)
	3	124.67	122.76
1	5	131.72	122.55
	10	124.93	133.15
	3	128.65	114.75
3	5	135.90	122.07
	10	125.39	132.96
	3	127.28	114.76
7	5	132.83	122.23
	10	128.80	132.91

The pressure effect on T_g was also investigated on the UD-R2-MWCNT. Midpoint T_g values under 1, 3 and 7 bar pressures are 136.51, 134.99 and 128.43 °C, respectively. These test results were obtained from the 3^{rd} cycle, based on the dynamic tests performed at 10 °C/min. It is believed that this effect cannot be attributed to the degree of cure owing to the residual cure amount that comes out from the 3^{rd} cycle tests is 0 J/g. Therefore, it was concluded that when pressure was applied in prepregs, which were exposed to a heat

again after curing, the chain movements in the epoxy resin were affected more quickly by this heat and chain movements started at lower temperatures. This means that the composite would lose its mechanical properties at lower temperatures in pressurized environments.

Table 19. Tg variation according to different pressure conditions for UD-R2-MWCNT

	10 °C/min			
	Pressure (bar)	Midpoint T _g (°C)	Inflect. Pt. T _g (°C)	
UD-R2-MWCNT	1	136.51	122.5	
	3	134.99	117.17	
	7	128.43	116.5	

In addition to all these, it should be noted that the variation of the change in T_g values obtained from the DSC device may be high. T_g behavior can best be interpreted by evaluating the results from the DMA measurement. Explanations about the test results from the DMA will be made in the following sections.

With all this, it was observed that the cure degrees did not change with pressure and no trend was seen when the results were examined.

3.2.4. Model Free Kinetics (MFK) analysis – UD-R2 and UD-R2-MWCNT

In order to predict the cure mechanism of isothermal reactions and the cure time and degrees against temperature, MFK analysis was used, which provides information by analyzing a minimum of three test results made with different heating rates in dynamic DSC tests. It is possible to learn the cure kinetics of your sample with this method, and the temperatures and times to be selected while determining the cure cycle can be predicted from these data and even directly used. This analysis method offers rapid optimizations for production.

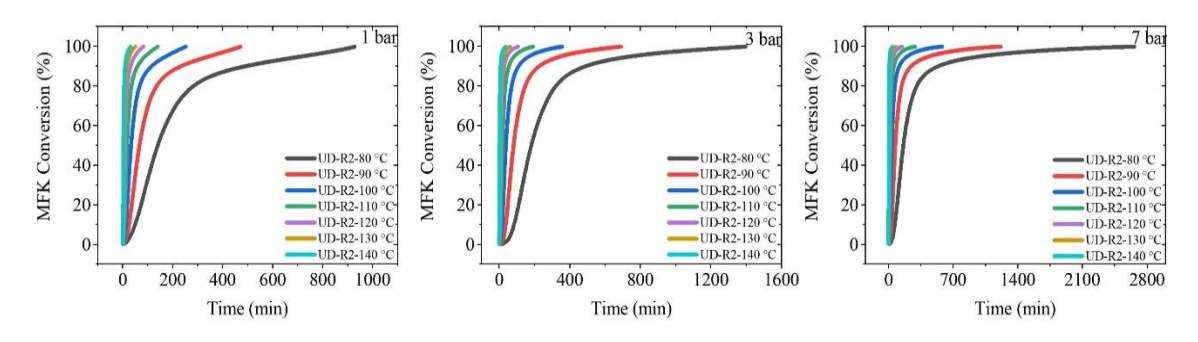


Figure 36. UD-R2 MFK Analysis isothermal cure degree estimation curves at 80, 90, 100, 120, 130 and 140 °C temperatures under 1, 3, and 7 bar pressures

MFK estimations for the UD-R2 and UD-R2-MWCNT were also made at different temperatures apart from isothermal test temperatures (**Figure 36**, **Figure 37**, **Table 20**, **Table 21**). In this way, observations could be made about the reaction kinetics broader. To give an example, with the MFK analysis applied to UD-R2 prepreg, it was found that different cure percentages such as 20, 60, 99% occur in the minute for 80, 90, 100, 110, 120, 130 and 140 °C temperatures. These analyses were examined separately at 1, 3 and 7 bar pressures. For instance, for UD-R2, it was seen that 99.9% cure will take place in 87.50 minutes at 120 °C under 3 bar pressures.

Table 20. UD-R2 MFK analysis estimation of cure degree versus time

	1 bar						
Conversion	Conversion MFK Conversion at Different Temperatures (min)						
(%)	80 °C	90 °C	100 °C	110 °C	120 °C	130 °C	140 °C
10	49.87	25.12	13.25	7.30	4.18	2.49	1.54
50	140.56	67.38	33.77	17.64	9.58	5.40	3.16
70	212.92	101.84	50.84	26.42	14.25	7.97	4.60
90	495.6	235.52	116.66	60.05	32.03	17.67	10.06
95	724.7	348.89	174.97	91.12	49.15	27.38	15.73
97	821.34	402.36	205.53	109.12	60.05	34.15	20.03
98	864.72	428.56	221.79	119.47	66.79	38.64	23.08
99	903.88	454.15	238.92	131.18	74.96	44.44	27.27
			3 bar				
Conversion		MFK C	onversion a	t Different T	Temperatur	es (min)	
(%)	80 °C	90 °C	100 °C	110 °C	120 °C	130 °C	140 °C
10	84.55	37.31	17.21	8.27	4.12	2.13	1.14
50	182.58	82.01	38.47	18.78	9.51	4.98	2.70
70	257.73	117.12	55.56	27.41	14.03	7.43	4.06
90	494.16	229.36	111.01	55.84	29.11	15.68	8.71
95	758.49	354.1	172.3	87.09	45.6	24.66	13.75
97	960.55	452.77	222.38	113.43	59.91	32.68	18.36
98	1098.06	522.62	259.18	133.48	71.18	39.20	22.24
99	1258.85	609.14	307.32	161.11	87.5	49.09	28.39
			7 bar				
Conversion		MFK C	onversion a	t Different T	Temperature	es (min)	
(%)	80 °C	90 °C	100 °C	110 °C	120 °C	130 °C	140 °C
10	68.33	31.76	15.38	7.74	4.03	2.17	1.21
50	160.68	74.12	35.64	17.81	9.22	4.93	2.72
70	233.77	108.14	52.14	26.12	13.55	7.27	4.02
90	544.41	247.52	117.47	58.00	29.7	15.73	8.59
95	1015.63	448.50	207.2	99.78	49.92	25.88	13.86
97	1433.07	629.14	288.96	138.36	68.83	35.48	18.90
98	1743.12	767.4	353.35	169.56	84.53	43.65	23.29
99	2153.56	959.22	446.75	216.79	109.25	57.02	30.74

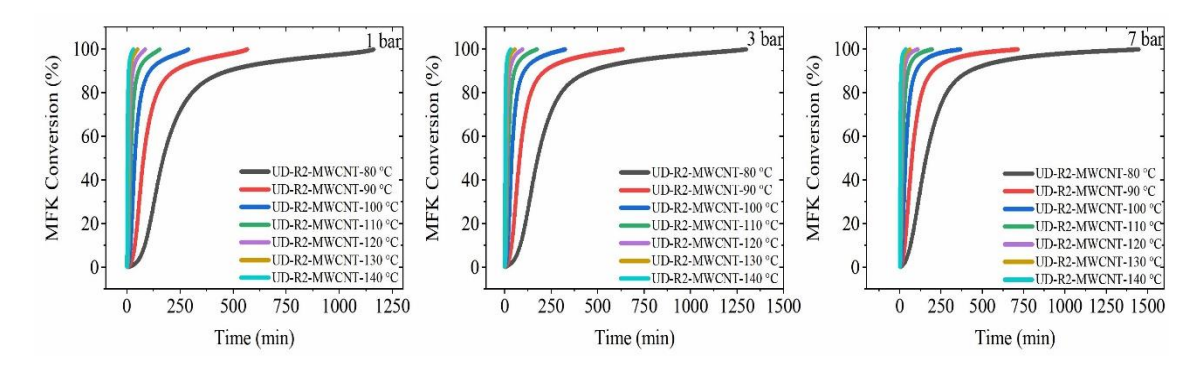


Figure 37. UD-R2-MWCNT MFK Analysis isothermal cure degree estimation curves at 80, 90, 100, 110, 120, 130 and 140 °C temperatures under 1, 3, 5.6 and 7 bar pressures Moreover, it was seen that the same cure degrees were reached in longer periods with pressure such as 99% curing was achieved in 454 minutes at 90 °C under 1 bar pressure, while this time was 609 minutes at 5.6 bar and 959 minutes at 7 bar for UD-R2. Although the same trend was examined for the UD-R2-MWCNT prepreg system and the increase in times with the effect of pressure was not as much as the UD-R2. For instance, at 90 °C, under 1 bar pressure, 99% curing was achieved in 544 minutes, while at 5.6 bar this time was 580 minutes, and at 7 bar it was 596 minutes.

Table 21. UD-R2-MWCNT MFK analysis estimation of cure degree versus time

	1 bar						
Conversion (9/)		MFK Co	nversion at	Different T	emperatur	es (min)	
Conversion (%)	80 °C	90 °C	100 °C	110 °C	120 °C	130 °C	140 °C
10	83.78	37.37	17.46	8.52	4.32	2.27	1.24
50	171.35	78.44	37.52	18.69	9.66	5.17	2.86
70	242.25	112.04	54.09	27.17	14.15	7.62	4.24
90	480.79	224.76	109.55	55.48	29.11	15.78	8.82
95	760.4	354.48	172.27	86.98	45.49	24.58	13.69
97	954.28	448.43	219.61	111.71	58.85	32.02	17.96
98	1054.51	500.61	247.76	127.4	67.86	37.34	21.18
99	1130.61	544.59	273.97	143.47	77.98	43.87	25.48
			3 bars				
Conversion (%)		MFK Co	nversion at	Different T	erent Temperatures (min)		
Conversion (%)	80 °C	90 °C	100 °C	110 °C	120 °C	130 °C	140 °C
10	83.49	36.96	17.19	8.37	4.25	2.25	1.23
50	177.81	80.51	38.15	18.86	9.69	5.16	2.84
70	244.72	112.46	54.03	27.04	14.05	7.56	4.20
90	469.91	219.39	106.88	54.14	28.43	15.44	8.64
95	736.59	343.3	166.87	84.31	44.14	23.88	13.32
97	937.87	439.84	215.04	109.24	57.48	31.25	17.51
98	1067.92	505.04	248.96	127.50	67.63	37.06	20.93
99	1208.82	580.47	290.75	151.39	81.69	45.56	26.19
7 bars							
Conversion (%)		MFK Co	nversion at	Different T	emperatur	es (min)	
Conversion (%)	80 °C	90 °C	100 °C	110 °C	120 °C	130 °C	140 °C
10	64.89	30.58	15.10	7.80	4.20	2.35	1.37
50	159.55	74.21	36.08	18.27	9.62	5.25	2.96

Table 21 continued							
70	227.88	106.62	52.07	26.47	13.96	7.62	4.30
90	427.75	202.96	100.37	51.57	27.45	15.10	8.56
95	654.77	310.57	153.45	78.74	41.84	22.96	12.99
97	853.67	406.00	201.08	103.39	55.03	30.25	17.13
98	1010.92	482.90	240.16	123.97	66.22	36.52	20.75
99	1234.18	596.04	299.64	156.3	84.36	46.99	26.96

3.2.5. Sample preparation and isothermal test methods for HP-DSC tests

The test sample preparation method in **Section 3.2.1** was used while preparing the isothermal test samples. As the isothermal test method, a different method was followed from the test methods used in **Section 2.2.7**, and the isothermal test was carried out only at 120 °C. For the reasons explained in **Section 3.2.1**, 1, 3 and 7 bar pressures were used as the pressure value. The reason why only 120 °C was chosen as the isothermal temperature value is that the gel time starts in this temperature range in the temperature sweep rheology data to be explained in **Section 3.3.1** and **3.3.2**, and the 100% cure degree is reached in an optimum time at this temperature. Therefore, as an isothermal test method, the temperature was increased from 25 °C to 120 °C with a heating rate of 190 °C/min in 0.30 sec for isothermal tests under pressures of 1, 3 and 7 bar. As stated, the test times were determined based on the MFK estimations. Nevertheless, the test was continued for longer periods than the MFK estimations in order to prove the workability of MFK analyses. Residual cure test methods were applied to all tests.

3.2.6. HP-DSC isothermal test results and comparison with MFK analysis results – UD-R2

Curing and conversion curves obtained in dynamic tests are shown in **Figure 38**. Enthalpy and conversion values can be checked via **Table 22** and **Table 23**. Closer inspection of the **Table 22** showed that the curing enthalpies are 127.20 J/g, 118.13 J/g, and 120.42 J/g under 1 bar, 3 bar and 7 bar pressures, respectively. It could be concluded that the enthalpy values are close to each other, and no change was observed with the pressure. Besides, the results are in same range within UD-R2 dynamic test results. This also differs with the changes related to the increase of enthalpy values in isothermal tests compared to the dynamic test results, which were examined in **Chapter 2**. It could be deduced that the result obtained from these test results is the same as the situation encountered in dynamic tests and since no physical barrier occurs in front of the reactions due to the fabric type in UD-R2, the effect of pressure is not needed.

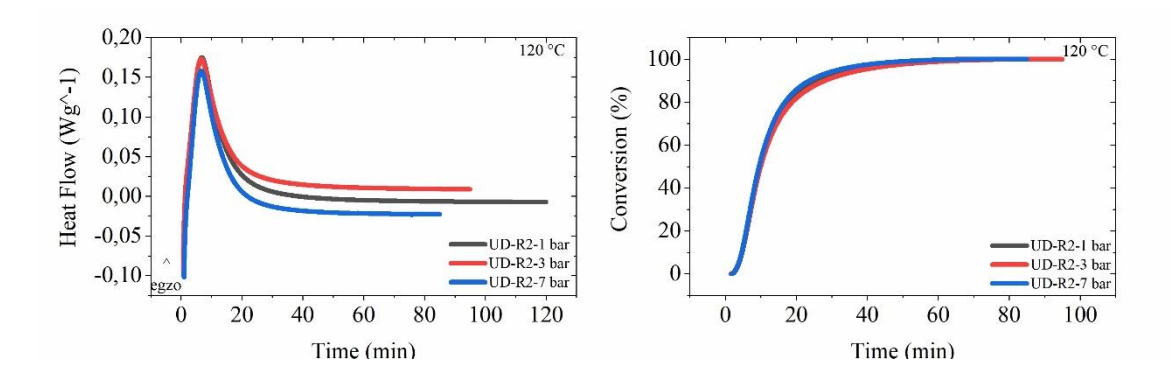


Figure 38. Isothermal enthalpy (left) and conversion (right) curves carried out for UD-R2 under 1, 3, 5.6 and 7 bar pressures at 90, 100, 110, 120 °C temperatures

Table 22. UD-R2 isothermal cure enthalpies

Pressure (bar)	Temperature (°C/min)	Normalized Enthalpy (Jg^-1)
1	120	127.20
3	120	118.13
7	120	120.42

If the MFK analysis and isothermal test results were compared, the **Table 20**, **Table 23** and **Figure 39** illustrate that the curves are compatible with each other, and the final curing times are very close to each other except 7 bar. Also, the curing times increased with the pressure with 3 bar, and decreased with 7 bar.

Table 23. UD-R2 isothermal cure degree according to time

1 bar		3 bar		7 bar	
120 °C		120 °C		120 °C	
Conversion (%)	Time (min)	Conversion (%)	Time (min)	Conversion (%)	Time (min)
50	9.89	50	9.92	50	9.46
60	11.71	60	11.84	60	11.13
70	14.17	70	14.52	70	13.36
80	18.00	80	18.85	80	16.77
90	25.64	90	28.07	90	23.70
95	34.09	95	38.69	95	31.86
98	44.84	98	52.80	98	43.09
99	51.82	99	62.34	99	51.14
100	74.36	100	94.38		

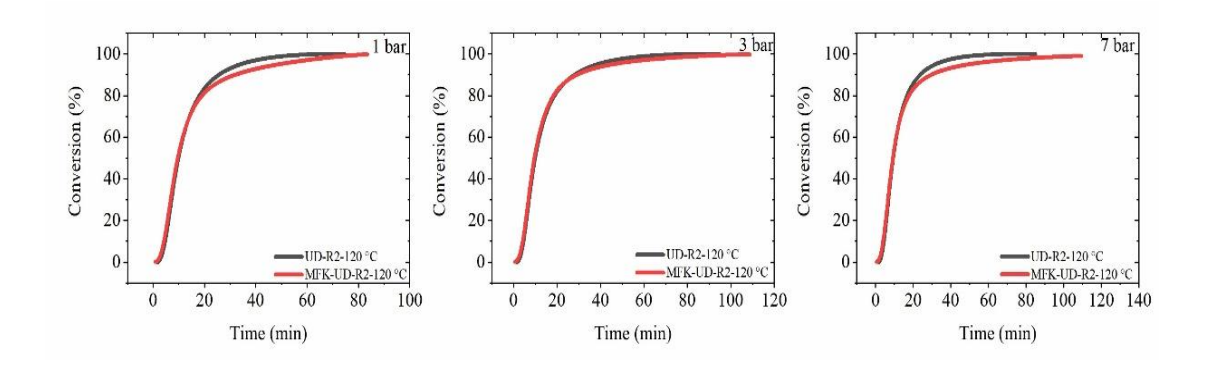


Figure 39. Comparison of UD-R2 MFK analysis estimations and isothermal curves

3.2.7. HP-DSC isothermal test results and comparison with MFK analysis results – UD-R2-MWCNT

Curing and conversion curves obtained in dynamic tests are shown in **Figure 40**. Enthalpy and conversion values can be checked via **Table 24** and **Table 25**. This table presented that the cure enthalpies are 125.32 J/g, 138.37 J/g, and 128.60 J/g under pressure values of 1 bar, 3 bar and 7 bar, respectively. It was also asserted that no changing occurred with the pressure when the enthalpy values were examined, and likewise, these results are in a similar scale with the enthalpy values obtained by dynamic tests. The explanation for UD-R2 (**Section 3.2.2**) is valid as the reason for this effect.

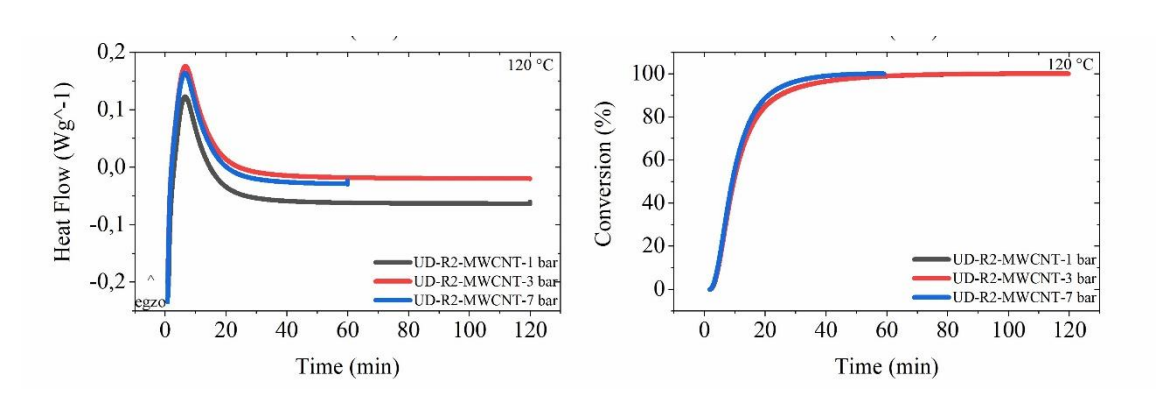


Figure 40. Isothermal enthalpy (left) and conversion (right) curves carried out for UD-R2-MWCNT under 1, 3, 5.6 and 7 bar pressures at 90, 100, 110, 120 °C temperatures

Table 24. UD-R2-MWCNT isothermal cure enthalpies

Pressure (bar)	Temperature (°C/min)	Normalized Enthalpy (Jg^-1)
1	120	125.32
3	120	138.37
7	120	128.26

When comparing conversions of UD-R2 and UD-R2-MWCNT, the consideration in **Table 23** and **Table 25** is curing times. That is, the curing time of UD-R2-MWCNT at

99% conversion was shorter compared to UD-R2. This is because the functional groups of MWCNTs, especially the one functionalized with -COOH, have a catalytic effect in the reactions. These functional groups attack the epoxy ring and rapidly open the epoxy ring. However, due to the large surface area of MWCNT, the reaction kinetics are accelerated with the increased intermolecular reaction surface area, and thus curing occurs faster.

Table 25. UD-R2-MWCNT isothermal cure degree according to time

1 bar		3 bar		7 bar	
120 °C		120 °C		120 °C	
Conversion (%)	Time (min)	Conversion (%)	Time (min)	Conversion (%)	Time (min)
50	9.530	50	9.67	50	9.19
60	11.20	60	11.40	60	10.80
70	13.50	70	13.80	70	12.80
80	17.10	80	17.30	80	15.70
90	24.60	90	24.80	90	21.00
95	34.50	95	36.30	95	27.00
98	50.10	98	53.20	98	35.10
99	62.40	99	66.10	99	40.50

The MFK analysis results and isothermal test results were compared and found that a very similar curing mechanism was observed in the progress rate of the reaction at 1 and 7 bar pressure values, and some differences were observed at 3 bar pressure (Figure 41). However, 99% curing time was found less according to MFK analysis estimation and especially curing time under the 7 bar pressure took a short time like 40 minutes similar to the UD-R2 test result. It has been mentioned in Chapter 1 that different pressure values may have a distinct effect on the cure kinetics of different resin systems. Here, it could be seen that the 3 bar pressure also provides adequate effect on results. However, it could be seen that the 7 bar pressure has a greater effect on the curing times in R2-based prepreg systems than in R1-based prepreg systems. On the other hand, it was observed that the MFK analysis could not figure out the mechanism by which MWCNTs accelerated crosslink formation in UD-R2-MWCNT, since the effect of nanomaterial factor was not used in creating mathematical formulas before. However, it is known that researchers are aware of this, and various modification studies are carried out on the subject [4]. Considering that the use of nanomaterial reinforced prepregs in the composite industry will increase in the future, it is believed that perhaps a coefficient for this effect should be defined in the kinetic equations created and the equations should be modified.

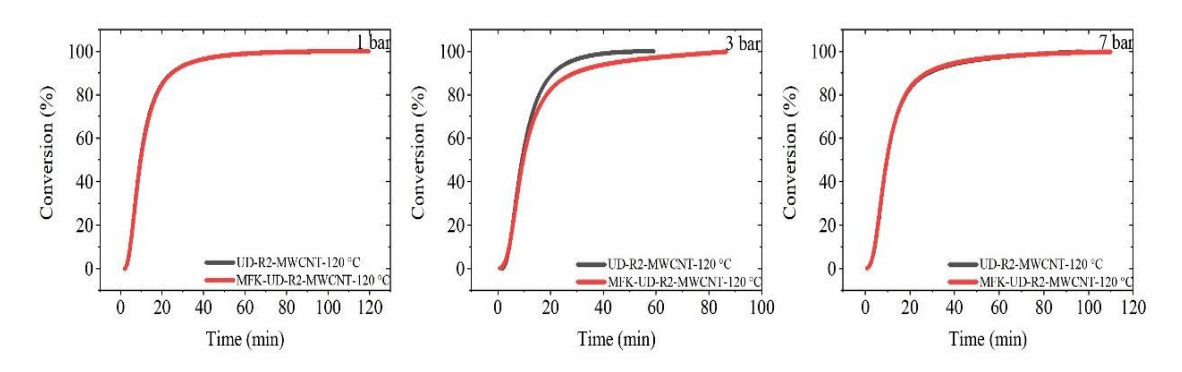


Figure 41. Comparison of UD-R2-MWCNT MFK analysis estimations and isothermal curves

3.3. Experimental - Rheometer

UD-R2 and UD-R2-MWCNT prepregs were tested with Anton-Paar MCR 302 Rheometer device. Temperature sweep test was carried out between 50-200 °C based on EN6043 A standard and as a result of the data obtained from this test, gel time tests were carried out at temperatures at 90 and 120 °C according to EN6043 B standard, as in Chapter 1. Measurements were made in shear strain mode, amplitude gamma 10% and angular frequency omega 10 rad/s, and gap ranged from 0.50 to 0.70.

3.3.1. Temperature sweep and gel time – UD-R2

As shown in **Figure 42** and **Table 26**, complex viscosity values are 2,135.30 Pa.s at 50 °C and 586.03 Pa.s at 120 °C. The gelation time of the temperature sweep is 36.896 min at 123.30 °C and the complex viscosity value is 3382.80 Pa.s. As in **Chapter 2**, the temperatures at which complex viscosity drops were determined on the temperature sweep curves and evaluated as the dwell temperature parameter to be used in the cure cycle.

The gel time test at 90 °C, the complex viscosity value in the first minute of reaching this temperature (3.5 minutes for test time) was found to be 559.73 Pa.s, and after 81.87 minutes at this temperature gelation occurs and the complex viscosity value reached 28,549.00 Pa.s.

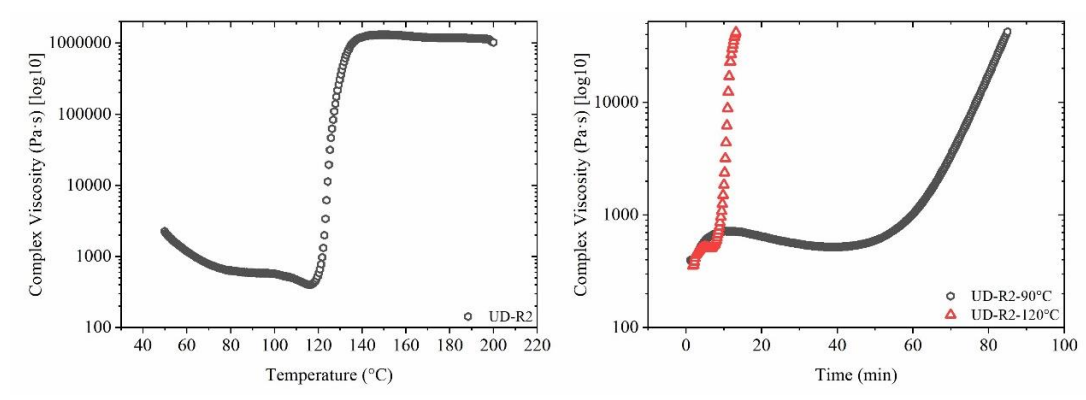


Figure 42. UD-R2 temperature sweep (left) and gel time curves (right)

The information about the gel time test performed at 120 °C is as follows. The time 120 °C per minute was reached (3.6 minutes for test time), the complex viscosity value is 519.86 Pa.s. Also, the gel time at 120 °C is 9.12 minutes and the complex viscosity value is 4,397.10 Pa.s.

Table 26. Complex viscosity of UD-R2 temperature sweep and gel time

Temperature sweep					
Time (min)	Temperature (°C)	Complex Viscosity (Pa·s)			
0.502	50.31	2,135.30			
5.27	60.06	1,182.90			
17.8	85.18	606.97			
20.3	90.20	596.89			
35.4	120.30	586.03			
Gel Time (36.326 min)	123.30	3,382.80			
	Gel time				
Time (min)	Temperature (°C)	Complex Viscosity (Pa·s)			
3.5	90.00	559.73			
Gel Time (74.336 min)	90.00	28,549.00			
Gel time					
Time (min)	Temperature (°C)	Complex Viscosity (Pa·s)			
3.6	120.00	519.86			
Gel Time (9.1261 min)	120.00	4,397.10			

It is apparent that when the TW-R1 and UD-R2 test results were compared, the viscosity values of UD-R2 are lower at different temperatures obtained from the temperature sweep test. As mentioned in **Chapter 2**, one of the reasons for the modification of the R1 resin was to lower the viscosity. One of the reasons for the modification was that the viscosity of the R2 resin is high and this sometimes causes difficulties during the production processes and creates some difficulties in the dispersion of MWCNTs in the resin to be reinforced with the nanomaterial. However, it was seen that the viscosity values of UD-R2 are higher in the gel time tests performed at 90 and 120 °C. The reason is that other components used to increase the cross-link structure in the R2 resin. Inherently, the

viscosity of the R2 resin increased faster with the rising of the crosslink density in the early stage at 90 and 120 °C. If the complex viscosity values after the gel point were analyzed the complex viscosity results are 12,817.00 and 28,549.00 Pa.s for TW-R1 and UD-R2, respectively at 90 °C. It could be concluded that the crosslinking agents could display their effects when they have more time for molecular mobilities

3.3.2. Temperature sweep and gel time – UD-R2-MWCNT

As indicated in **Figure 43** and **Table 27**, the complex viscosity values obtained as a result of temperature sweep are 2847 and 953.39 Pa.s for 50 and 120 °C, respectively. The gel point is at 123.30 °C in 36.92 minutes and the viscosity value is 3,639.60 Pa.s.

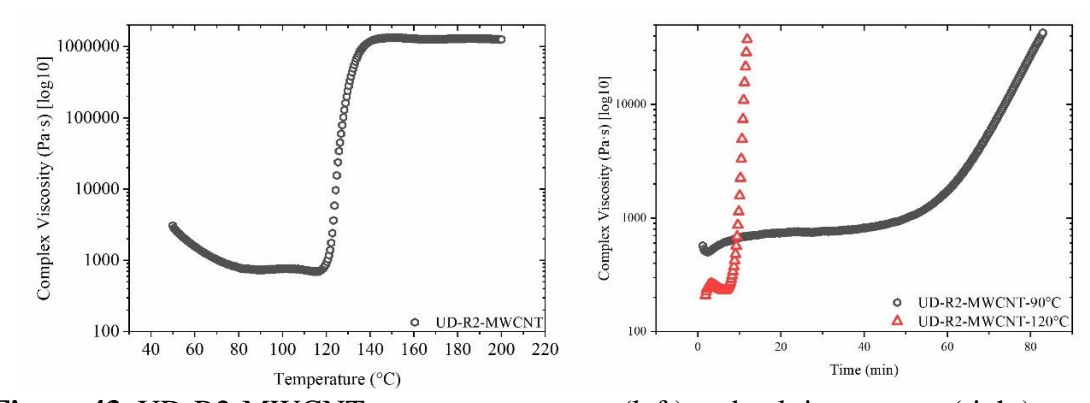


Figure 43. UD-R2-MWCNT temperature sweep (left) and gel time curves (right) The gel time value at 90 °C is 560.15 Pa.s at 3.5.min, and after 78.47 minutes, gelation occurs, and the viscosity value rises to 24,951 Pa.s.

Table 27. Complex viscosity of UD- R2-MWCNT temperature sweep and gel time

Temperature Sweep						
Time (min)	Temperature (°C)	Complex Viscosity (Pa·s)				
0.502	50.44	2,847.00				
5.27	60.07	1,563.80				
17.8	85.19	755.45				
20.3	90.19	740.54				
35.4	120.28	953.39				
Gel Time (36.923 min)	123.30	3,639.60				
Gel time						
Time (min)	Temperature (°C)	Complex Viscosity (Pa·s)				
3.5	90.00	560.15				
Gel Time (78.476 min)	90.00	24,951.00				
Gel time						
Time (min)	Temperature (°C)	Complex Viscosity (Pa·s)				
3.2	120.00	243.04				
Gel Time (9.0186 min)	120.00	4,969.70				

If these values are mentioned for 120 °C, the complex viscosity value becomes 243.04 Pa.s at 3.2 minutes and 120 °C and gel point takes place very rapidly in 9 minutes and the viscosity value becomes 4,969.7 Pa.s.

The test results revealed that an increase in complex viscosity values obtained from temperature sweep test was observed due to its nanomaterial reinforced structure as expected. However, when the viscosity values in the 90 and 120 °C gel time test were examined, it was seen that the values are very close to each other. The reason for this is thought to be related to the fact that both are based on the same resin content and the density of the crosslink structure which starts to increase in the same amount.

3.4. Experimental - Important parameters for cure cycle steps and cure cycle determination

The cure cycle should be design as follows. Cure cycle should maximize the interface bond between fiber and matrix and reduce the void ratio below 1% to give the best thermal and mechanical properties, while minimizing energy consumption and costs. The effect of pressure in cure cycle is very important in keeping the fiber-resin ratio at an optimum level and minimizing the void ratio. Pressure uses the viscosity of the resin while reducing the void ratio. The resin viscosity should be low enough to provide homogeneous distribution in the composite laminate to be produced and to remove a certain amount of bleed from the system by carrying air bubbles and water vapor with it. For the UD-R2 and UD-R2-MWCNT systems, this isothermal holding temperature was found to be 90 °C based on the temperature sweep test results. The heating rate required to reach this temperature was chosen as 3 °C/min, thus, significant time was provided for molecular mobilities. The dwell time at this temperature was determined as 20 minutes based on the gel time test result at 90 °C. Although this system does not contain a large amount of void content, as the temperature increases micro-voids will form and homogeneous distribution of the resin should be ensured.

The second isothermal step of the cure cycle was selected as the temperature at which the curing reactions would be completed, and this temperature was determined as 120 °C for both systems based on the isothermal and rheology test results. This temperature should be high enough to allow 100% curing of the resin in an optimum time, however not too high so as not to waste much energy. The heating rate to 120 °C was also chosen as 3 °C/min, which would allow molecule and chain movements. The times to be held at 120

°C was determined as follows. First of all, it should be noted that the number of autoclave manufacturing runs required for both UD-R2 and UD-R2-MWCNT prepreg systems are four based on the isothermal test results under 3 bar and 7 bar pressures. Besides, the characterization and mechanical tests performed for the manufactured parts have to be repeated. Considering the cost of the autoclave production process and carefully examining the test results, it was decided that a common denominator could be found for these two systems and manufactured two autoclave cycles instead of four. That is, two different pressure conditions will be tested for these two systems for the same durations. It would be seen that the time required to reach 98% cure degree for both systems under 3 bar pressure is 53 minutes and this time was determined as an isothermal hold time at 120 °C in cure cycle when the detailed examination was made from **Table 23** and **Table 25**. This cure cycle will also be referred to as CC3 (**Figure 44**).

However, if the isothermal test results of 7 bar pressure are examined, it can be seen that the time required to reach 99% curing degree for UD-R2 is 50 minutes, this time is 40 minutes for UD-R2-MWCNT system. Here, the common denominator was found as follows. Since the curing time required for the UD-R2 system is longer than that of UD-R2-MWCNT and holding longer in the autoclave will not have any disadvantages, the holding time at 120 °C was chosen as 50 minutes. This cure cycle will also be referred to as CC4 (**Figure 45**). However, there is a reference cure cycle applied for these systems and it is applied to both systems in the same way. This cycle will also be referred to as CCRef-2.

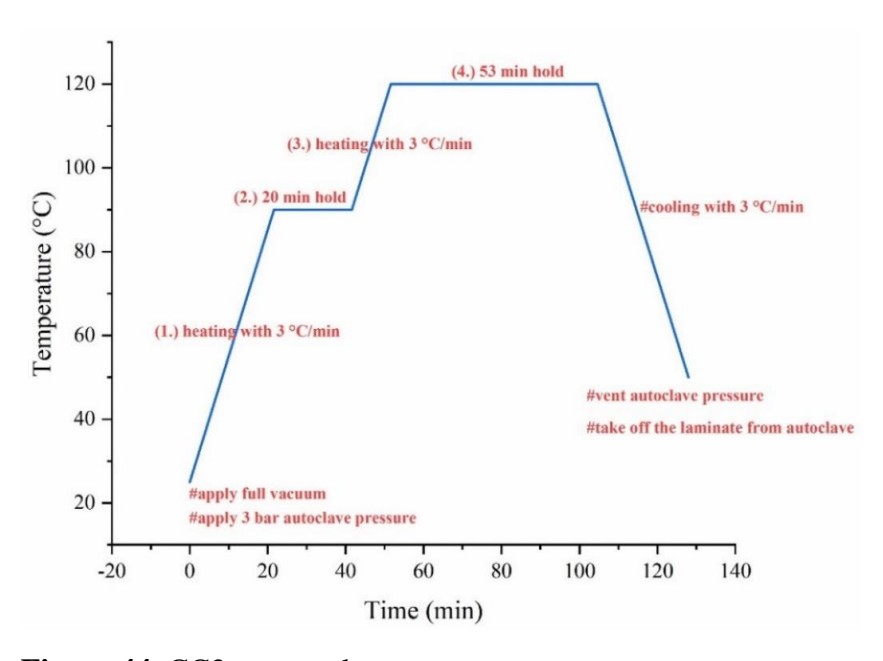


Figure 44. CC3 cure cycle

After the hold stage at 120 °C, composite laminate was cooled in an autoclave up to 50 °C at a low cooling rate of 3 °C/min in order to avoid shrinkage and then left to cool at room temperature.

CC3 cure cycle workability was checked through some characterization and mechanical tests. Besides, CC4 cure cycle workability was checked through some characterization tests. For this purpose, DSC test for residual cure control, DMA test in accordance with EN6032 standard to measure T_g behavior, tests in accordance with ASTM D792 and ASTM D3171 standards to learn composite density and component content were performed. In addition, the tensile strength test was applied according to ASTM D3039 standard and the interlaminar shear stress (ILSS) test, which is one of the mechanical properties most affected by the void ratio, was applied in according to with ASTM D2344.

All of the test data were presented in **Table 28** since the data of these test results belong to two different prepreg systems and their two different cure cycles. This has emerged as a situation that seems necessary to be done in order to avoid confusion.

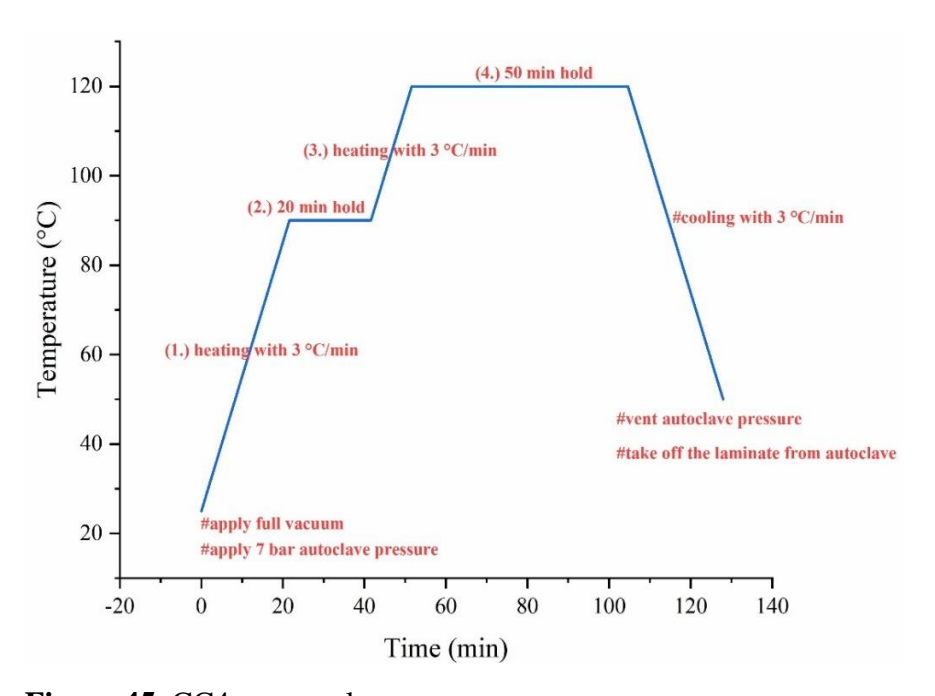


Figure 45. CC4 cure cycle

Firstly, the characterization test results of the CC3 and CC4 cure cycles were examined. It should be remembered that while determining CC3 cure cycles, the time that will give a cure degree of 98% was chosen as the second isothermal holding time. When the residual cure test results of the CC3 curing cycle were examined, the cure degree was calculated as 98.67% when the enthalpy value that should be found in the system is taken as 121 J/g on average for UD-R2. The cure degree was found as 98.88% when the total

enthalpy value of UD-R2-MWCNT was taken as 128 J/g. In other words, it can be concluded that the CC3 completed the curing reactions for UD-R2 and UD-R2-MWCNT.

Table 28. Comparison of the characterization test results of CC3 and CC4 cure cycles with CCRef-2

	UD-R2- CCRef-2	UD- R2- CC3	UD- R2- CC4	UD-R2- MWCNT- CCRef-2	UD-R2- MWCNT- CC3	UD-R2- MWCNT- CC4
Residual Cure Enthalpy (J/g)	-	1.60	1.10	2.13	1.43	2.17
Pycnometer density (g/cm ³)	1.53	1.55	1.55	1.54	1.53	1.53
Percentage of resin weight in composite W _m (%)	35.07	35.30	35.23	37.26	37.51	37.95
Percentage of fiber weight in composite W_r (%)	64.93	64.70	64.77	62.74	62.49	62.05
Void Content V _v (%)	-0.62	-1.62	-1.74	-0.68	-0.16	-0.09
Tan δ T _g (°C)	163,25	151.80	158.74	154.09	149.46	157.57

While determining the CC4 cure cycle, the second isothermal hold time was chosen as the time to give a 99% cure degree. When the residual cure test results of the CC4 cure cycle were examined, the curing degree was calculated as 99.09% when the enthalpy value required to be found in the system is taken on average 121 J/g for UD-R2. If the total enthalpy value of UD-R2-MWCNT is taken as 128 J/g, the cure degree was found to be 98.30%. That is, it can be concluded that for the CC4 curing cycle the curing reactions for UD-R2 and UD-R2-MWCNT were also completed.

Based on the density test conducted with the ASTM D792 standard for UD-R2 and UD-R2-MWCNT, it is seen that the densities obtained as a result of CC3 and CC4 are the same as the composite laminate obtained from the reference cure cycle. Likewise, in the constituent content tests based on the ASTM D3171 standard for UD-R2 and UD-R2-MWCNT, CC3 and CC4 cure cycles did not cause any change in fiber-resin weight ratios, and dwell time did not cause any resin loss. When the void content was examined, very low values were obtained. The reason why void contents give negative values is that the density test was not performed for each batch taken from the resin manufacturer and constituent content calculations were made over the determined reference value. It was concluded that the void ratio remained within the aviation standards.

The last of the characterization tests was DMA, which was performed using the EN6032 standard. It was observed that it was 7% less than the value of the reference composite production when the tan δ T_g value for UD-R2 was examined for the CC3 cure cycle.

However, for the CC4 cure cycle, this value is 2.76%. When the tan δ T_g values for UD-R2-MWCNT were examined, it was found that the T_g value of CC3 production was 3% less than the reference value. Besides, the tan δ T_g value of CC4 production is 2.20% higher than the reference composite production.

Table 29. Comparison of the mechanical test results of CC3 and CC4 cure cycles with CCRef-2

	UD-R2-CCRef-2	UD-R2-CC3	UD-R2-CC4
Tensile Strength (MPa)	2399.37	2294.38	2517.12
Tensile Modulus (GPa)	149.63	127.93	139.10
Short Beam Strength (MPa)	69.91	73.47	73.75

When the mechanical test results were examined, it was found that the tensile strength of the UD-R2 prepreg decreased by 4.37% in CC3 cycle with respect to the reference as a result of the test obtained based on the ASTM D3039 standard. However, when the tensile test results were examined for CC4, the tensile strength of UD-R2 prepreg was 4.7% higher than the reference tensile strength.

Lastly, when the short beam strength test results of ASTM D2344 ILSS test were examined, it was observed that the CC3 and CC4 cure cycles gave the desired values for UD-R2. In addition, ILSS and tensile test results can be checked in **Figure 46**, **Figure 47**.

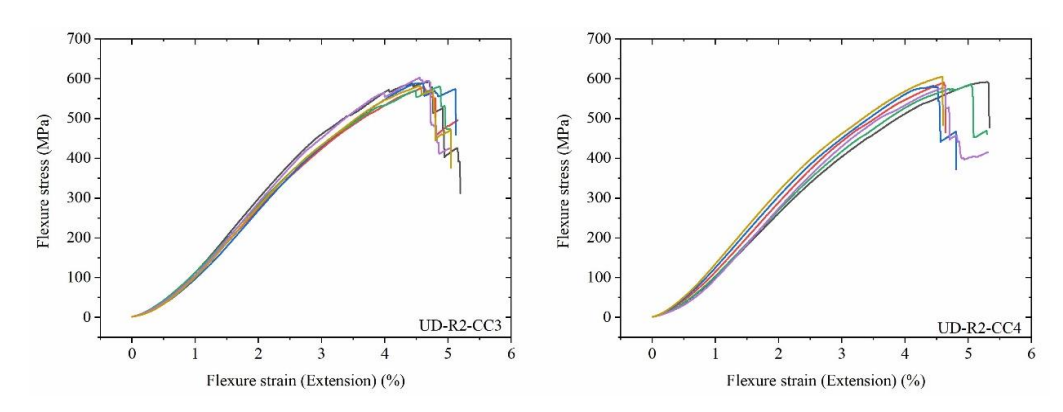


Figure 46. UD-R2 CC3 (left) and CC4 (right) interlaminar shear stress (ILSS) test results curves

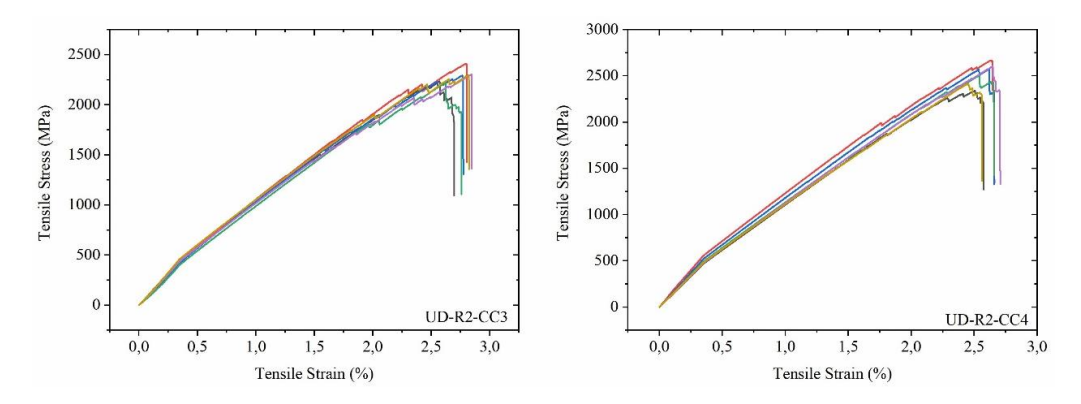


Figure 47. UD-R2 CC3 (left) and CC4 (right) tensile test results curves

When all these are considered, the test results in T_g value and tensile strength provide very important information. While the values in the CC3 cure cycle with a pressure value of 3 bar are lower than the reference T_g and tensile strength values, the values in the CC4 production with a pressure value of 7 bar are in the same range with the reference values. In this case, it has been proven that not every type of resin can work under all pressure conditions, as pointed out in introduction of **Chapter 2**. R2 resin gives higher values when it is manufactured with the cure cycle at 7 bar pressure. This case also showed the importance of studying the cure kinetics of the prepregs to be used during the manufacturing of composite parts.

CHAPTER 4

4. Conclusions

The cure cycle determination is very important for the improvement and optimization of the mechanical properties of carbon/epoxy composite materials. Multiple parameters in the cure cycle such as isothermal hold temperatures and times and heating and cooling rates must be carefully determined. These parameters are mostly related to the cure kinetics of the epoxy resin component of the carbon/epoxy composite, which is mainly the rate of chemical reactions occurring during epoxy resin curing. The rate of chemical reactions in epoxy resins is affected by temperature, surface area, the presence of a catalyst, and pressure. The effect of these parameters on the cure kinetics of epoxy resins and prepregs were investigated in this thesis using HP-DSC and rheometer. The obtained cure kinetic results were used to determine the cure cycle for prepregs with two different resin formulations and weave types, and a nano-material reinforced version of one of these prepregs, under two different pressure conditions.

The thesis was divided into two parts. In the first part, cure kinetic studies of a commercial epoxy resin and the prepreg obtained through combination of this epoxy resin with a 2x2 twill fabric were performed and the HP-DSC and rheology results were compared with each other under different heating rates, temperatures and pressures. When the enthalpy values of the prepreg were normalized based on the resin content, it was found that the normalized enthalpy values of the prepreg were less than the theoretically calculated enthalpy values, which were obtained from the enthalpy values of the neat resin in the dynamic HP-DSC tests. This was attributed to the prepreg being pre-cured to a B-stage during manufacturing by exposing it to heat. That is, some of the reactions already carried out, causing the total enthalpy to decrease. When the effect of pressure on enthalpy was examined, it was observed that an increase in pressure did not change the enthalpy values of the resin; whereas, it increased the enthalpy values of the prepreg to some degree. This behavior can be explained by the presence of the voids in the prepreg. The voids already present between the woven fibers (in crimp zones) in the twill prepreg and the voids formed during the evaporation of the moisture, which is also present in the crimp zones, upon temperature increase during curing restricted the progress of the reactions by forming physical barriers. These voids, which are either evacuated or reduced in size with the application of pressure, increased the surface area of the reactions and allowed more reactions to take place resulting in an increase in the enthalpy value of the prepreg. The examination of the enthalpy values at three different heating rates indicated that the increase in enthalpy values at low heating rates was more pronounced, which is considered to be due to the fact that the molecular mobility at lower conversions is more at low heating rates since more time and heat dissipitaion is provided for curing at lower temperatures, which result in more homegenous distribution of the resin in the prepreg before reaching the gel point, where the mobility is more limited. In addition, the enthalpy values obtained from the isothermal HP-DSC tests were higher than the enthalpy values of the dynamic HP-DSC tests for these reasons mentioned. That is, the reason for this is considered to be the extended time of curing for the isothermal tests as opposed to the dynamic tests. Although the reaction rates of the resin and the prepreg under pressure are similar until the gel point, which can be seen when the resin and prepreg isothermal conversion tables and the data in the gel time tables are analyzed together, there is a substantial decrease in the reaction rate of the resin after the gel point as opposed to that of the prepreg. This behavior can be explained as follows. The increase in crosslink density at the gel point constitues a sigificant obstacle to the molecular mobility in the resin, which lowers the reaction rate and increases the time to reach full conversion. Although a similar observation is made for the prepreg, the decrease in the reaction rate of the prepregis less than the resin since the prepreg contains fibers and its physical structure is different than the resin. The crosslink density, that can be found in the resin as a bulk, has to spread over a certain volume in the prepreg due to fibers creating physical barriers to the increase in the local crosslink density. In addition to the HP-DSC results, the rheological behavior of the resin and the prepreg was examined by a temperature sweep study using a rheometer, which showed that the complex viscosity of the resin was considerably lower than that of the prepreg at the beginning of the curing, which is due to the prepreg being at the B-stage. A through examination of dynamic and isothermal HP-DSC results along with the rheological behavior of the resin and the prepreg resulted in the determination of cure cyles (CC1 and CC2, respectively) for the resin and the prepreg.

In the second part of the thesis, the cure kinetics of two prepregs prepared by the combination of another epoxy resin, which is a modified version of the commercial epoxy resin used in the first part of the thesis, either in its neat form or in its nanomaterial reinforced form with a UD fabric were examined. The effect of both the use of a UD fabric instead of a twill fabric and the utilization of nanomaterial reinforcement on the

cure kinetics was investigated. The cure kinetics was tested at three pressures to determine the effect of pressure on the UD neat and nano-reinforced prepregs. When the HP-DSC test results were examined for the prepreg produced using a UD fabric, which consists of fibers oriented in one direction, as opposed to the twill fabric, it was observed that there was not a significant amount of voids present with the prepreg, which may be due to the fact that there are not crimp zones that will entrap air bubbles and water vapor in the UD fabric. Therefore, pressure did not change the enthalpy results. The resin used in the UD prepreg was a modified version of the commercial epoxy resin used in the first part of the thesis with various crosslinking and viscosity reducing agents, which increased the T_g and the curing time. A slight increase in curing enthalpy was observed when the prepreg was reinforced with the MWCNT. The reason was thought to be the participation of MWCNTs in the curing reaction. It was observed that the time required to reach 100% cure is less than the neat prepreg since MWCNTs increased the molecular interactions by increasing the surface area, thus, the rate of curing reactions. Additionally, when the rheological behaviors obtained from temperature sweep studies were examined, it was observed that the complex viscosity increased in the prepreg reinforced with nanomaterial since the molecular weight increased with the inclusion of MWCNTs in the molecular structure.

In the light of all results obtained in this study, cure cycles were determined. Since it was observed that the effect of pressure was more pronounced in the prepreg as opposed to the resin in the first part of the thesis, it was thought that it would be more reasonable to determine the cure cycles using the cure kinetic data obtained from the prepreg studies. For TW-R1, UD-R2, and UD-R2-MWCNT prepregs, individual cure cycles were determined using the data from HP-DSC and rheology, and the workability of these cure cycles was examined by thermal and mechanical characterization. The logic behind the cure cycle determination was as follows. First, it was decided that there should be two target isothermal hold temperatures. The first isothermal hold temperature not only would help the evacuation of the voids and excess resin from the system and but also would distribute the resin more homogeneously in the prepreg. The second target isothermal temperature hold would be the place where the curing reactions would be completed. For the first isothermal target temperature, the temperature was determined using the DSC and rheology data in a way that curing would not start and the viscosity would be low enough to distribute the resin homogeneously in the prepreg and evacuate the voids, yet

high enough not to cause resin loss. The holding time at this temperature was determined using the gel time data (taking the first point where the low viscosity value starts to rise), considered these parameters. The heating rate required to reach this temperature was determined to be 3 °C/min considering the longer time provided with this heating rate for the molecular mobility. The second target isothermal hold temperature, on the other hand, was chosen as the temperature at which the curing reactions would be completed without taking long periods of time and would not cause thermal distortion from the resin by causing short-term high enthalpy incereases. The hold time at this temperature was determined as the time to give 100% curing from the HP-DSC data. The cooling rate was chosen as a slow rate that would not cause shrinkage of the resin.

The pressure used in the cure cycle of the TW-R1 was determined to be 3 bar since it is the lowest pressure value that first changes the curing kinetic behavior that changes with the pressure mentioned above respect to the data obtained from the HP-DSC. However, since 7 bar is another pressure value that changes the curing kinetics and is frequently used in the industry, it was chosen as another pressure to be applied in the same curing cycle. As a result of the characterization and mechanical tests applied to the carbon/epoxy composite laminates manufactured with the these cure cycle applied under two different pressures, it was seen that both cure cycles were successful. Both cure cycles fully satisfied the residual cure, fiber-resin-void content, Tg and tensile and short beam strengths of the reference manufacturing. With all this, when determining the cure cycles for UD-R2 and UD-R2-MWCNT, the same cure cycles were applied as these prepregs showed similar cure kinetic behavior under 3 and 7 bar pressure. The reason for choosing 7 bar pressure value is that it has the most effect on the curing times and changes the curing kinetics in this direction, in line with the information obtained from the isothermal HP-DSC data. The reason for testing a pressure of 3 bar was to see if it had an effect on the cure kinetic behavior at a larger surface area, although there was no effect on the cure kinetics according to the information obtained from the HP-DSC test results working with small weights and to enable comparison with the information from Chapter 2. In the characterization and mechanical test results of carbon/epoxy composite laminate productions made with these two cure cycles, it was observed that 3 bar pressure did not satisfied T_g and tensile and short beam strengths values of the reference production, however 7 bar pressure fully satisfied the residual cure, fiber-resin-void content, Tg and tensile and short beam strengths. As a result, it was thought that the pressure value of 3

bar, which was not found to affect the curing kinetics in the tests performed on the HP-DSC device, could not reach the reference values in the cure cycle, and that the pressure value definitely should be determined by examining the curing kinetic behavior changes while determining the cure cycle. However, although the isothermal temperature and hold times were the same (it is thought that these values are the same due to the same base resins), in the cure cycles determined by the test results obtained as a result of the studies performed with HP-DSC and rheometer in Chapters 2 and 3, it was observed that these cure cycles only under different pressure values satisfy the highest thermal, physical and mechanical properties of carbon/epoxy laminate.

As a result of this thesis, it was understood that if only the cure kinetics is known and the cure cycle are determined for each prepreg system respect to cure kinetics data, maximum thermal, physical and mechanical properties can only be achieved in carbon/epoxy composites. In addition, it can be concluded that the cure cycle of carbon/epoxy composites can be determined easily by making various optimizations in accordance with parameters such as the size of the composite part, curved structure of the composite part, energy and cost efficiency using the cure kinetics data which are obtained HP-DSC and rheometer.

References

- [1] Drakonakis V M, Seferis J C and Doumanidis C C 2013 Curing pressure influence of out-of-autoclave processing on structural composites for commercial aviation Adv. Mater. Sci. Eng. 2013
- [2] Varma I K and Gupta V B Thermosetting Resin DProperties
- [3] America D of D of the U S of 2002 Composite Materials Handbook Vol. 3: Polymer Matrix Composites MIL Handb. 3 1–690
- [4] Anon 1986 Ashby, M. F., Ashby, M. F., & Jones, D. R. H. (1986). Engineering materials 2: An introduction to microstructures, processing, and design . (Engineering materials.) Oxford [Oxfordshire: Pergamon Press. 1986
- [5] IMAMURA T and YAMAGUCHI Y 1995 Composite Materials for Aircraft Structures. vol 43
- [6] Anon 2000 Craver, C. D., & Carraher, C. E. (2000). Applied polymer science: 21st century . Amsterdam [Netherlands: Elsevier. 2000
- [7] Acebo C, Ramis X and Serra A 2017 Improved epoxy thermosets by the use of poly(ethyleneimine) derivatives Phys. Sci. Rev. 2 1–31
- [8] Acocella M R, Corcione C E, Giuri A, Maggio M, Maffezzoli A and Guerra G 2016 Graphene oxide as a catalyst for ring opening reactions in amine crosslinking of epoxy resins RSC Adv. 6 23858–65
- [9] Wang R and Schuman T 2015 Towards green: A review of recent developments in bio-renewable epoxy resins from vegetable oils vol 2015-Janua
- [10] Anon 1975 BRANDRUP, J., IMMERGUT, E. H., & MCDOWELL, W. (1975). Polymer handbook . New York, Wiley. 1975
- [11] Campbell Jr F C 2003 Chapter 6 Curing: It's a Matter of Time (t), Temperature (T) and Pressure (P) Manuf. Process. Adv. Compos. 2004
- [12] Anon 1989 Allen, G., & Bevington, J. C. (1989). Comprehensive polymer science: The synthesis, characterization, reactions & applications of polymers. (Polymer characterization.) Oxford, England: Pergamon Press. 1989
- [13] Lo J and Nutt S 2019 Method for in situ analysis of volatiles generated during cure of composites Compos. Part A Appl. Sci. Manuf. 123 141–8
- [14] Callister W D 2007 Materials Science and Engineering: An Introduction. New York: John Wiley & Sons 1997
- [15] Anon 2003 Advani, S.G., & Sozer, E.M. (Eds.). (2003). Process Modeling in Composites Manufacturing (1st ed.). CRC Press. https://doi.org/10.1201/9780203910061 2003
- [16] Gorbatikh L and Lomov S V. 2016 Damage accumulation in textile composites (Elsevier)
- [17] Özdemir H, Içten B M and Doğan A 2018 Experimental investigation of the tensile and impact properties of twill and twill derivative woven fabric reinforced

- composites Tekst. ve Konfeksiyon 28 258–72
- [18] Wang L, Wu J, Chen C, Zheng C, Li B, Joshi S C and Zhou K 2017 Progressive failure analysis of 2D woven composites at the meso-micro scale Compos. Struct. 178 395–405
- [19] Hardis R 2012 Cure kinetics characterization and monitoring of an epoxy resin for thick composite structures A thesis 55
- [20] Maria J, Paiva F De, Mayer S and Cerqueira M 2006 Paiva 2006 Carbon Epoxy 9 83–9
- [21] Wang P H, Sterkenburg R, Kim G and He Y 2019 Investigating the void content, fiber content, and fiber orientation of 3D printed recycled carbon fiber Key Eng. Mater. 801 KEM 276–81
- [22] Drakonakis V M, Seferis J C and Doumanidis C C 2013 Curing pressure influence of out-of-autoclave processing on structural composites for commercial aviation Adv. Mater. Sci. Eng. 2013
- [23] Loos A C and Springer G S 1983 Curing of Epoxy Matrix Composites J. Compos. Mater. 17 135–69
- [24] Park S Y and Choi W J 2017 3 Production Control Effect on Composite Material Quality and Stability for Aerospace Usage Adv. Compos. Mater. Prop. Appl. 112–94
- [25] Clausse D, Gomez F, Pezron I, Komunjer L and Dalmazzone C 2005 Morphology characterization of emulsions by differential scanning calorimetry Adv. Colloid Interface Sci. 117 59–74
- [26] Quintanilla L, Rodríguez-Cabello J C, Jawhari T and Pastor J M 1993 Structural analysis of injection-moulded semicrystalline polymers by Fourier transform infrared spectroscopy with photoacoustic detection and differential scanning calorimetry: 1. Poly(ethylene terephthalate) Polymer (Guildf). 34 3787–95
- [27] Deyme M and Madelmont G 1990 Differential scanning calorimetry Biomaterials 11 141–2
- [28] Porter C E and Blum F D 2002 Thermal characterization of adsorbed polystyrene using modulated differential scanning calorimetry Macromolecules 35 7448–52
- [29] Drzeżdżon J, Jacewicz D, Sielicka A and Chmurzyński L 2019 Characterization of polymers based on differential scanning calorimetry based techniques TrAC Trends Anal. Chem. 110 51–6
- [30] Legrand M and Bellenger V 2001 Estimation of the cross-linking ratio and glass transition temperature during curing of amine-cross-linked epoxies Compos. Sci. Technol. 61 1485–9
- [31] Weldon D G 2014 Differential scanning calorimetry J. Prot. Coatings Linings 31 21–3
- [32] Mettler-Toledo AG A Thermal Analysis Excellence DSC 1
- [33] Shawe J, Riesen R, Widmann J and Schubnell M 2000 UserCom Mettler Toledo 1–28

- [34] MettlerToledo 2010 User Com 1–24
- [35] Analysis T Advanced Model Free Kinetics 2–3
- [36] Vyazovkin S, Burnham A K, Favergeon L, Koga N, Moukhina E, Pérez-Maqueda L A and Sbirrazzuoli N 2020 ICTAC Kinetics Committee recommendations for analysis of multi-step kinetics Thermochim. Acta 689
- [37] Anon Espenson, J. H. (2002). Chemical kinetics and reaction mechanisms. New York McGraw-Hill.pdf
- [38] Anon Laidler, K. J. (1987). Chemical kinetics New York Harper & Row.pdf
- [39] Anon Shenoy, A. V. (1999). Rheology of filled polymer systems Dordrecht Kluwer.pdf
- [40] Giesekus H 1961 Rheology, Theory and Applications. Zeitschrift für Phys. Chemie 30 287–8
- [41] Costa M L, Botelho E C, De Paiva J M F and Rezende M C 2005 Characterization of cure of carbon/epoxy prepreg used in aerospace field Mater. Res. 8 317–22
- [42] Shakya N, Roux J A and Jeswani A L 2013 Effect of resin viscosity in fiber reinforcement compaction in resin injection pultrusion process Appl. Compos. Mater. 20 1173–93
- [43] Guide R MCR Evolution Series
- [44] WenjunLi 2003 R ~ Oeoutv
- [45] López J, Ramírez C, Torres A, Abad M J, Barral L, Cano J and Díez F J 2002 Isothermal curing by dynamic mechanical analysis of three epoxy resin systems: Gelation and vitrification J. Appl. Polym. Sci. 83 78–85
- [46] METTLER TOLEDO METTLER TOLEDO STAR System DMA/SDTA861 Operating Instructions 342
- [47] Rude T J, Strait L H and Ruhala L A 2000 Measurement of fiber density by helium pycnometry J. Compos. Mater. 34 1948–58
- [48] Viet N V., Zaki W and Umer R 2018 Interlaminar shear stress function for adhesively bonded multi-layer metal laminates Int. J. Adhes. Adhes. 82 14–20
- [49] Abali F, Pora A and Shivakumar K 2003 Modified short beam shear test for measurement of interlaminar shear strength of composites J. Compos. Mater. 37 453–64
- [50] Lu X and Liu D 1992 An interlaminar shear stress continuity theory for both thin and thick composite laminates J. Appl. Mech. Trans. ASME 59 502–9
- [51] Aslan Z 2015 Apparent interlaminar shear strength measurement by four point short beam test Adv. Compos. Lett. 24 27–32
- [52] Markham M F and Dawson D 1975 Interlaminar shear strength of fibre-reinforced composites Composites 6 173–6
- [53] Davies L W, Day R J, Bond D, Nesbitt A, Ellis J and Gardon E 2007 Effect of cure cycle heat transfer rates on the physical and mechanical properties of an epoxy

- matrix composite Compos. Sci. Technol. 67 1892–9
- [54] Vertuccio L, Russo S, Raimondo M, Lafdi K and Guadagno L 2015 Influence of carbon nanofillers on the curing kinetics of epoxy-amine resin RSC Adv. 5 90437–50
- [55] Atarsia A and Boukhili R 2000 Relationship between isothermal and dynamic cure of thermaosets via the isoconversion representation Polym. Eng. Sci. 40 607–20
- [56] Di Vizio F, Santillo F, Squeo E A, Mirante N, Di Cosmo A, Lillo F and SpA A 2015 Curing kinetics analysis of carbon/epoxy prepreg for solid rocket motor casings application
- [57] Pongsa U, Samthong C, Praserthdam P and Somwangthanaroj A 2016 Influence of diaminobenzoyl-functionalized multiwalled carbon nanotubes on the nonisothermal curing kinetics, dynamic mechanical properties, and thermal conductivity of epoxy-anhydride composites J. Appl. Polym. Sci. 133 1–10
- [58] Gerami G, Bagheri R and Darvishi R 2019 Investigation of isothermal and dynamic cure kinetics of epoxy resin/nadic methyl anhydride/dicyandiamide by differential scanning calorimetry (DSC) J. Therm. Anal. Calorim. 137 575–82
- [59] Boey F Y C and Lye S W 1992 Void reduction in autoclave processing of thermoset composites. Part 1: High pressure effects on void reduction Composites 23 261–5
- [60] Lundström T S and Gebart B R 1994 Influence from process parameters on void formation in resin transfer molding Polym. Compos. 15 25–33
- [61] Olivier P, Cottu J P and Ferret B 1995 Effects of cure cycle pressure and voids on some mechanical properties of carbon/epoxy laminates Composites 26 509–15
- [62] Lee B L and Yang T W MOISTURE EFFECTS ON PMC.pdf 3 1217–31
- [63] Nakamae K, Nishino T, AiRu X and Takatsuka K 1991 Pressure dependence of the curing behavior of epoxy resin Polym. J. 23 1157–62
- [64] Boey F Y C and Lye S W 1992 Void reduction in autoclave processing of thermoset composites. Part 2: Void reduction in a microwave curing process Composites 23 266–70
- [65] Xu Y, He Q, Yang W, Sun T and Tang Q 2018 Study on relationships between curing pressures and mechanical properties for epoxy adhesive films Chem. Eng. Trans. 66 43–8
- [66] Koushyar H, Alavi-Soltani S, Minaie B and Violette M 2012 Effects of variation in autoclave pressure, temperature, and vacuum-application time on porosity and mechanical properties of a carbon fiber/epoxy composite J. Compos. Mater. 46 1985–2004
- [67] Anon 2018 ZWEBEN, C. H., & BEAUMONT, P. W. R. (2018). Comprehensive composite materials II . https://www.sciencedirect.com/science/referenceworks/9780081005347. 2018
- [68] Park S Y, Choi C H, Choi W J and Hwang S S 2019 A Comparison of the Properties of Carbon Fiber Epoxy Composites Produced by Non-autoclave with Vacuum Bag Only Prepreg and Autoclave Process Appl. Compos. Mater. 26 187–

- [69] Anon 1977 Browning, C., Husman, G., & Whitney, J. (1977). Moisture Effects in Epoxy Matrix Composites. ASTM special technical publications, 481-496. 1977
- [70] Nele L, Caggiano A and Teti R 2016 Autoclave Cycle Optimization for High Performance Composite Parts Manufacturing Procedia CIRP 57 241–6
- [71] Dong A, Zhao Y, Zhao X and Yu Q 2018 Cure cycle optimization of rapidly cured out-of-autoclave composites Materials (Basel). 11
- [72] Harper J F, Miller N A and Yap S C 1993 Influence of temperature and pressure during the curing of prepreg carbon fiber epoxy resin Polym. Plast. Technol. Eng. 32 269–75
- [73] Selvaraj S and Madhavan M 2019 Strengthening of Laterally Restrained Steel Beams Subjected to Flexural Loading Using Low-Modulus CFRP J. Perform. Constr. Facil. 33 04019032
- [74] Budriene S 2002 Polymer Synthesis: Theory and Practice vol 2002
- [75] Saeb M R, Bakhshandeh E, Khonakdar H A, Mäder E, Scheffler C and Heinrich G 2013 Cure kinetics of epoxy nanocomposites affected by MWCNTs functionalization: A review Sci. World J. 2013
- [76] Shen J, Huang W, Wu L, Hu Y and Ye M 2007 Thermo-physical properties of epoxy nanocomposites reinforced with amino-functionalized multi-walled carbon nanotubes Compos. Part A Appl. Sci. Manuf. 38 1331–6
- [77] Allaoui A and El Bounia N 2009 How carbon nanotubes affect the cure kinetics and glass transition temperature of their epoxy composites? A review Express Polym. Lett. 3 588–94
- [78] Prolongo S G, Gude M R and Ureña A 2010 The curing process of epoxy/aminofunctionalized MWCNTs: Calorimetry, molecular modelling, and electron microscopy J. Nanotechnol.